Volume 3

MICROWAVE AND RF DESIGN

NETWORKS

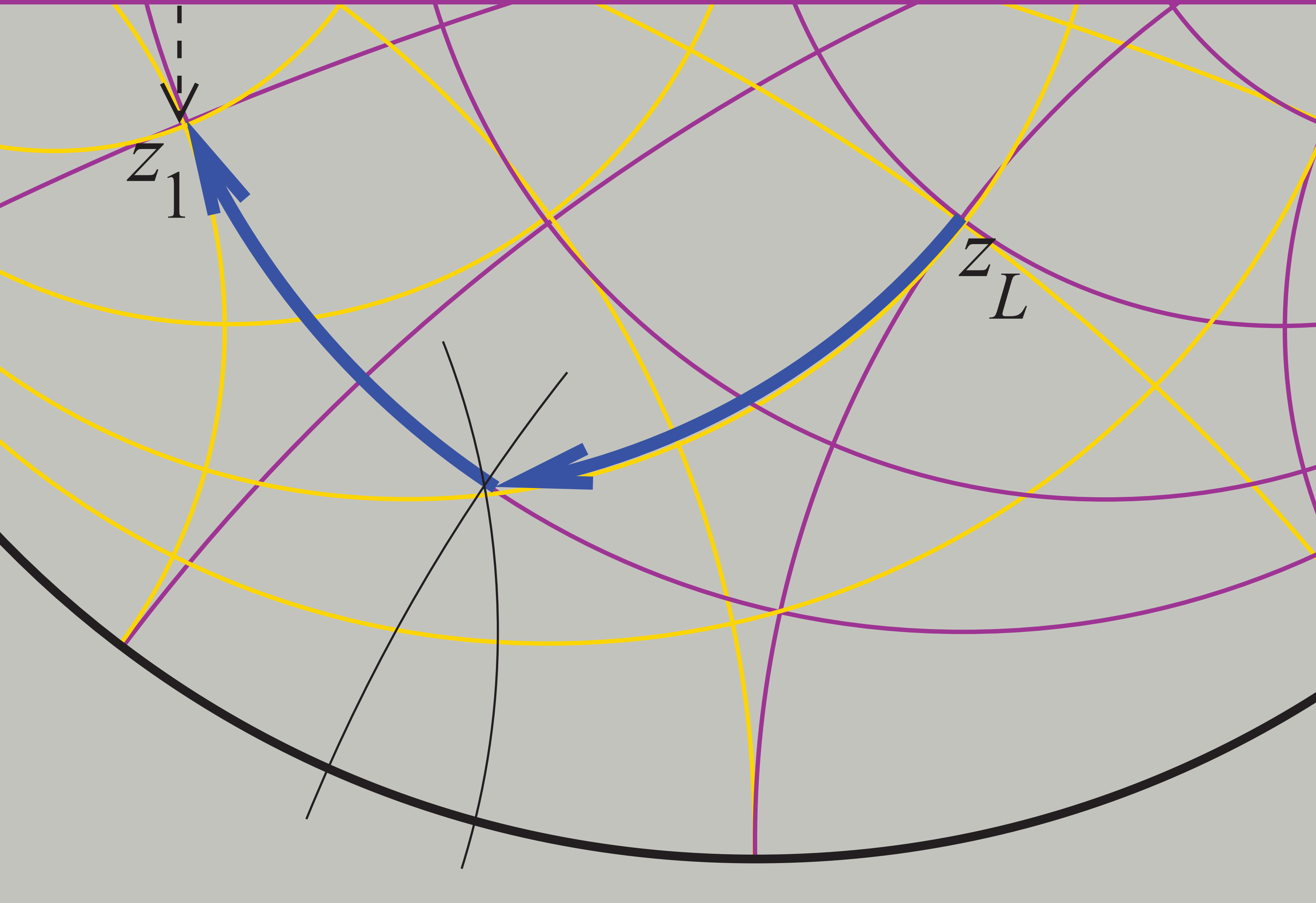

Michael Steer

Third Edition

Microwave and RF Design
Networks

Volume 3

Third Edition

Michael Steer

Microwave and RF Design
Networks

Volume 3

Third Edition

Michael Steer

Citation: Steer, Michael. *Microwave and RF Design: Networks*. Volume 3. (Third Edition), NC State University, 2019. doi: https//doi.org/10.5149/9781469656953 Steer

ISBN 978-1-4696-5694-6 (paperback)
ISBN 978-1-4696-5695-3 (open access ebook)

Published by NC State University

NC STATE UNIVERSITY

Distributed by the University of North Carolina Press
www.uncpress.org

Printing: 1

To

Alison

Preface

The book series *Microwave and RF Design* is a comprehensive treatment of radio frequency (RF) and microwave design with a modern "systems-first" approach. A strong emphasis on design permeates the series with extensive case studies and design examples. Design is oriented towards cellular communications and microstrip design so that lessons learned can be applied to real-world design tasks. The books in the Microwave and RF Design series are:

- Microwave and RF Design: Radio Systems, Volume 1
- Microwave and RF Design: Transmission Lines, Volume 2
- Microwave and RF Design: Networks, Volume 3
- Microwave and RF Design: Modules, Volume 4
- Microwave and RF Design: Amplifiers and Oscillators, Volume 5

The length and format of each is suitable for automatic printing and binding.

Rationale

The central philosophy behind this series's popular approach is that the student or practicing engineer will develop a full appreciation for RF and microwave engineering and gain the practical skills to perform system-level design decisions. Now more than ever companies need engineers with an ingrained appreciation of systems and armed with the skills to make system decisions. One of the greatest challenges facing RF and microwave engineering is the increasing level of abstraction needed to create innovative microwave and RF systems. This book series is organized in such a way that the reader comes to understand the impact that system-level decisions have on component and subsystem design. At the same time, the capabilities of technologies, components, and subsystems impact system design. The book series is meticulously crafted to intertwine these themes.

Audience

The book series was originally developed for three courses at North Carolina State University. One is a final-year undergraduate class, another an introductory graduate class, and the third an advanced graduate class. Books in the series are used as supplementary texts in two other classes. There are extensive case studies, examples, and end of chapter problems ranging from straight-forward to in-depth problems requiring hours to solve. A companion book, *Fundamentals of Microwave and RF Design*, is more suitable for an undergraduate class yet there is a direct linkage between the material in this book and the series which can then be used as a career-long reference text. I believe it is completely understandable for senior-level students where a microwave/RF engineering course is offered. The book series is a comprehensive RF and microwave text and reference, with detailed index, appendices, and cross-references throughout. Practicing engineers will find the book series a valuable systems primer, a refresher as needed, and a reference tool in the field. Additionally, it can serve as a valuable, accessible resource for those outside RF circuit engineering who need to understand how they can work with RF hardware engineers.

Organization

This book is a volume in a five volume series on RF and microwave design. The first volume in the series, *Microwave and RF Design: Radio Systems*, addresses radio systems mainly following the evolution of cellular radio. A central aspect of microwave engineering is distributed effects considered in the second volume of this book series, *Microwave and RF Design: Transmission Lines*. Here transmission lines are treated as supporting forward- and backward-traveling voltage and current waves and these are related to electromagnetic effects. The third volume, *Microwave and RF Design: Networks*, covers microwave network theory which is the theory that describes power flow and can be used with transmission line effects. Topics covered in *Microwave and RF Design: Modules*, focus on designing microwave circuits and systems using modules introducing a large number of different modules. Modules is just another term for a network but the implication is that is is packaged and often available off-the-shelf. Other topics that are important in system design using modules are considered including noise, distortion, and dynamic range. Most microwave and RF designers construct systems using modules developed by other engineers who specialize in developing the modules. Examples are filter and amplifier modules which once designed can be used in many different systems. Much of microwave design is about maximizing dynamic range, minimizing noise, and minimizing DC power consumption. The fifth volume in this series, *Microwave and RF Design: Amplifiers and Oscillators*, considers amplifier and oscillator design and develops the skills required to develop modules.

Volume 1: Microwave and RF Design: Radio Systems

The first book of the series covers RF systems. It describes system concepts and provides comprehensive knowledge of RF and microwave systems. The emphasis is on understanding how systems are crafted from many different technologies and concepts. The reader gains valuable insight into how different technologies can be traded off in meeting system requirements. I do not believe this systems presentation is available anywhere else in such a compact form.

Volume 2: Microwave and RF Design: Transmission Lines

This book begins with a chapter on transmission line theory and introduces the concepts of forward- and backward-traveling waves. Many examples are included of advanced techniques for analyzing and designing transmission line networks. This is followed by a chapter on planar transmission lines with microstrip lines primarily used in design examples. Design examples illustrate some of the less quantifiable design decisions that must be made. The next chapter describes frequency-dependent transmission line effects and describes the design choices that must be taken to avoid multimoding. The final chapter in this volume addresses coupled-lines. It is shown how to design coupled-line networks that exploit this distributed effect to realize novel circuit functionality and how to design networks that minimize negative effects. The modern treatment of transmission lines in this volume emphasizes planar circuit design and the practical aspects of designing around unwanted effects. Detailed design of a directional coupler is used to illustrate the use of coupled lines. Network equivalents of coupled lines are introduced as fundamental building blocks that are used later in the synthesis of coupled-line filters. The text, examples, and problems introduce the often hidden design requirements of designing to mitigate parasitic effects and unwanted modes of operation.

Volume 3: Microwave and RF Design: Networks

Volume 3 focuses on microwave networks with descriptions based on S parameters and $ABCD$ matrices, and the representation of reflection and transmission information on polar plots called Smith charts. Microwave measurement and calibration technology are examined. A sampling of the wide variety of microwave elements based on transmission lines is presented. It is shown how many of these have lumped-element equivalents and how lumped elements and transmission lines can be combined as a compromise between the high performance of transmission line structures and the compactness of lumped elements. This volume concludes with an in-depth treatment of matching for maximum power transfer. Both lumped-element and distributed-element matching are presented.

Volume 4: Microwave and RF Design: Modules

Volume 4 focuses on the design of systems based on microwave modules. The book considers the wide variety of RF modules including amplifiers, local oscillators, switches, circulators, isolators, phase detectors, frequency multipliers and dividers, phase-locked loops, and direct digital synthesizers. The use of modules has become increasingly important in RF and microwave engineering. A wide variety of passive and active modules are available and high-performance systems can be realized cost effectively and with stellar performance by using off-the-shelf modules interconnected using planar transmission lines. Module vendors are encouraged by the market to develop competitive modules that can be used in a wide variety of applications. The great majority of RF and microwave engineers either develop modules or use modules to realize RF systems. Systems must also be concerned with noise and distortion, including distortion that originates in supposedly linear elements. Something as simple as a termination can produce distortion called passive intermodulation distortion. Design techniques are presented for designing cascaded systems while managing noise and distortion. Filters are also modules and general filter theory is covered and the design of parallel coupled line filters is presented in detail. Filter design is presented as a mixture of art and science. This mix, and the thought processes involved, are emphasized through the design of a filter integrated throughout this chapter.

Volume 5: Microwave and RF Design: Amplifiers and Oscillators

The fifth volume presents the design of amplifiers and oscillators in a way that enables state-of-the-art designs to be developed. Detailed strategies for amplifiers and voltage-controlled oscillators are presented. Design of competitive microwave amplifiers and oscillators are particularly challenging as many trade-offs are required in design, and the design decisions cannot be reduced to a formulaic flow. Very detailed case studies are presented and while some may seem quite complicated, they parallel the level of sophistication required to develop competitive designs.

Case Studies

A key feature of this book series is the use of real world case studies of leading edge designs. Some of the case studies are designs done in my research group to demonstrate design techniques resulting in leading performance. The case studies and the persons responsible for helping to develop them are as follows.

1. Software defined radio transmitter.
2. High dynamic range down converter design. This case study was developed with Alan Victor.
3. Design of a third-order Chebyshev combline filter. This case study was developed with Wael Fathelbab.
4. Design of a bandstop filter. This case study was developed with Wael Fathelbab.
5. Tunable Resonator with a varactor diode stack. This case study was developed with Alan Victor.
6. Analysis of a 15 GHz Receiver. This case study was developed with Alan Victor.
7. Transceiver Architecture. This case study was developed with Alan Victor.
8. Narrowband linear amplifier design. This case study was developed with Dane Collins and National Instruments Corporation.
9. Wideband Amplifier Design. This case study was developed with Dane Collins and National Instruments Corporation.
10. Distributed biasing of differential amplifiers. This case study was developed with Wael Fathelbab.
11. Analysis of a distributed amplifier. This case study was developed with Ratan Bhatia, Jason Gerber, Tony Kwan, and Rowan Gilmore.
12. Design of a WiMAX power amplifier. This case study was developed with Dane Collins and National Instruments Corporation.
13. Reflection oscillator. This case study was developed with Dane Collins and National Instruments Corporation.
14. Design of a C-Band VCO. This case study was developed with Alan Victor.
15. Oscillator phase noise analysis. This case study was developed with Dane Collins and National Instruments Corporation.

Many of these case studies are available as captioned YouTube videos and qualified instructors can request higher resolution videos from the author.

Course Structures

Based on the adoption of the first and second editions at universities, several different university courses have been developed using various parts of what was originally one very large book. The book supports teaching two or three classes with courses varying by the selection of volumes and chapters. A standard microwave class following the format of earlier microwave texts can be taught using the second and third volumes. Such a course will benefit from the strong practical design flavor and modern treatment of measurement technology, Smith charts, and matching networks. Transmission line propagation and design is presented in the context of microstrip technology providing an immediately useful skill. The subtleties of multimoding are also presented in the context of microstrip lines. In such a class the first volume on microwave systems can be assigned for self-learning.

Another approach is to teach a course that focuses on transmission line effects including parallel coupled-line filters and module design. Such a class would focus on Volumes 2, 3 and 4. A filter design course would focus on using Volume 4 on module design. A course on amplifier and oscillator design would use Volume 5. This course is supported by a large number of case studies that present design concepts that would otherwise be difficult to put into the flow of the textbook.

Another option suited to an undergraduate or introductory graduate class is to teach a class that enables engineers to develop RF and microwave systems. This class uses portions of Volumes 2, 3 and 4. This class then omits detailed filter, amplifier, and oscillator design.

The fundamental philosophy behind the book series is that the broader impact of the material should be presented first. Systems should be discussed up front and not left as an afterthought for the final chapter of a textbook, the last lecture of the semester, or the last course of a curriculum.

The book series is written so that all electrical engineers can gain an appreciation of RF and microwave hardware engineering. The body of the text can be covered without strong reliance on this electromagnetic theory, but it is there for those who desire it for teaching or reader review. The book is rich with detailed information and also serves as a technical reference.

The Systems Engineer

Systems are developed beginning with fuzzy requirements for components and subsystems. Just as system requirements provide impetus to develop new base technologies, the development of new technologies provides new capabilities that drive innovation and new systems. The new capabilities may arise from developments made in support of other systems. Sometimes serendipity leads to the new capabilities. Creating innovative microwave and RF systems that address market needs or provide for new opportunities is the most exciting challenge in RF design. The engineers who can conceptualize and architect new RF systems are in great demand. This book began as an effort to train RF systems engineers and as an RF systems resource for practicing engineers. Many RF systems engineers began their careers when systems were simple. Today, appreciating a system requires higher levels of abstraction than in the past, but it also requires detailed knowledge or the ability to access detailed knowledge and expertise. So what makes a systems engineer? There is not a simple answer, but many partial answers. We know that system engineers have great technical confidence and broad appreciation for technologies. They are both broad in their knowledge of a large swath of technologies and also deep in knowledge of a few areas, sometimes called the "T" model. One book or course will not make a systems engineer. It is clear that there must be a diverse set of experiences. This book series fulfills the role of fostering both high-level abstraction of RF engineering and also detailed design skills to realize effective RF and microwave modules. My hope is that this book will provide the necessary background for the next generation of RF systems engineers by stressing system principles immediately, followed by core RF technologies. Core technologies are thereby covered within the context of the systems in which they are used.

Supplementary Materials

Supplementary materials available to qualified instructors adopting the book include PowerPoint slides and solutions to the end-of-chapter problems. Requests should be directed to the author. Access to downloads of the books, additional material and YouTube videos of many case studies are available at `https://www.lib.ncsu.edu/do/open-education`

Acknowledgments

Writing this book has been a large task and I am indebted to the many people who helped along the way. First I want to thank the more than 1200 electrical engineering graduate students who used drafts and the first two editions at NC State. I thank the many instructors and students who have provided feedback. I particularly thank Dr. Wael Fathelbab, a filter expert, who co-wrote an early version of the filter chapter. Professor Andreas Cangellaris helped in developing the early structure of the book. Many people have reviewed the book and provided suggestions. I thank input on the structure of the manuscript: Professors Mark Wharton and Nuno Carvalho of Universidade de Aveiro, Professors Ed Delp and Saul Gelfand of Purdue University, Professor Lynn Carpenter of Pennsylvania State University, Professor Grant Ellis of the Universiti Teknologi Petronas, Professor Islam Eshrah of Cairo University, Professor Mohammad Essaaidi and Dr. Otman Aghzout of Abdelmalek Essaadi Univeristy, Professor Jianguo Ma of Guangdong University of Technology, Dr. Jayesh Nath of Apple, Mr. Sony Rowland of the U.S. Navy, and Dr. Jonathan Wilkerson of Lawrence Livermore National Laboratories, Dr. Josh Wetherington of Vadum, Dr. Glen Garner of Vadum, and Mr. Justin Lowry who graduated from North Carolina State University.

Many people helped in producing this book. In the first edition I was assisted by Ms. Claire Sideri, Ms. Susan Manning, and Mr. Robert Lawless who assisted in layout and production. The publisher, task master, and chief coordinator, Mr. Dudley Kay, provided focus and tremendous assistance in developing the first and second editions of the book, collecting feedback from many instructors and reviewers. I thank the Institution of Engineering and Technology, who acquired the original publisher, for returning the copyright to me. This open access book was facilitated by John McLeod and Samuel Dalzell of the University of North Carolina Press, and by Micah Vandergrift and William Cross of NC State University Libraries. The open access ebooks are host by NC State University Libraries.

The book was produced using LaTeX and open access fonts, line art was drawn using xfig and inkscape, and images were edited in gimp. So thanks to the many volunteers who developed these packages.

My family, Mary, Cormac, Fiona, and Killian, gracefully put up with my absence for innumerable nights and weekends, many more than I could have ever imagined. I truly thank them. I also thank my academic sponsor, Dr. Ross Lampe, Jr., whose support of the university and its mission enabled me to pursue high risk and high reward endeavors including this book.

Michael Steer
North Carolina State University
Raleigh, North Carolina
mbs@ncsu.edu

List of Trademarks

3GPP® is a registered trademark of the European Telecommunications Standards Institute.

802® is a registered trademark of the Institute of Electrical & Electronics Engineers .

APC-7® is a registered trademark of Amphenol Corporation.

AT&T® is a registered trademark of AT&T Intellectual Property II, L.P.

AWR® is a registered trademark of National Instruments Corporation.

AWRDE® is a trademark of National Instruments Corporation.

Bluetooth® is a registered trademark of the Bluetooth Special Interest Group.

GSM® is a registered trademark of the GSM MOU Association.

Mathcad® is a registered trademark of Parametric Technology Corporation.

MATLAB® is a registered trademark of The MathWorks, Inc.

NEC® is a registered trademark of NEC Corporation.

OFDMA® is a registered trademark of Runcom Technologies Ltd.

Qualcomm® is a registered trademark of Qualcomm Inc.

Teflon® is a registered trademark of E. I. du Pont de Nemours.

RFMD® is a registered trademark of RF Micro Devices, Inc.

SONNET® is a trademark of Sonnet Corporation.

Smith is a registered trademark of the Institute of Electrical and Electronics Engineers.

Touchstone® is a registered trademark of Agilent Corporation.

WiFi® is a registered trademark of the Wi-Fi Alliance.

WiMAX® is a registered trademark of the WiMAX Forum.

All other trademarks are the properties of their respective owners.

Contents

CHAPTER 1

Introduction to RF and Microwave Networks

1.1 Introduction to Microwave Networks

At microwave frequencies a ground plane cannot always be defined as circuits are large enough that a "ground" in one part of a circuit is not the same as a "ground" in another spatially separated part of the circuit. If they were the same "ground" then charges would need to be able to instantaneously redistribute and this is not possible because of the finite speed of causality (that is, the speed of light). One of the consequences of this is that voltage and current occur as forward- and backward-traveling voltage and current waves on transmission lines, or in microwave networks as incident and reflected voltage and current waves at interfaces between different parts of a circuit. At any point the sum of the forward-traveling (or incident) voltage wave and the backward-traveling (or reflected) voltage wave is the total voltage used with low-frequency circuits. A similar description applies to currents. A voltage wave directly relates to the movement of power or what are called power waves. Because of this, the conventional circuit parameters, the y and z parameters defined when there is a single ground, prove to be inadequate to describe signals in microwave circuits. Scattering parameters, or S parameters, are the most convenient network parameters to use with microwave circuits as they neatly describe the properties of traveling waves of voltage and current. A further attribute is that the S parameters relate directly to power flow.

In the early days of electrical engineering all circuits were called networks. That usage remains with microwave circuits but it is more commonly used with circuits that operate at microwave frequencies but only the external terminals are presented and internal details often hidden. The use of the network term also conveys a subtle reminder that there is not necessarily a universal ground. S parameters are defined even when there is not a universal ground.

Most RF and microwave design is concerned with the movement of signal power and minimizing noise power to maintain a high signal-to-noise ratio in a circuit. This maximizes the performance of communication, radar and sensor systems. Thus maximizing power transfer is critical and the design technique that does this is called matching.

1.2 Book Outline

Chapter 2 presents microwave network analysis and in particular S parameters and other parameters that are useful in design. One of the characteristics of a microwave designer is thatthey work very well with graphical information about a network. The visual display is the fastest way to convey information to the human brain. A human recognizes patterns very well so it is not surprising that microwave design methods have evolved to make extensive use of graphical means of representing network information, and of design strategies that are based on graphical manipulations. Graphical methods for representing the description of microwave networks are considered in the third chapter of this book, Chapter 3, entitled Graphical Network Analysis. The all important Smith chart is described here. Working knowledge of S parameters and of Smith charts are the two biggest 'barriers to entry' to microwave design. They are the two main topics that must be understood and absorbed before one can become a competent microwave designer or even converse with other engineers about microwave designs. There is no simpler way to describe the intended or actual performance of a microwave circuit design.

The fourth chapter, Chapter 4, discusses microwave measurements and how information about a network can be interpreted from the graphical display of measured information or from a design solution sketched out on a Smith chart. The Smith chart is the microwave engineer's 'back-of-the-envelope' sketch pad.

Chapter 5 introduces many novel microwave elements and these rarely have an analog below microwave frequencies. These circuit elements exploit distributed effects, i.e. transmission line effects. Sometimes there are a few low frequency analogs but these were developed by first conceiving the microwave element and then replacing transmission lines by their approximate LC equivalent circuits. This chapter introduces transmission line stubs, hybrids (which are four-port circuits that route signal power), baluns (which interface balanced and unbalanced circuits), and power combiners and dividers.

The final two chapters in this book, Chapter 6 on impedance matching, i.e. matching for maximum power transfer, and Chapter 7 on broadband matching are concerned with the design of impedance matching networks, with managing the bandwidth of these networks, and with describing the performance of microwave circuit elements.

This book is the third volume in a series on microwave and RF design. The first volume in the series addresses radio systems [1] mainly following the evolution of cellular radio. A central aspect of microwave engineering is distributed effects considered in the second volume of his book series [2]. Here the transmission lines are treated as supporting forward- and backward-traveling voltage and current waves and these are related to electromagnetic effects. The fourth volume [3] focuses on designing microwave circuits and systems using modules introducing a large number of different modules. Modules is just another term for a network but the implication is that is is packaged and often available off-the-shelf. Other topics in this chapter that are important in system design using modules are considered including metrics for describing noise, distortion, and dynamic range. Most microwave and RF designers construct systems using modules developed by other engineers who specialize in developing the modules. Examples are filter and amplifier chip modules which once designed can be used in many different systems. Much of microwave design is about maximizing dynamic range, minimizing noise, and minimizing DC power consumption. The fifth volume in this series [4] considers amplifier and oscillator design and develops the skills required to develop modules.

The books in the Microwave and RF Design series are:

- Microwave and RF Design: Radio Systems
- Microwave and RF Design: Transmission Lines
- Microwave and RF Design: Networks
- Microwave and RF Design: Modules
- Microwave and RF Design: Amplifiers and Oscillators

1.3 References

[1] M. Steer, *Microwave and RF Design, Radio Systems*, 3rd ed. North Carolina State University, 2019.

[2] ——, *Microwave and RF Design, Transmission Lines*, 3rd ed. North Carolina State University, 2019.

[3] ——, *Microwave and RF Design, Modules*, 3rd ed. North Carolina State University, 2019.

[4] ——, *Microwave and RF Design, Amplifiers and Oscillators*, 3rd ed. North Carolina State University, 2019.

CHAPTER 2

Microwave Network Analysis

2.1 Introduction

Analog circuits at frequencies up to a few tens of megahertz are characterized by admittances, impedances, voltages, and currents. Above these frequencies it is not possible to measure voltage, current, or impedance directly. One reason for this is that measurement equipment is separated from the device by lengths of transmission line that are electrically long (i.e., at least an appreciable fraction of a wavelength long). It is better to use quantities such as voltage reflection and transmission coefficients that can be quite readily measured and are related to power flow. As well, in RF and microwave circuit design the power of signals and of noise is always of interest. Thus there is a predisposition to focus on measurement parameters that are related to the reflection and transmission of power.

Scattering parameters, S parameters, embody the effects of reflection and transmission. As will be seen, it is easy to convert these to more familiar network parameters such as admittance and impedance parameters. In this chapter S parameters will be defined and related to impedance and admittance parameters, then it will be demonstrated that the use of S parameters helps in the design and interpretation of RF circuits. S parameters have become the most important parameters for RF and microwave engineers and many design methodologies have been developed around them.

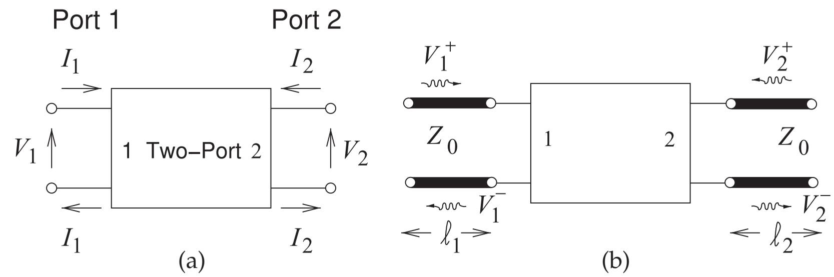

Figure 2-1: A two-port network: (a) port voltages; and (b) with transmission lines at the ports.

This chapter presents microwave circuit theory which is based on the representation of distributed structures that are too large to be considered to be dimensionless, by lumped element circuits. The origins of microwave circuit theory were in the 1940s, 1950s and 1960s [1–3] with extensions for networks with lossy transmission lines [4, 5].

2.2 Two-Port Networks

Many of the techniques employed in analyzing circuits require that the voltage at each terminal of a circuit be referenced to a common point such as ground. In microwave circuits it is generally difficult to do this. Recall that with transmission lines it is not possible to establish a common ground point. However, with transmission lines (and circuit elements that utilize distributed effects) it was seen that for each signal current there is a signal return current. Thus at radio frequencies, and for circuits that are distributed, ports are used, as shown in Figure 2-1(a), which define the voltages and currents for what is known as a two-port network, or just two-port.[1] The network in Figure 2-1(a) has four terminals and two ports. A port voltage is defined as the voltage difference between a pair of terminals with one of the terminals in the pair becoming the reference terminal. The current entering the network at the top terminal of Port 1 is I_1 and there is an equal current leaving the reference terminal. This arrangement clearly makes sense when transmission lines are attached to Ports 1 and 2, as in Figure 2-1(b). With transmission lines at Ports 1 and 2 there will be traveling-wave voltages, and at the ports the traveling-wave components add to give the total port voltage. In dealing with nondistributed circuits it is preferable to use the total port voltages and currents—V_1, I_1, V_2, and I_2, shown in Figure 2-1(a). However, with distributed elements it is preferable to deal with traveling voltages and currents—V_1^+, V_1^-, V_2^+, and V_2^-, shown in Figure 2-1(b). RF and microwave design necessarily requires switching between the two forms.

2.2.1 Reciprocity, Symmetry, Passivity, and Linearity

Reciprocity, symmetry, passivity, and linearity are fundamental properties of networks. A network is linear if the response (voltages and currents) is linearly dependent on the drive level, and superposition also applies. So if the two-port shown in Figure 2-1(a) is linear, the currents I_1 and I_2 are linear functions of V_1 and V_2. An example of a linear network would be one with resistors and capacitors. A network with a diode would be an example of a nonlinear network.

[1] Even when the term "two-port" is used on its own, the hyphen is used, as it is referring to a two-port network.

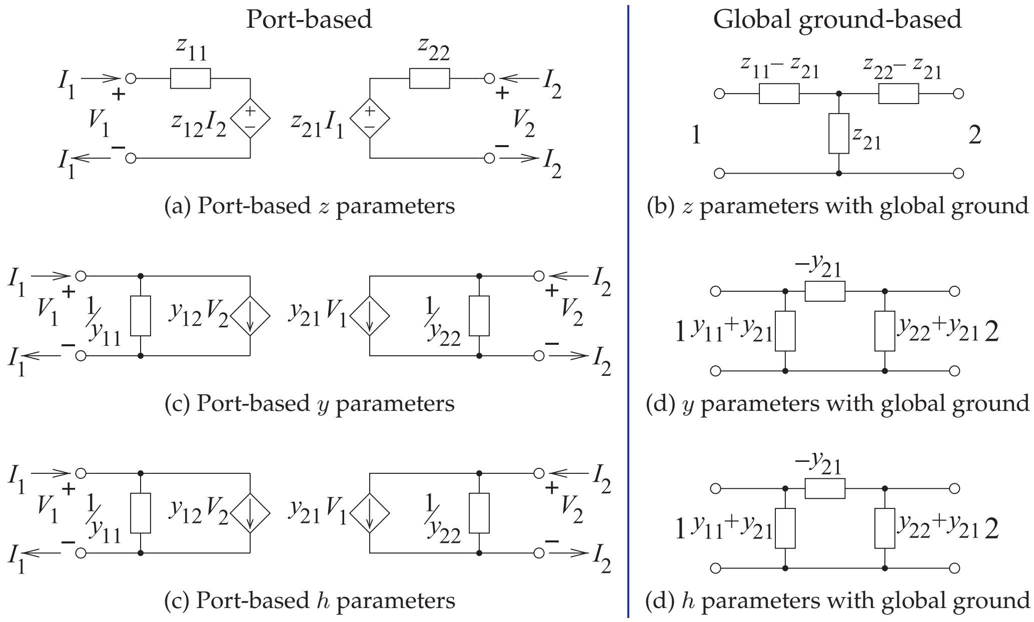

Figure 2-2: The z-, y-, and h- parameter equivalent circuits for port-based and global ground representations. The immittances are shown as impedances.

A passive network has no internal sources of power and so a network with an embedded battery is not a passive network. A symmetrical two-port has the same characteristics at each of the ports. An example of a symmetrical network is a transmission line with a uniform cross section.

A reciprocal two-port has a response at Port 2 from an excitation at Port 1 that is the same as the response at Port 1 to the same excitation at Port 2. As an example, consider the two-port in Figure 2-1(a) with $V_2 = 0$. If the network is reciprocal, then the ratio I_2/V_1 with $V_2 = 0$ will be the same as the ratio I_1/V_2 with $V_1 = 0$. Most networks with resistors, capacitors, and transmission lines, for example, are reciprocal. A transistor amplifier is not reciprocal, as gain, analogous to the ratio V_2/V_1, is in just one direction (or unidirectional).

2.2.2 Parameters Based on Total Voltage and Current

Here port-based impedance (z), admittance (y), and hybrid (h) parameters will be described. These are similar to the more conventional z, y, and h parameters defined with respect to a common or global ground. The contrasting circuit representations of the parameters are shown in Figure 2-2.

Impedance parameters

First, port-based impedance parameters will be considered based on total port voltages and currents as defined for the two-port in Figure 2-1. These parameters are also referred to as port impedance parameters or just impedance parameters when the context is understood to be ports.

Port-based impedance parameters, or z parameters, are defined as

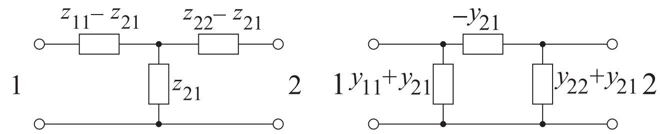

(a) z parameters (b) y parameters

Figure 2-3: Circuit equivalence of the z and y parameters for a reciprocal network (in (b) the elements are admittances).

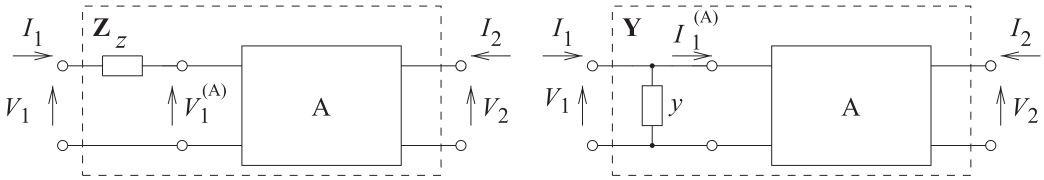

(a) Series connection (b) Parallel or shunt connection

Figure 2-4: Connection of a two-terminal element to a two-port.

$$V_1 = z_{11}I_1 + z_{12}I_2 \qquad (2.1) \qquad\qquad V_2 = z_{21}I_1 + z_{22}I_2, \qquad (2.2)$$

or in matrix form as $\mathbf{V} = \mathbf{ZI}$. (2.3)

The double subscript on a parameter is ordered so that the first refers to the output and the second refers to the input, so z_{ij} relates the voltage output at Port i to the current input at Port j. If the network is reciprocal, then $z_{12} = z_{21}$, but this simple type of relationship does not apply to all network parameters. The reciprocal circuit equivalence of the z parameters is shown in Figure 2-3(a). It will be seen that the z parameters are convenient parameters to use when an element is in series with one of the ports, as then the operation required in developing the z parameters of the larger network is just addition.

Figure 2-4(a) shows the series connection of a two-terminal element with a two-port designated as network A. The z parameters of network A are

$$\mathbf{Z}_A = \begin{bmatrix} z_{11}^{(A)} & z_{12}^{(A)} \\ z_{21}^{(A)} & z_{22}^{(A)} \end{bmatrix}, \qquad (2.4)$$

so that $V_1^{(A)} = z_{11}^{(A)}I_1 + z_{12}^{(A)}I_2$ (2.5) $\qquad V_2 = z_{21}^{(A)}I_1 + z_{22}^{(A)}I_2.$ (2.6)

Now $\qquad V_1 = zI_1 + V_1^{(A)} = zI_1 + z_{11}^{(A)}I_1 + z_{12}^{(A)}I_2,$ (2.7)

so the z parameters of the whole network can be written as

$$\mathbf{Z} = \begin{bmatrix} z & 0 \\ 0 & 0 \end{bmatrix} + \mathbf{Z}_A. \qquad (2.8)$$

EXAMPLE 2.1 Thevenin equivalent of a source with a two-port

What is the Thevenin equivalent circuit of the source-terminated two-port network on the right.

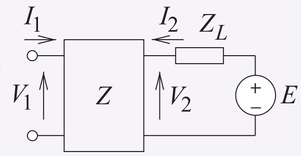

Original circuit

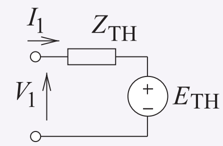

Thevenin equivalent

Solution:

From the original circuit

$$V_1 = Z_{11} I_1 + Z_{12} I_2 \tag{2.9}$$

$$V_2 = Z_{21} I_1 + Z_{22} I_2 \tag{2.10}$$

$$V_2 = E - I_2 Z_L \tag{2.11}$$

Substituting Equation (2.11) in Equation (2.10)

$$E = Z_{21} I_1 + (Z_{22} + Z_L) I_2 \tag{2.12}$$

Multiplying Equation (2.9) by $(Z_{22} + Z_L)$ and Equation (2.12) by Z_{12}

$$(Z_{22} + Z_L)V_1 = (Z_{22} + Z_L)Z_{11} I_1 + (Z_{22} + Z_L)Z_{12} I_2 \tag{2.13}$$

$$Z_{12}E = Z_{12} Z_{21} I_1 + Z_{12}(Z_{22} + Z_L) I_2 \tag{2.14}$$

Subtracting Equation (2.14) from Equation (2.13)

$$(Z_{22} + Z_L)V_1 - Z_{12}E = [(Z_{22} + Z_L)Z_{11} -] I_1$$

$$V_1 = \frac{Z_{12}E}{Z_{22} + Z_L} + \left(Z_{11} - \frac{Z_{12} Z_{21}}{Z_{22} + Z_L} \right) I_1 \tag{2.15}$$

For the Thevenin equivalent circuit $V_1 = E_{\mathrm{TH}} + I_1 Z_{\mathrm{TH}}$ and so

$$Z_{\mathrm{TH}} = \left(Z_{11} - \frac{Z_{12} Z_{21}}{Z_{22} + Z_L} \right) \quad \text{and} \quad E_{\mathrm{TH}} = \frac{Z_{12}E}{Z_{22} + Z_L} \tag{2.16}$$

Admittance parameters

When an element is in shunt with a two-port, port-based admittance parameters, or y parameters, are the most convenient to use. These are defined as

$$I_1 = y_{11} V_1 + y_{12} V_2 \tag{2.17}$$

$$I_2 = y_{21} V_1 + y_{22} V_2, \tag{2.18}$$

or in matrix form as

$$\mathbf{I} = \mathbf{YV}. \tag{2.19}$$

Now, for reciprocity, $y_{12} = y_{21}$ and the circuit equivalence of the y parameters is shown in Figure 2-3(b). Consider the shunt connection of an element shown in Figure 2-4(b) where the y parameters of network A are

$$\mathbf{Y}_A = \begin{bmatrix} y_{11}^{(A)} & y_{12}^{(A)} \\ y_{21}^{(A)} & y_{22}^{(A)} \end{bmatrix} = \mathbf{Z}_A^{-1}. \tag{2.20}$$

The port voltages and currents are related as follows

$$I_1^{(A)} = y_{11}^{(A)} V_1 + y_{12}^{(A)} V_2 \quad \text{and} \quad I_2 = y_{21}^{(A)} V_1 + y_{22}^{(A)} V_2 \tag{2.21}$$

$$I_1 = y V_1 + I_1^{(A)} = (y + y_{11}^{(A)}) V_1 + y_{12}^{(A)} V_2. \tag{2.22}$$

Thus the y parameters of the whole network are

$$\mathbf{Y} = \begin{bmatrix} y & 0 \\ 0 & 0 \end{bmatrix} + \mathbf{Y}_A. \tag{2.23}$$

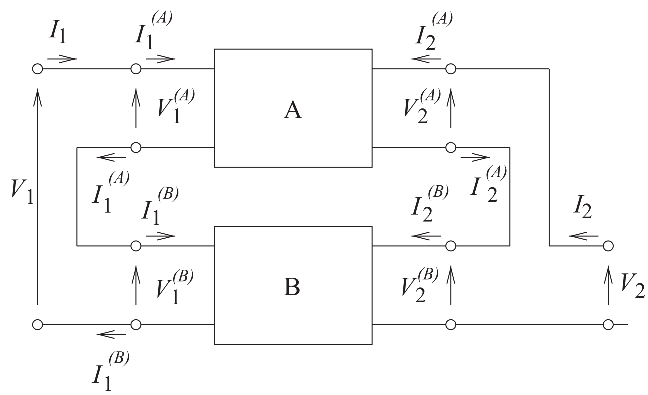

Figure 2-5: Series connection of two two-port networks.

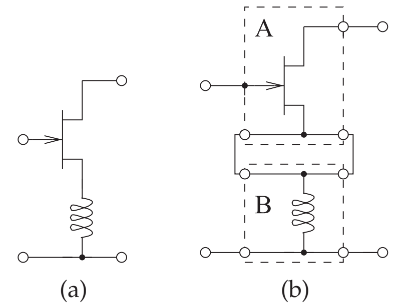

Figure 2-6: Example of a series connection of two-port networks: (a) an amplifier; and (b) its components represented as two-port networks.

Hybrid parameters

Sometimes it is more convenient to use hybrid parameters, or h parameters, defined by

$$V_1 = h_{11}I_1 + h_{12}V_2 \qquad \text{and} \qquad I_2 = h_{21}I_1 + h_{22}V_2, \tag{2.24}$$

or in matrix form as

$$\begin{bmatrix} V_1 \\ I_2 \end{bmatrix} = \mathbf{H} \begin{bmatrix} I_1 \\ V_2 \end{bmatrix}. \tag{2.25}$$

These parameters are convenient to use with transistor circuits, as they describe a voltage-controlled current source that is a simple model of a transistor.

The choice of which network parameters to use depends on convenience, but as will be seen throughout this text, some parameters naturally describe a particular characteristic desired in a design. For example, with Port 1 being the input port of an amplifier and Port 2 being the output port, h_{21} describes the current gain of the amplifier.

2.2.3 Series Connection of Two-Port Networks

A series connection of two two-ports is shown in Figure 2-5. An example of when the series connection occurs is shown in Figure 2-6, which is the schematic of a transistor amplifier configuration with an inductor in the source leg. The transistor and the inductor can each be represented as two-ports so that the circuit of Figure 2-6(a) is the series connection of two two-ports, as shown in Figure 2-6(b). In the following, two-port parameters of the complete circuit are developed using the two-port parameter descriptions of the component two-ports. The procedure with any interconnection is to write down the relationships between the voltages and currents of the constituent networks. Which network parameters to use requires identification of the arithmetic path requiring the fewest operations.

Simple algebra relates the various total voltage and current parameters. From Figure 2-5,

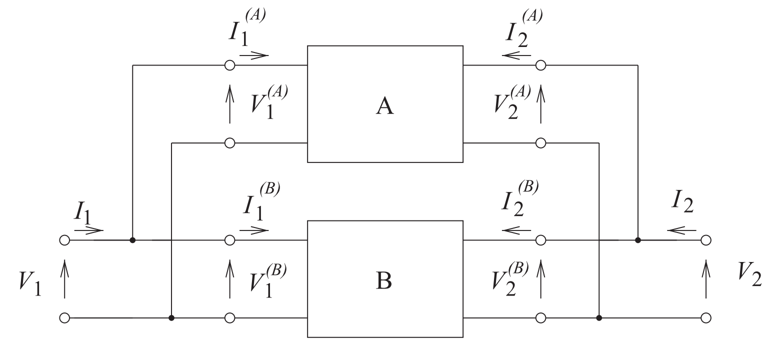

Figure 2-7: Parallel connection of two-port networks.

$$I_1^{(A)} = I_1^{(B)} = I_1, \;\; I_2^{(A)} = I_2^{(B)} = I_2, \;\; V_1 = V_1^{(A)} + V_1^{(B)}, \;\; V_2 = V_2^{(A)} + V_2^{(B)},$$

which in matrix form becomes

$$\begin{bmatrix} V_1^{(A)} \\ V_2^{(A)} \end{bmatrix} = \begin{bmatrix} z_{11}^{(A)} & z_{12}^{(A)} \\ z_{21}^{(A)} & z_{22}^{(A)} \end{bmatrix} \begin{bmatrix} I_1^{(A)} \\ I_2^{(A)} \end{bmatrix}; \begin{bmatrix} V_1^{(B)} \\ V_2^{(B)} \end{bmatrix} = \begin{bmatrix} z_{11}^{(B)} & z_{12}^{(B)} \\ z_{21}^{(B)} & z_{22}^{(B)} \end{bmatrix} \begin{bmatrix} I_1^{(B)} \\ I_2^{(B)} \end{bmatrix} \tag{2.26}$$

or

$$\begin{bmatrix} V_1 \\ V_2 \end{bmatrix} = (\mathbf{Z}^A + \mathbf{Z}^B) \begin{bmatrix} I_1 \\ I_2 \end{bmatrix}. \tag{2.27}$$

Thus the impedance matrix of the series connection of two-ports is

$$\mathbf{Z} = \mathbf{Z_A} + \mathbf{Z_B}. \tag{2.28}$$

2.2.4 Parallel Connection of Two-Port Networks

Admittance parameters are most conveniently combined to obtain the overall parameters of the two-port parallel connection of Figure 2-7. The total voltage and current are related by

$$V_1^{(A)} = V_1^{(B)} = V_1 \tag{2.29}$$

$$V_2^{(A)} = V_2^{(B)} = V_2 \tag{2.30}$$

$$I_1 = I_1^{(A)} + I_1^{(B)} \tag{2.31}$$

$$I_2 = I_2^{(A)} + I_2^{(B)} \tag{2.32}$$

and

$$\begin{bmatrix} I_1^{(A)} \\ I_2^{(A)} \end{bmatrix} = \begin{bmatrix} y_{11}^{(A)} & y_{12}^{(A)} \\ y_{21}^{(A)} & y_{22}^{(A)} \end{bmatrix} \begin{bmatrix} V_1^{(A)} \\ V_2^{(A)} \end{bmatrix} \tag{2.33}$$

$$\begin{bmatrix} I_1^{(B)} \\ I_2^{(B)} \end{bmatrix} = \begin{bmatrix} y_{11}^{(B)} & y_{12}^{(B)} \\ y_{21}^{(B)} & y_{22}^{(B)} \end{bmatrix} \begin{bmatrix} V_1^{(B)} \\ V_2^{(B)} \end{bmatrix}. \tag{2.34}$$

So the overall y parameter relation is

$$\begin{bmatrix} I_1 \\ I_2 \end{bmatrix} = (\mathbf{Y}_A + \mathbf{Y}_B) \begin{bmatrix} V_1 \\ V_2 \end{bmatrix}. \tag{2.35}$$

Figure 2-8 is an example of subcircuits that can be represented as two-ports that are then connected in parallel.

2.2.5 Series-Parallel Connection of Two-Port Networks

A similar approach to that in the preceding subsection is followed in developing the overall network parameters of the series-parallel connection of

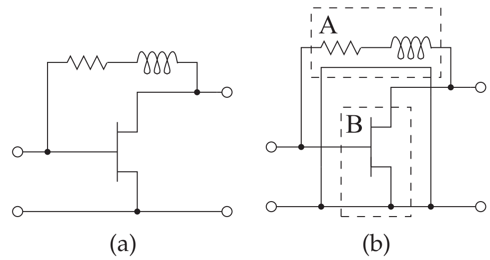

Figure 2-8: Example of the parallel connection of two two-ports: (a) a feedback amplifier; and (b) its components represented as two-port networks A and B.

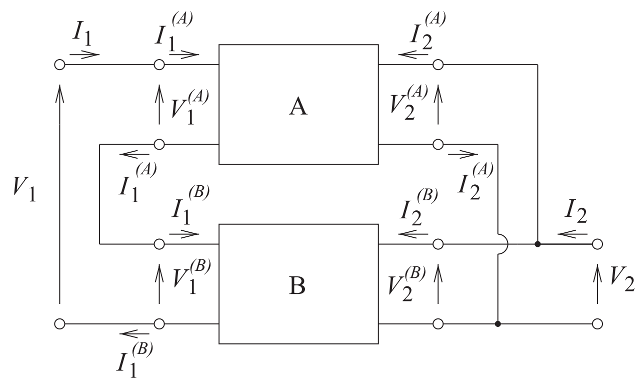

Figure 2-9: Series-parallel connection of two-ports.

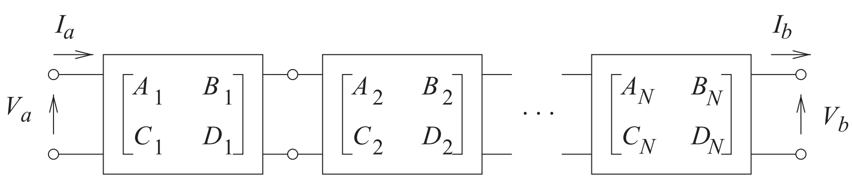

Figure 2-10: Cascade of two-port networks.

two-ports shown in Figure 2-9. Now,

$$I_1^{(A)} = I_1^{(B)} = I_1 \tag{2.36}$$

$$V_2^{(A)} = V_2^{(B)} = V_2 \tag{2.37}$$

$$V_1 = V_1^{(A)} + V_1^{(B)} \tag{2.38}$$

$$I_2 = I_2^{(A)} + I_2^{(B)}, \tag{2.39}$$

and so, using hybrid parameters,

$$\begin{bmatrix} V_1^{(A)} \\ I_2^{(A)} \end{bmatrix} = \begin{bmatrix} h_{11}^{(A)} & h_{12}^{(A)} \\ h_{21}^{(A)} & h_{22}^{(A)} \end{bmatrix} \begin{bmatrix} I_1^{(A)} \\ V_2^{(A)} \end{bmatrix} \tag{2.40}$$

$$\begin{bmatrix} V_1^{(B)} \\ I_2^{(B)} \end{bmatrix} = \begin{bmatrix} h_{11}^{(B)} & h_{12}^{(B)} \\ h_{21}^{(B)} & h_{22}^{(B)} \end{bmatrix} \begin{bmatrix} I_1^{(B)} \\ V_2^{(B)} \end{bmatrix}. \tag{2.41}$$

Putting this in compact form:

$$\begin{bmatrix} V_1 \\ I_2 \end{bmatrix} = (\mathbf{H}_A + \mathbf{H}_B) \begin{bmatrix} I_1 \\ V_2 \end{bmatrix}. \tag{2.42}$$

2.2.6 $ABCD$ Matrix Characterization of Two-Port Networks

$ABCD$ parameters are the best parameters to use when cascading two-ports, as in Figure 2-10, and total voltage and current relationships are required. First, consider Figure 2-11, which puts the voltages and currents

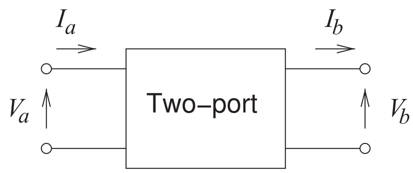

Figure 2-11: Two-port network with cascadable voltage and current definitions.

in cascadable form with the input variables in terms of the output variables:

$$\begin{bmatrix} V_a \\ I_a \end{bmatrix} = \begin{bmatrix} A & B \\ C & D \end{bmatrix} \begin{bmatrix} V_b \\ I_b \end{bmatrix}. \tag{2.43}$$

The reciprocity relationship of the $ABCD$ parameters is not as simple as for the z and y parameters. To see this, first express $ABCD$ parameters in terms of z parameters. Note that the current at Port 2 is in the opposite direction to the usual definition of the two-port current shown in Figure 2-1(a). So

$$V_a = V_1 \tag{2.44}$$
$$I_a = I_1 \tag{2.45}$$
$$V_a = z_{11}I_a - z_{12}I_b \tag{2.46}$$
$$V_b = V_2 \tag{2.47}$$
$$I_b = -I_2 \tag{2.48}$$
$$V_b = z_{21}I_a - z_{22}I_b. \tag{2.49}$$

From Equation (2.49),
$$I_a = \frac{z_{22}}{z_{21}}I_b + \frac{1}{z_{21}}V_b, \tag{2.50}$$

and substituting this into Equation (2.46) yields

$$V_a = \frac{z_{11}}{z_{21}}V_b + \left(z_{11}\frac{z_{22}}{z_{21}} - z_{12}\right) I_b. \tag{2.51}$$

Comparing Equations (2.50) and (2.51) to Equation (2.43) leads to

$$\begin{array}{ll} A = z_{11}/z_{21} & B = \Delta_z/z_{21} \\ C = 1/z_{21} & D = z_{22}/z_{21}, \end{array} \tag{2.52}$$

where
$$\Delta_z = z_{11}z_{22} - z_{12}z_{21}. \tag{2.53}$$

Rearranging,

$$\begin{array}{ll} z_{11} = A/C & z_{12} = (AD - BC)/C \\ z_{21} = 1/C & z_{22} = D/C. \end{array} \tag{2.54}$$

Now the reciprocity condition in terms of $ABCD$ parameters can be determined. For z parameters, $z_{12} = z_{21}$ for reciprocity; that is, from Equation (2.54), for a reciprocal network,

$$\frac{AD - BC}{C} = \frac{1}{C} \quad \text{and} \quad AD - BC = 1. \tag{2.55}$$

Thus for a two-port network to be reciprocal, $AD - BC = 1$. The utility of these parameters is that the $ABCD$ matrix of the cascade connection of N two-ports in Figure 2-10 is equal to the product of the $ABCD$ matrices of the individual two-ports:

$$\begin{bmatrix} A & B \\ C & D \end{bmatrix} = \begin{bmatrix} A_1 & B_1 \\ C_1 & D_1 \end{bmatrix} \begin{bmatrix} A_2 & B_2 \\ C_2 & D_2 \end{bmatrix} \cdots \begin{bmatrix} A_N & B_N \\ C_N & D_N \end{bmatrix}. \tag{2.56}$$

See Table 2-1 for the $ABCD$ parameters of several two-port networks.

Table 2-1: $ABCD$ parameters of several two-ports. The transmission line is lossless with a propagation constant of β. ($\beta\ell$ and θ are electrical lengths of transmission lines in radians.)

Series impedance, z 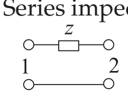 $A = 1 \quad B = z$ $C = 0 \quad D = 1$	Shunt admittance, y 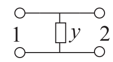 $A = 1 \quad B = 0$ $C = y \quad D = 1$
Transmission line, length ℓ, $Z_0 = 1/Y_0$ 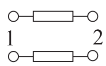 $A = \cos(\beta\ell) \quad B = \jmath Z_0 \sin(\beta\ell)$ $C = \jmath Y_0 \sin(\beta\ell) \quad D = \cos(\beta\ell)$	Transformer, ratio n:1 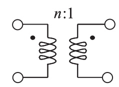 $A = n \quad B = 0$ $C = 0 \quad D = 1/n$
Pi network 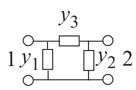 $A = 1 + y_2/y_3 \quad B = 1/y_3$ $C = y_1 + y_2 + y_1 y_2/y_3$ $D = 1 + y_1/y_3$	Tee network 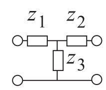 $A = 1 + z_1/z_3$ $B = z_1 + z_2 + z_1 z_2/z_3$ $C = 1/z_3 \quad D = 1 + z_2/z_3$
Series shorted stub, electrical length θ 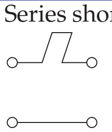 $A = 1 \quad B = \jmath Z_0 \tan\theta$ $C = 0 \quad D = 1$	Series open stub, electrical length θ 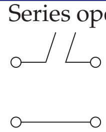 $A = 1 \quad B = -\jmath Z_0/(\tan\theta)$ $C = 0 \quad D = 1$
Shunt shorted stub, electrical length θ 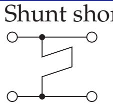 $A = 1 \quad B = 0$ $C = -\jmath/(Z_0 \tan\theta) \quad D = 1$	Shunt open stub, electrical length θ 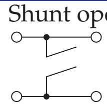 $A = 1 \quad B = 0$ $C = \jmath \tan\theta/Z_0 \quad D = 1$

2.3 Scattering Parameters

Direct measurement of the z, y, h, and $ABCD$ parameters requires that the ports be terminated in either short or open circuits. For active circuits, such terminations could result in undesired behavior, including oscillation or destruction. Also, at RF it is difficult to realize a good open or short. Since RF circuits are designed with close attention to maximum power transfer conditions, resistive terminations are preferred, as these are closer to the actual operating conditions. Thus the effect of measurement errors will have less impact than when parameter extraction relies on imperfect opens and shorts. The essence of scattering parameters (or S parameters[2]) is that they relate forward- and backward-traveling waves on a transmission line, thus S parameters are related to power flow.

The discussion of S parameters begins by considering the reflection coefficient, which is the S parameter of a one-port network.

2.3.1 Reflection Coefficient

The reflection coefficient, Γ, of a load, as in Figure 2-12, can be determined by separately measuring the forward- and backward-traveling voltages on the transmission line:

$$\Gamma(x) = \frac{V^-(x)}{V^+(x)}. \tag{2.57}$$

[2] For historical reasons a capital "S" is used when referring to S parameters. For most other network parameters, lowercase is used (e.g., z parameters for impedance parameters).

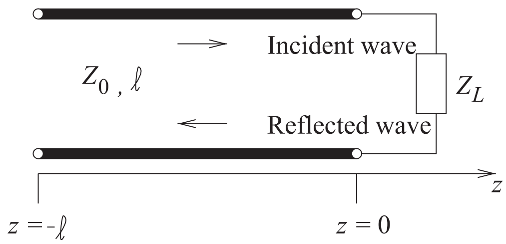

Figure 2-12: Transmission line of characteristic impedance Z_0 and length ℓ terminated in a load of impedance Z_L.

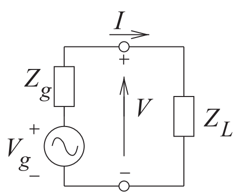

Figure 2-13: A Thevenin equivalent source with generator V_g and source impedance Z_g terminated in a load Z_L.

Γ at the load is related to the impedance Z_L by

$$\Gamma(0) = \frac{Z_L - Z_0}{Z_L + Z_0}, \tag{2.58}$$

where Z_0 is the characteristic impedance of the connecting transmission line. This can also be written as

$$\Gamma(0) = \frac{Y_0 - Y_L}{Y_0 + Y_L}, \tag{2.59}$$

where $Y_0 = 1/Z_0$ and $Y_L = 1/Z_L$.

2.3.2 Reflection Coefficient with Complex Reference Impedance

Here the reflection coefficient of Z_L in Figure 2-13 will be developed with respect to the complex reference impedance Z_g.The total voltage and current at the load are

$$V = V_g \frac{Z_L}{Z_g + Z_L} \quad (2.60) \qquad \text{and} \qquad I = \frac{V_g}{Z_g + Z_L}. \quad (2.61)$$

To develop the reflection coefficient, first define equivalent forward- and backward-traveling waves. This can be done by imagining that between the generator and the load there is a transmission line of characteristic impedance Z_g which has infinitesimal length. The incident voltage and current waves (V^+, I^+) are the total voltage and current obtained when the generator is conjugately matched to the load (i.e., $Z_L = Z_g^*$). So the equations of forward-traveling voltage and current become[3]

$$V^+ = V_g \frac{Z_g^*}{Z_g + Z_g^*} = V_g Z_g^* 2\mathcal{R}\{Z_g\} \quad (2.62) \qquad I^+ = V_g \frac{1}{2\mathcal{R}\{Z_g\}}\,. \quad (2.63)$$

Now return to considering the actual load, Z_L. The reflected voltage and current (V^-, I^-) are obtained by calculating the actual voltage and current at the source using the relationships

$$V = V^+ + V^- \quad (2.64) \qquad I = I^+ + I^- \quad (2.65)$$

[3] Here $\Re$ is the real operator, which yields the real part of a complex number.

to determine the backward-traveling components. In Equations (2.64) and (2.65) the forward-traveling components are those in Equations (2.62) and (2.63). From Equation (2.62),

$$V_g = V^+ \frac{Z_g + Z_g^*}{Z_g^*}, \tag{2.66}$$

and from Equations (2.60), (2.64), and (2.66),

$$\begin{aligned} V^- = V - V^+ = V_g \frac{Z_L}{Z_g + Z_L} - V^+ &= \left[\frac{Z_g + Z_g^*}{Z_g^*} \frac{Z_L}{Z_g + Z_L} - 1 \right] V^+ \\ &= \left[\frac{Z_g Z_L + Z_g^* Z_L - Z_g^* Z_g - Z_g^* Z_L}{Z_g^*(Z_g + Z_L)} \right] V^+ \\ &= \underbrace{\left(\frac{Z_L - Z_g^*}{Z_L + Z_g} \right) \frac{Z_g}{Z_g^*}}_{\Gamma^V} V^+ = \Gamma^V \, V^+. \end{aligned} \tag{2.67}$$

Similarly $$I^- = -\underbrace{\left(\frac{Z_L - Z_g^*}{Z_L + Z_g} \right) \frac{Z_g}{Z_g^*}}_{\Gamma^I} I^+ = \Gamma^I \, I^+. \tag{2.68}$$

Γ^V is the voltage reflection coefficient, which is usually denoted as just Γ, while Γ^I is the current reflection coefficient. It is clear that $\Gamma^V = 0 = \Gamma^I$ when $Z_L = Z_g^*$ and $\Gamma^V = -\Gamma^I = (Z_L - R_g)/(Z_L + R_g)$ when Z_g is purely resistive (i.e., when $Z_g = R_g$). Generally the reflection coefficients are defined using a purely resistive Z_g. This becomes the reference resistance, which is more commonly referred to as the reference impedance, Z_0, or, if the same reference impedance is used throughout, the system impedance.

2.3.3 Two-Port S Parameters

Two-port S parameters are defined in terms of traveling waves on transmission lines with real characteristic impedance Z_0 attached to each of the ports of the network, see Figure 2-1(b):

$$V_1^- = S_{11} V_1^+ + S_{12} V_2^+ \tag{2.69}$$ $$V_2^- = S_{21} V_1^+ + S_{22} V_2^+, \tag{2.70}$$

where S_{ij} are the individual S parameters. In matrix form the equations above become

$$\begin{bmatrix} V_1^- \\ V_2^- \end{bmatrix} = \begin{bmatrix} S_{11} & S_{12} \\ S_{21} & S_{22} \end{bmatrix} \begin{bmatrix} V_1^+ \\ V_2^+ \end{bmatrix} = \mathbf{S} \begin{bmatrix} V_1^+ \\ V_2^+ \end{bmatrix}. \tag{2.71}$$

Individual S parameters are determined by measuring the forward- and backward-traveling waves with loads $Z_L = Z_0$ at the ports. For the output line the load cannot reflect power and so $V_2^+ = 0$, then

$$S_{11} = \left. \frac{V_1^-}{V_1^+} \right|_{V_2^+ = 0}. \tag{2.72}$$

The remaining three parameters are determined similarly and so S_{22} is found as

$$S_{22} = \left.\frac{V_2^-}{V_2^+}\right|_{V_1^+=0} \tag{2.73}$$

and the transmission parameter as

$$S_{21} = \left.\frac{V_2^-}{V_1^+}\right|_{V_2^+=0}. \tag{2.74}$$

S_{21} is also called the transmission coefficient, T. In the reverse direction,

$$S_{12} = \left.\frac{V_1^-}{V_2^+}\right|_{V_1^+=0}. \tag{2.75}$$

In the above Z_0 is referred to as the **normalization impedance** or equivalently the **reference impedance**. In some circumstances $Z_{\rm REF}$ is used to denote reference impedance to avoid possible confusion with a transmission line impedance that is not the same as the reference impedance. The S parameters here are also called normalized S parameters, and the S parameters are normalized to the same reference impedance at each port. Calling them **normalized S parameters** also carrys the additional meaning that the S parameters are referenced to the one real impedance.

The relationships between the two-port S parameters and the common network parameters are given in Table 2-2. It is interesting to note that $S_{21}/S_{12} = z_{21}/z_{12} = y_{21}/y_{12} = h_{21}/h_{12}$. That is, the ratio of the forward to reverse parameters (at least for S, z, y, and h parameters) are the same and this ratio is one for a reciprocal device. An S parameter is a voltage ratio, so when it is expressed in decibels $S_{ij}|_{\rm dB} = 20\log(S_{ij})$.

A reciprocal network has $S_{12} = S_{21}$. If unit power flows into a two-port (with ports terminated in the reference impedance), a fraction, $|S_{11}|^2$, is reflected and a further fraction, $|S_{21}|^2$, is transmitted through the network.

EXAMPLE 2.2 Two-Port S Parameters

What are the S parameters of a 30 dB attenuator?

Solution:

An attenuator is shown with a system impedance of Z_0. An ideal attenuator has no reflection at each of the two ports when the attenuator is embedded in its system impedance. Thus $\Gamma_{\rm in} = 0 = \Gamma_{\rm out}$. Since there is no reflection from the load or the source, this implies that $S_{11} = 0 = S_{22}$.

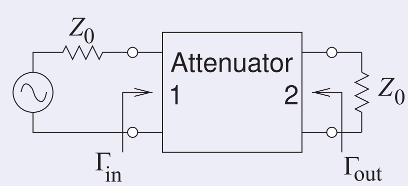

Since this is a 30 dB attenuator, the power delivered to the load impedance Z_0 is 30 dB below the power available from the source, thus $S_{21} = -30$ dB $= 0.0316$. The attenuator is reciprocal and so $S_{12} = S_{21}$. Thus the S parameters of the attenuator are

$$\mathbf{S} = \begin{bmatrix} 0 & 0.0316 \\ 0.0316 & 0 \end{bmatrix}. \tag{2.76}$$

Note that the reference impedance did not need to be known to develop the S parameters.

Table 2-2: Two-port S parameter conversion chart. The z, y, and h parameters are normalized to Z_0. Z', Y', and H' are the actual parameters. For $ABCD$ parameter conversion see Section 2.7.2.

	S	In terms of S
z	$Z'_{11} = z_{11}Z_0 \quad Z'_{12} = z_{12}Z_0$	$Z'_{21} = z_{21}Z_0 \quad Z'_{22} = z_{22}Z_0$
	$\delta_z = (1 + z_{11})(1 + z_{22}) - z_{12}z_{21}$	$\delta_S = (1 - S_{11})(1 - S_{22}) - S_{12}S_{21}$
	$S_{11} = [(z_{11} - 1)(z_{22} + 1) - z_{12}z_{21}]/\delta_z$	$z_{11} = [(1 + S_{11})(1 - S_{22}) + S_{12}S_{21}]/\delta_S$
	$S_{12} = 2z_{12}/\delta_z$	$z_{12} = 2S_{12}/\delta_S$
	$S_{21} = 2z_{21}/\delta_z$	$z_{21} = 2S_{21}/\delta_S$
	$S_{22} = [(z_{11} + 1)(z_{22} - 1) - z_{12}z_{21}]/\delta_z$	$z_{22} = [(1 - S_{11})(1 + S_{22}) + S_{12}S_{21}]/\delta_S$
y	$Y'_{11} = y_{11}/Z_0 \quad Y'_{12} = y_{12}/Z_0$	$Y'_{21} = y_{21}/Z_0 \quad Y'_{22} = y_{22}/Z_0$
	$\delta_y = (1 + y_{11})(1 + y_{22}) - y_{12}y_{21}$	$\delta_S = (1 + S_{11})(1 + S_{22}) - S_{12}S_{21}$
	$S_{11} = [(1 - y_{11})(1 + y_{22}) + y_{12}y_{21}]/\delta_y$	$y_{11} = [(1 - S_{11})(1 + S_{22}) + S_{12}S_{21}]/\delta_S$
	$S_{12} = -2y_{12}/\delta_y$	$y_{12} = -2S_{12}/\delta_S$
	$S_{21} = -2y_{21}/\delta_y$	$y_{21} = -2S_{21}/\delta_S$
	$S_{22} = [(1 + y_{11})(1 - y_{22}) + y_{12}y_{21}]/\delta_y$	$y_{22} = [(1 + S_{11})(1 - S_{22}) + S_{12}S_{21}]/\delta_S$
h	$H'_{11} = h_{11}Z_0 \quad H'_{12} = h_{12}$	$H'_{21} = h_{21} \quad H'_{22} = h_{22}/Z_0$
	$\delta_h = (1 + h_{11})(1 + h_{22}) - h_{12}h_{21}$	$\delta_S = (1 - S_{11})(1 + S_{22}) + S_{12}S_{21}$
	$S_{11} = [(h_{11} - 1)(h_{22} + 1) - h_{12}h_{21}]/\delta_h$	$h_{11} = [(1 + S_{11})(1 + S_{22}) - S_{12}S_{21}]/\delta_S$
	$S_{12} = 2h_{12}/\delta_h$	$h_{12} = 2S_{12}/\delta_S$
	$S_{21} = -2h_{21}/\delta_h$	$h_{21} = -2S_{21}/\delta_S$
	$S_{22} = [(1 + h_{11})(1 - h_{22}) + h_{12}h_{21}]/\delta_h$	$h_{22} = [(1 - S_{11})(1 - S_{22}) - S_{12}S_{21}]/\delta_S$

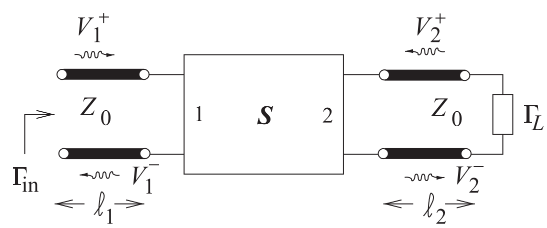

Figure 2-14: A terminated two-port network with transmission lines of infinitesimal length at the ports.

2.3.4 Input Reflection Coefficient of a Terminated Two-Port Network

A two-port is shown in Figure 2-14 that is terminated at Port 2 in a load with a reflection coefficient Γ_L. The lines at each of the ports are of infinitesimal length (i.e., $\ell_1 \to 0$ and $\ell_2 \to 0$) and are used to make it easier to visualize the separation of the voltage into forward- and backward-traveling components. The aim in this section is to develop a formula for the input reflection coefficient $\Gamma_{\text{in}} = V_1^-/V_1^+$. For the circuit in Figure 2-14 three equations can be developed:

$$V_1^- = S_{11}V_1^+ + S_{12}V_2^+ \tag{2.77}$$

$$V_2^- = S_{21}V_1^+ + S_{22}V_2^+ \tag{2.78}$$

$$V_2^+ = \Gamma_L V_2^-, \quad \text{i.e.,} \quad V_2^- = V_2^+/\Gamma_L. \tag{2.79}$$

Note that V_2^- is the voltage wave that leaves the two-port but is incident on the load Γ_L. The aim here is to eliminate V_2^+ and V_2^-. Substituting Equation

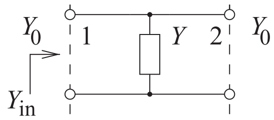

Figure 2-15: Shunt element in the form of a two-port.

(2.79) into Equation (2.78) leads to

$$V_2^+/\Gamma_L = S_{21}V_1^+ + S_{22}V_2^+ \tag{2.80}$$

$$V_2^+\left(\frac{1 - S_{22}\Gamma_L}{\Gamma_L}\right) = S_{21}V_1^+ \tag{2.81}$$

$$V_2^+ = \left(\frac{S_{21}\Gamma_L}{1 - S_{22}\Gamma_L}\right)V_1^+. \tag{2.82}$$

Now substituting Equation (2.82) in Equation (2.77) yields

$$V_1^- = S_{11}V_1^+ + S_{12}\left(\frac{S_{21}\Gamma_L}{1 - S_{22}\Gamma_L}\right)V_1^+ \tag{2.83}$$

and so

$$\Gamma_{\text{in}} = S_{11} + \frac{S_{12}S_{21}\Gamma_L}{1 - S_{22}\Gamma_L}. \tag{2.84}$$

2.3.5 Evaluation of the Scattering Parameters of an Element

Scattering parameters can be derived analytically for various circuit configurations and in this section the procedure is illustrated for the shunt element of Figure 2-15. The procedure to find S_{11} is to match Port 2 so that $V_2^+ = 0$, then S_{11} is the reflection coefficient at Port 1:

$$S_{11} = \frac{Y_0 - Y_{\text{in}}}{Y_0 + Y_{\text{in}}}, \tag{2.85}$$

where $Y_{\text{in}} = Y_0 + Y$, since the matched termination at Port 2 (i.e., $Y_0 = 1/Z_0$) shunts the admittance Y. Thus

$$S_{11} = \frac{Y_0 - Y_0 - Y}{2Y_0 + Y} = \frac{-Y}{2Y_0 + Y}. \tag{2.86}$$

From the symmetry of the two-port,

$$S_{22} = S_{11}. \tag{2.87}$$

S_{21} is evaluated by determining the transmitted wave, V_2^-, with the output line matched so that again an admittance, Y_0, is placed at Port 2 and $V_2^+ = 0$. After some algebraic manipulation,

$$S_{21} = 2Y_0/(Y + 2Y_0) \tag{2.88}$$

is obtained. Since this is clearly a reciprocal network, $S_{12} = S_{21}$ and all four S parameters are obtained. A similar procedure of selectively applying matched loads is used to obtain the S parameters of other networks.

EXAMPLE 2.3 Calculation of the *S* Parameters of a Two-Port Network

Derive the two-port 50 Ω S parameters of the resistive circuit to the right.

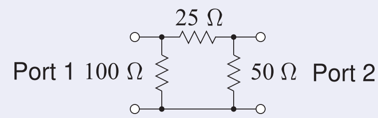

Solution:

Calculation of S_{11}. This involves terminating Port 2 in the system reference impedance, 50 Ω, and then calculating the input impedance of the augmented network. This is then converted to a reflection coefficient, which here is S_{11}. The circuit for calculation is to the right. Now

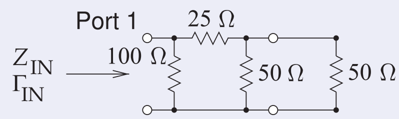

$$Z_{\text{IN}} = 100 \parallel [25 \, \$ \, (50 \parallel 50)] \; \Omega = 100 \parallel 50 \; \Omega = 33.33 \; \Omega, \tag{2.89}$$

where $\parallel$ indicates the parallel-connection calculation and \$ indicates the series-connection calculation. Thus

$$S_{11} = \Gamma_{\text{IN}} = \frac{Z_{\text{IN}} - Z_0}{Z_{\text{IN}} + Z_0} = \frac{33.33 - 50}{33.33 + 50} = -0.2. \tag{2.90}$$

Calculation of S_{21}. This involves terminating Port 2 in the system reference impedance, 50 Ω, and then calculating the forward-traveling voltage wave at Port 1 and the reverse-traveling voltage wave at Port 2. Note that the reverse-traveling voltage wave at Port 2 is leaving the two-port.

Since there is no wave reflected from the termination at Port 2, the total voltage at Port 2 is just V_2^-. The circuit for calculation is on the right.

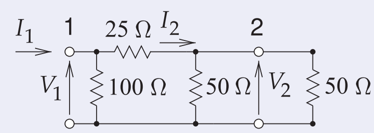

$$V_1 = V_1^+ + V_1^- = V_1^+ (1 + S_{11}) \rightarrow V_1^+ = \frac{V_1}{1 + S_{11}} = 1.25 V_1. \tag{2.91}$$

The voltage at Port 1 is

$$V_1 = I_1 Z_{\text{IN}} = 33.33 I_1 \rightarrow V_1^+ = 1.25 \cdot 33.33 I_1 = 41.66 I_1. \tag{2.92}$$

The next step is to find an expression for I_2:

$$V_1 = I_1 Z_{\text{IN}} = 33.33 I_1 = I_2 (25 \, \$ \, 50 \parallel 50) = 50 I_2. \tag{2.93}$$

Rearranging,

$$I_2 = I_1 \frac{33.33}{50} = 0.6667 I_1. \tag{2.94}$$

Now

$$V_2^- = V_2 = I_2 (50 \parallel 50) = 25 I_2 = 16.67 I_1. \tag{2.95}$$

So

$$S_{21} = \frac{V_2^-}{V_1^+} = \frac{16.67}{41.66} = 0.4. \tag{2.96}$$

Calculation of S_{12}. The two-port is a reciprocal network (as are all networks with only lumped R, L, and C elements) and so $S_{12} = S_{21}$.

Calculation of S_{22}. Using a similar procedure to that used for finding S_{11}, the circuit for the calculation is on the right:

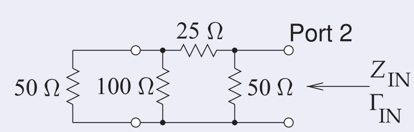

$$Z_{\rm IN} = 50 \parallel [25 \,\$\, (100 \parallel 50)]\ \Omega = 50 \parallel (25\$33.33) = 50 \parallel 58.33 = 26.92\ \Omega. \tag{2.97}$$

Therefore

$$S_{22} = \Gamma_{\rm IN} = \frac{26.92 - 50}{26.92 + 50} = -0.3. \tag{2.98}$$

Collecting the individual S parameters:

$$\mathbf{S} = \begin{bmatrix} -0.2 & 0.4 \\ 0.4 & -0.3 \end{bmatrix}. \tag{2.99}$$

2.3.6 Properties of a Two-Port in Terms of S Parameters

The properties of most interest are whether the two-port network is lossless, passive, or reciprocal.

If a network is lossless, all of the power input to the network must leave the network. The power incident on Port 1 of a network is

$$P_1^+ = \left| \frac{\frac{1}{2} V_1^+}{Z_0} \right|^2 \tag{2.100}$$

and the power leaving Port 1 is

$$P_1^- = \left| \frac{\frac{1}{2} V_1^-}{Z_0} \right|^2. \tag{2.101}$$

This can be repeated for Port 2 and the factor $\frac{1}{2}/Z_0$ appears in all expressions. So cancelling this factor, the condition for the network to be lossless is

$$|S_{11}|^2 + |S_{21}|^2 = 1 \quad \text{and} \quad |S_{12}|^2 + |S_{22}|^2 = 1. \tag{2.102}$$

For a network to be passive, no more power can leave the network than enters it. So the condition for passivity is

$$|S_{11}|^2 + |S_{21}|^2 \le 1 \quad \text{and} \quad |S_{12}|^2 + |S_{22}|^2 \le 1. \tag{2.103}$$

Reciprocity requires that $S_{21} = S_{12}$.

2.3.7 Scattering Transfer or T Parameters

S parameters relate reflected waves to incident waves, thus mixing the quantities at the input and output ports. However, in dealing with cascaded networks it is preferable to relate the traveling waves at the input ports to the output ports. Such parameters are called the scattering transfer (or ST) parameters, which for a two-port network are defined by

$$\begin{bmatrix} V_1^- \\ V_1^+ \end{bmatrix} = \begin{bmatrix} {}^ST_{11} & {}^ST_{12} \\ {}^ST_{21} & {}^ST_{22} \end{bmatrix} \begin{bmatrix} V_2^+ \\ V_2^- \end{bmatrix}, \tag{2.104}$$

where

$${}^S\mathbf{T} = \begin{bmatrix} {}^ST_{11} & {}^ST_{12} \\ {}^ST_{21} & {}^ST_{22} \end{bmatrix}. \tag{2.105}$$

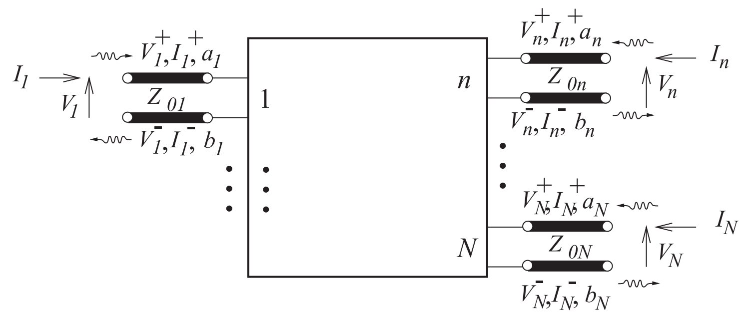

Figure 2-16: N-port network with traveling voltage and current waves.

The two-port ST parameters and S parameters are related by

$$\begin{bmatrix} {}^ST_{11} & {}^ST_{12} \\ {}^ST_{21} & {}^ST_{22} \end{bmatrix} = \begin{bmatrix} -(S_{11}S_{22} - S_{12}S_{21})/S_{21} & (S_{11}/S_{21}) \\ -(S_{22}/S_{21}) & (1/S_{21}) \end{bmatrix} \tag{2.106}$$

and

$$\begin{bmatrix} S_{11} & S_{12} \\ S_{21} & S_{22} \end{bmatrix} = \begin{bmatrix} {}^ST_{12}{}^ST_{22}^{-1} & ({}^ST_{11} - {}^ST_{12}{}^ST_{22}^{-1}{}^ST_{21}) \\ {}^ST_{22}^{-1} & -{}^ST_{22}^{-1}{}^ST_{21} \end{bmatrix}. \tag{2.107}$$

Very often the ST parameters are called T parameters, but there are at least two types of T parameters, so it is necessary to be specific. (Another form will be introduced in Section 2.6.) If networks A and B have parameters ${}^S\mathbf{T}_A$ and ${}^S\mathbf{T}_B$, then the ${}^S\mathbf{T}$ parameters of the cascaded network are

$${}^S\mathbf{T} = {}^S\mathbf{T}_A \cdot {}^S\mathbf{T}_B. \tag{2.108}$$

There are two forms of the scattering T parameters. Here the scattering transfer parameters are designated as the ST parameters but often T on its own is used. The other more common form are the chain scattering parameters which will be considered in Section 2.6.

2.4 Generalized Scattering Parameters

The scattering parameters up to now are known as normalized S parameters because they have the same reference impedance at each port. However the qualification 'normalized' is not used unless it is necessary to distinguish them from a more general form of S parameters. In this section generalized S parameters that have different reference impedances at each of the ports are considered. These are particularly useful in designing amplifiers but are also useful in measurements where the system impedance of a design may not be the same as the reference impedance of the measurement system. For example an RFIC may have a system impedance of $100\ \Omega$, but the measurement system have a reference impedance of $50\ \Omega$.

2.4.1 The N-Port Network

The N-port network is a generalization of a two-port, as you may have guessed. A network with many ports is shown in Figure 2-16. Again, each port consists of a pair of terminals, one of which is the reference for voltage. Each port has equal and opposite currents at the two terminals. The incident and reflected voltages at any port can be related to each other using the voltage scattering parameter matrix relation:

$$\begin{bmatrix} V_1^- \\ V_2^- \\ \vdots \\ V_N^- \end{bmatrix} = \begin{bmatrix} S_{11} & S_{12} & \dots & S_{1N} \\ S_{21} & S_{22} & \dots & S_{2N} \\ \vdots & & \ddots & \\ S_{N1} & S_{N2} & \dots & S_{NN} \end{bmatrix} \begin{bmatrix} V_1^+ \\ V_2^+ \\ \vdots \\ V_N^+ \end{bmatrix}, \tag{2.109}$$

or in compact form as $\mathbf{V}^- = \mathbf{S}\mathbf{V}^+$. (2.110)

Notice that

$$S_{ij} = \left. \frac{V_i^-}{V_j^+} \right|_{V_k^+=0 \text{ for } k \neq j}. \tag{2.111}$$

In words, S_{ij} is found by driving Port j with an incident wave of voltage V_j^+ and measuring the reflected wave V_i^- at Port i, with all ports other than j terminated in a matched load. Reflection and transmission coefficients can also be defined using the above relationship, provided that the ports are terminated in matched loads:

- S_{ii} : reflection coefficient seen looking into Port i
- S_{ij} : transmission coefficient from j to i.

2.4.2 Power Waves

The S parameters used so far have the same reference impedance at each port. These can be generalized so that the reference impedances at each port can be different. These are useful if the actual system being considered has different loading conditions at the ports. Generalized S parameters, denoted here as ${}^{G}S$, are defined in terms of what are called root power waves, which in turn are defined using forward- and backward-traveling voltage waves. Consider the N-port network of Figure 2-16, where the nth port has a reference transmission line of characteristic impedance Z_{0n}, which can have infinitesimal length. The transmission line at the nth port serves to separate the forward- and backward-traveling voltage (V_n^+ and V_n^-) and current (I_n^+ and I_n^-) waves.

The reference characteristic impedance matrix $\mathbf{Z}_0$ is a diagonal matrix, $\mathbf{Z}_0$ = diag($Z_{01} \dots Z_{0n} \dots Z_{0N}$), and the **root power waves** at the nth port, a_n and b_n, are defined by

$$a_n = V_n^+ / \sqrt{\Re\{Z_{0n}\}} \quad \text{and} \quad b_n = V_n^- / \sqrt{\Re\{Z_{0n}\}}, \tag{2.112}$$

and shown in Figure 2-17 and are often called just **power waves**. The unit of the a and b values is root power, that is, in the SI unit system, $\sqrt{\text{W}}$. In matrix form

$$\mathbf{a} = \mathbf{Z}_0^{-1/2}\mathbf{V}^+ = \mathbf{Y}_0^{1/2}\mathbf{V}^+, \qquad \mathbf{b} = \mathbf{Z}_0^{-1/2}\mathbf{V}^- = \mathbf{Y}_0^{1/2}\mathbf{V}^-, \tag{2.113}$$

$$\mathbf{V}^+ = \mathbf{Z}_0^{1/2}\mathbf{a} = \mathbf{Y}_0^{-1/2}\mathbf{a}, \qquad \mathbf{V}^- = \mathbf{Z}_0^{1/2}\mathbf{b} = \mathbf{Y}_0^{-1/2}\mathbf{b}, \tag{2.114}$$

where

$$\mathbf{a} = [a_1 \dots a_n \dots a_N]^{\mathrm{T}}, \qquad \mathbf{b} = [b_1 \dots b_n \dots b_N]^{\mathrm{T}}, \tag{2.115}$$

$$\mathbf{V}^+ = [V_1^+ \dots V_n^+ \dots V_N^+]^{\mathrm{T}}, \qquad \mathbf{V}^- = [V_1^- \dots V_n^- \dots V_N^-]^{\mathrm{T}}, \tag{2.116}$$

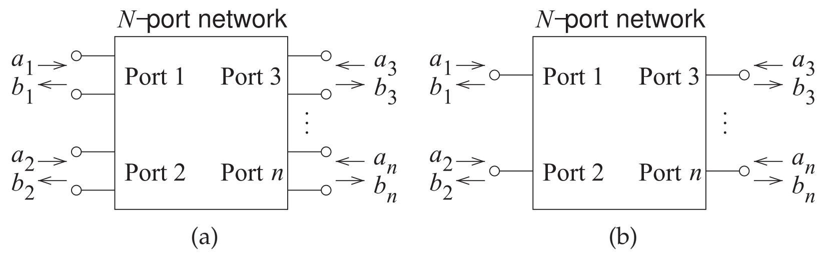

Figure 2-17: N-ports defining the a and b root power waves: (a) two-terminal ports; and (b) ports on their own.

and the characteristic admittance matrix is $\mathbf{Y}_0 = \mathbf{Z}_0^{-1}$. The power waves are interpreted as describing power flow:

$$\frac{1}{\sqrt{2}}|a_n| = \sqrt{\text{incident power at Port } n}$$
$$\text{and} \quad \frac{1}{\sqrt{2}}|b_n| = \sqrt{\text{power leaving at Port } n}. \tag{2.117}$$

That is, for example, the incident (or available) power at Port n, referenced to Z_{0n}, is $\frac{1}{2}|a_n|^2$ and the reflected power at the port is $\frac{1}{2}|b_n|^2$. Thus the power delivered by the nth port is $\frac{1}{2}(|b_n|^2 - |a_n|^2)$.

After some manipulation it can be shown that on each reference line the power waves can be related to the total voltages and currents as

$$\mathbf{a} = \frac{\mathbf{V} + \mathbf{Z}_0\mathbf{I}}{2\sqrt{\Re\{\mathbf{Z}_0\}}} \quad \text{and} \quad \mathbf{b} = \frac{\mathbf{V} - \mathbf{Z}_0^*\mathbf{I}}{2\sqrt{\Re\{\mathbf{Z}_0\}}}, \tag{2.118}$$

where $\mathbf{V}$ and $\mathbf{I}$ are vectors of total voltage and total current. Now, generalized S parameters can be formally defined as

$$\mathbf{b} = {}^G\mathbf{S}\mathbf{a}, \tag{2.119}$$

thus $\mathbf{Y}_0^{1/2}\mathbf{V}^- = {}^G\mathbf{S}\mathbf{Y}_0^{1/2}\mathbf{V}^+$, and so $\mathbf{V}^- = \mathbf{Y}_0^{-1/2}{}^G\mathbf{S}\mathbf{Y}_0^{1/2}\mathbf{V}^+$. This reduces to $\mathbf{V}^- = {}^G\mathbf{S}\mathbf{V}^+$ when all of the reference transmission lines have the same characteristic impedance. However, when the ports have different reference impedances, $\mathbf{S}^V$ is used for voltage scattering parameters and $\mathbf{S}^I$ for current scattering parameters, where $\mathbf{V}^- = \mathbf{S}^V\mathbf{V}^+$ and $\mathbf{I}^- = \mathbf{S}^I\mathbf{I}^+$.

The following conversion relationships can also be derived:

$$\mathbf{S}^I = \Re\{\mathbf{Z}_0\}^{-\frac{1}{2}}\,{}^G\mathbf{S}\Re\{\mathbf{Z}_0\}^{\frac{1}{2}} \tag{2.120}$$
$$\mathbf{S}^V = \mathbf{Z}_0\Re\{\mathbf{Z}_0\}^{-\frac{1}{2}}\,{}^G\mathbf{S}\Re\{\mathbf{Z}_0\}^{\frac{1}{2}}\{\mathbf{Z}_0^*\}^{-1}, \tag{2.121}$$

where $\Re\{\mathbf{Z}_0\}^{\frac{1}{2}} = \text{diag}\{\sqrt{\Re\{Z_{01}\}}, \sqrt{\Re\{Z_{02}\}}, \ldots, \sqrt{\Re\{Z_{0n}\}}\}$.

Recall that ${}^G\mathbf{S}$ is in terms of $\mathbf{a}$ and $\mathbf{b}$, $\mathbf{S^I}$ is in terms of $\mathbf{I}^-$ and $\mathbf{I}^+$, and $\mathbf{S^V}$ is in terms of $\mathbf{V}^-$ and $\mathbf{V}^+$. When port impedances and reference resistances are real, Equations (2.120) and (2.121) assume the simpler forms

$$\mathbf{S}^I = -\mathbf{R}_o^{-\frac{1}{2}}\,{}^G\mathbf{S}\,\mathbf{R}_0^{\frac{1}{2}} = -{}^G\mathbf{S}, \tag{2.122}$$
$$\mathbf{S^V} = \mathbf{R}_0\,\mathbf{R}_0^{-\frac{1}{2}}\,{}^G\mathbf{S}\,\mathbf{R}_0^{\frac{1}{2}}\,\mathbf{R}_0^{*-1} = \mathbf{R}_0\,(\mathbf{R}_0^*)^{-1}\,{}^G\mathbf{S} = {}^G\mathbf{S}, \tag{2.123}$$

where $\mathbf{R}_0^{\frac{1}{2}} = \text{diag}\{\sqrt{R_{01}}, \sqrt{R_{02}}, \ldots, \sqrt{R_{0n}}\}$, with R_{0n} being the reference resistance at the nth port. In addition, if the reference resistances at each port are the same, all of the various scattering parameter definitions become equivalent (i.e., $\mathbf{S^V} = -\mathbf{S^I} = {}^G\mathbf{S} = \mathbf{S}$), where $\mathbf{S}$ is the normalized S parameter matrix, also called the normalized S parameter matrix.

The reciprocity condition for generalized S parameters is ${}^GS_{12} = {}^GS_{21}Z_{01}/Z_{02}$.

EXAMPLE 2.4 **Generalized Scattering Parameters of a Through Connection**

Develop the generalized scattering parameters of a through connection with a reference impedance Z_{01} at Port 1 and a reference impedance Z_{02} at Port 2.

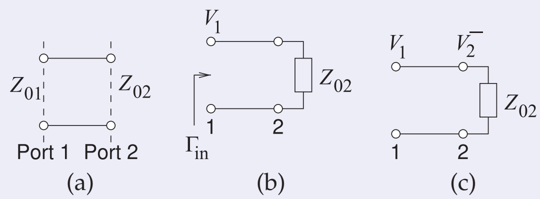

Solution:

The through connection is shown in (a) and in (b) is the configuration to determine S_{11} as $V_2^+ = 0 = a_2$ since Port 2 is terminated in Z_{02}. Then

$${}^GS_{11} = \Gamma_{\text{in}} = \frac{Z_{02} - Z_{01}}{Z_{02} + Z_{01}} \quad \text{and similarly} \quad {}^GS_{22} = \frac{Z_{01} - Z_{02}}{Z_{02} + Z_{01}} = -{}^GS_{11} \tag{2.124}$$

Figure (b) is used to determine S_{21} as here $V_2^+ = 0 = a_2$

$$V_2^- = b_2\sqrt{\Re\{Z_{02}\}} = V_1 = V_1^+ + V_1^- = V_1^+(1 + S_{11}) = a_1\sqrt{\Re\{Z_{01}\}}. \tag{2.125}$$

Thus,

$${}^GS_{21} = \left.\frac{b_2}{a_1}\right|_{a_2=0} = \frac{\sqrt{\Re\{Z_{01}\}}}{\sqrt{\Re\{Z_{02}\}}}(1 + {}^GS_{11}) \ \text{ and also } \ {}^GS_{12} = \frac{\sqrt{\Re\{Z_{02}\}}}{\sqrt{\Re\{Z_{01}\}}}(1 + {}^GS_{22}). \tag{2.126}$$

The generalized scattering parameter matrix of the through is

$${}^G\boldsymbol{S} = \frac{1}{Z_{01} + Z_{02}}\begin{bmatrix} Z_{02} - Z_{01} & 2Z_{01}\sqrt{\Re\{Z_{02}\}/\Re\{Z_{01}\}} \\ 2Z_{02}\sqrt{\Re\{Z_{01}\}/\Re\{Z_{02}\}} & Z_{01} - Z_{02} \end{bmatrix} \tag{2.127}$$

and for real Z_{01} and Z_{02} $\quad {}^G\boldsymbol{S} = \dfrac{1}{Z_{01} + Z_{02}}\begin{bmatrix} Z_{02} - Z_{01} & 2\sqrt{Z_{01}Z_{02}} \\ 2\sqrt{Z_{01}Z_{02}} & Z_{01} - Z_{02} \end{bmatrix}$ (2.128)

For normalized S parameters the reference impedances at the ports are the same, i.e. $Z_{01} = Z_0 = Z_{02}$, and the normalized S parameters of the through are (as expected)

$$\boldsymbol{S} = {}^N\boldsymbol{S} = \begin{bmatrix} 0 & 1 \\ 1 & 0 \end{bmatrix}. \tag{2.129}$$

2.4.3 Scattering Parameters in Terms of a and b waves

Previously S parameters were defined in terms of forward- and backward-traveling voltage waves, see Section 2.3.3 and Equation (2.71). That definition is adequate if only one reference impedance is used throughout. A more general form of S parameters uses the a and b root power waves. This is still valid if only one reference impedance is used but they can also be used when the ports have different reference impedances. This more general definition for a two-port network, with respect to Figure 2-18, is

$$\begin{bmatrix} b_1 \\ b_2 \end{bmatrix} = \begin{bmatrix} S_{11} & S_{12} \\ S_{21} & S_{22} \end{bmatrix}\begin{bmatrix} a_1 \\ a_2 \end{bmatrix}. \tag{2.130}$$

Even if the reference impedances at ports 1 and 2 are the different. If the references impedance are the same and real, the usual case, the scattering parameters are identical when used to relate traveling voltage waves as in the following:

$$\begin{bmatrix} V_1^- \\ V_2^- \end{bmatrix} = \begin{bmatrix} S_{11} & S_{12} \\ S_{21} & S_{22} \end{bmatrix} \begin{bmatrix} V_1^+ \\ V_2^+ \end{bmatrix}. \tag{2.131}$$

2.4.4 Normalized and Generalized S Parameters

S parameters measured with respect to a common reference resistance are referred to as normalized S parameters. In almost all cases, measured S parameters are normalized to 50 Ω, as 50 Ω cables and components are used in measurement systems. In other words, $Z_{01} = Z_{02} = \ldots = Z_{0N} = R_0$ (= 50 Ω). Generalized S parameters can be used to simplify the design process of devices such as amplifiers. For example, it is often convenient to use the input and output impedances of an amplifier as the normalization impedances. Also, it is often desirable to be able to convert between measured S parameters (normalized to 50 Ω) and generalized S parameters. Let ${}^N\mathbf{S}$ be the measured (normalized) S parameter matrix. (So ${}^N\mathbf{S}$ is the conventional S parameter matrix.) The development is tedious, but it can be shown that the generalized S parameters are

$${}^G\mathbf{S} = (\mathbf{D}^*)^{-1}({}^N\mathbf{S} - \mathbf{\Gamma}^*)(\mathbf{U} - \mathbf{\Gamma}\,{}^N\mathbf{S})^{-1}\mathbf{D}, \tag{2.132}$$

where $\mathbf{U}$ is the unit matrix ($\mathbf{U} = \mathrm{diag}(1, 1, \ldots, 1)$), R_0 is the reference impedance of the normalized S parameters, ${}^N\mathbf{S}$, and $\mathbf{D}$ is a diagonal matrix with elements

$$D_{ii} = |1 - \Gamma_i^*|^{-1}(1 - \Gamma_i)\sqrt{1 - |\Gamma_i|^2} \tag{2.133}$$

$$\Gamma_i = (Z_{0i} - R_0)(Z_{0i} + R_0)^{-1} \qquad i = 1, 2, \ \ldots \ , N, \tag{2.134}$$

and $\mathbf{\Gamma}$ is a diagonal matrix with elements Γ_i. Z_{0i} is the system impedance at Port i to which the generalized S parameters are to be referred.

2.4.5 Change of Reference Impedance

The result in the section above can be used to change scattering parameters referenced to a real impedance R_1 (i.e., ${}^{R1}\mathbf{S}$) to scattering parameters referenced to R_2 (i.e., ${}^{R2}\mathbf{S}$). Note that ${}^{R1}\mathbf{S}$ and ${}^{R2}\mathbf{S}$ are the conventional or normalized S parameters. The elements in Equations (2.133) and (2.134) become

$$D_{ii} = D = |1 - \Gamma_{R2}|^{-1}(1 - \Gamma_{R2})\sqrt{1 - |\Gamma_{R2}|^2} = \sqrt{1 - |\Gamma_{R2}|^2} \tag{2.135}$$

$$\Gamma_{R2} = (R_2 - R_1)(R_2 + R_1)^{-1}, \tag{2.136}$$

and $|\Gamma_{R2}| < 1$. So Equation (2.132) becomes

$${}^{R2}\mathbf{S} = \mathbf{D}^{-1}({}^{R1}\mathbf{S} - \mathbf{\Gamma})(\mathbf{U} - \mathbf{\Gamma}^{R1}\mathbf{S})^{-1}\mathbf{D} = ({}^{R1}\mathbf{S} - \mathbf{\Gamma})(\mathbf{U} - \mathbf{\Gamma}^{R1}\mathbf{S})^{-1} \tag{2.137}$$

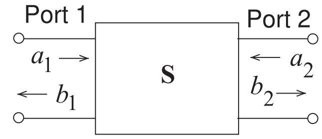

Figure 2-18: Definition of S parameters in terms of a and b root power waves. $a_1 = V_1^+/\Re\{\mathbf{Z}_{01}\}$, $b_1 = V_1^-/\Re\{\mathbf{Z}_{01}\}$, $a_2 = V_2^+/\Re\{\mathbf{Z}_{02}\}$, $b_2 = V_2^-/\Re\{\mathbf{Z}_{02}\}$. Incident power at Port 1 (2) is $|a_1|^2$ ($|a_2^2$). Power leaving Port 1 (2) is $|b_1|^2$ ($|b_2^2$)

since $\mathbf{D}$ is a diagonal matrix with all diagonal entries the same. So for a two-port

$$
\begin{aligned}
{}^{R2}\mathbf{S} &= \begin{bmatrix} {}^{R2}S_{11} & {}^{R2}S_{12} \\ {}^{R2}S_{21} & {}^{R2}S_{22} \end{bmatrix} \\
&= \begin{bmatrix} {}^{R1}S_{11} - \Gamma_{R2} & {}^{R1}S_{12} \\ {}^{R1}S_{21} & {}^{R1}S_{22} - \Gamma_{R2} \end{bmatrix} \begin{bmatrix} 1 - \Gamma_{R2}{}^{R1}S_{11} & -\Gamma_{R2}{}^{R1}S_{12} \\ -\Gamma_{R2}{}^{R1}S_{21} & 1 - \Gamma_{R2}{}^{R1}S_{22} \end{bmatrix}^{-1}.
\end{aligned}
\tag{2.138}
$$

EXAMPLE 2.5 Change of Reference Impedance

An attenuator has the 50 Ω S parameters:

$$
{}^{50}\mathbf{S} = \begin{bmatrix} 0 & 0.3162 \\ 0.3162 & 0 \end{bmatrix}. \tag{2.139}
$$

What are the S parameters referenced to 75 Ω?

Solution:

The conversion uses Equation (2.138) with $R_1 = 50\ \Omega$ and $R_2 = 75\ \Omega$.
So $\Gamma_{75} = (75 - 50)/(75 + 50) = 0.2$. Thus the S parameters referenced to 75 Ω are

$$
\begin{aligned}
{}^{75}\mathbf{S} &= \begin{bmatrix} {}^{50}S_{11} - \Gamma_{75} & {}^{50}S_{12} \\ {}^{50}S_{21} & {}^{50}S_{22} - \Gamma_{75} \end{bmatrix} \begin{bmatrix} 1 - \Gamma_{75}{}^{50}S_{11} & -\Gamma_{75}{}^{50}S_{12} \\ -\Gamma_{75}{}^{50}S_{21} & 1 - \Gamma_{75}{}^{50}S_{22} \end{bmatrix} \\
&= \begin{bmatrix} -0.2 & 0.3162 \\ 0.3162 & -0.2 \end{bmatrix} \begin{bmatrix} 1 & -0.2 \cdot 0.3162 \\ -0.2 \cdot 0.3162 & 1 \end{bmatrix} \\
&= \begin{bmatrix} -0.2 & 0.3162 \\ 0.3162 & -0.2 \end{bmatrix} \begin{bmatrix} 1 & 0.06324 \\ 0.06324 & 1 \end{bmatrix} = \begin{bmatrix} -0.18 & 0.3036 \\ 0.3036 & -0.18 \end{bmatrix}.
\end{aligned}
\tag{2.140}
$$

2.4.6 Passivity in Terms of Scattering Parameters

Consider an N-port characterized by its generalized scattering matrix $\mathbf{S}$. The time-averaged power dissipated in the N-port is

$$
P = \frac{1}{2}\sum_{i=1}^{N}(|\mathbf{a}_i|^2 - |\mathbf{b}_i|^2) = \tfrac{1}{2}\left(\mathbf{a}^{*\mathrm{T}}\mathbf{a} - \mathbf{b}^{*\mathrm{T}}\mathbf{b}\right), \tag{2.141}
$$

and so $$P = \tfrac{1}{2}\mathbf{a}^{*\mathrm{T}}\left[\mathbf{U} - (\mathbf{S}^*)^{\mathrm{T}}\mathbf{S}\right]\mathbf{a}. \tag{2.142}$$

In the above, the conjugate, $\mathbf{a}^*$, of the matrix $\mathbf{a}$ is obtained from $\mathbf{a}$ by taking the complex conjugate of each element. For a passive N-port,

$$
\mathbf{U} - (\mathbf{S}^*)^{\mathrm{T}}\mathbf{S} \geq 0 \quad \text{for all real } \omega, \tag{2.143}
$$

This can also be written in summation form as

$$
\sum_{k=1}^{N} S_{kj}S_{kj}^* = P_j. \tag{2.144}
$$

$P_j = 1$ for all j if the network is lossless. For a network to be passive $P_j \leq 1$ for all j. By examining the S parameters it can be determined quickly whether a network is lossless, lossy, or perhaps has gain.

For a lossless N-port, $$\mathbf{U} - \mathbf{S}^{*\mathrm{T}}\mathbf{S} = 0. \tag{2.145}$$

Rearranging, taking the transpose of both sides and noting that $\mathbf{U}^{\mathrm{T}} = \mathbf{U}$

$$\mathbf{S}^{*}\mathbf{S}^{\mathrm{T}} = \mathbf{U}. \tag{2.146}$$

This is known as the **unitary condition**. That is, for a lossless N-port

$$\mathbf{S}^{*} = \left(\mathbf{S}^{\mathrm{T}}\right)^{-1}. \tag{2.147}$$

The important result here is that for a lossless network (these are the unitary conditions)

$$\sum_{k=1}^{N} S_{kj} S_{kj}^{*} = 1 \tag{2.148}$$

$$\sum_{k=1}^{N} S_{ki} S_{kj}^{*} = 0 \quad \text{for } i \text{ not equal to } j. \tag{2.149}$$

2.4.7 Impedance Matrix Representation

In this section N-port S parameters are related to N-port z parameters. The basic relationship of voltage and current at any port using impedances is

$$\begin{bmatrix} V_1 \\ V_2 \\ \vdots \\ V_N \end{bmatrix} = \begin{bmatrix} z_{11} & z_{12} & \dots & z_{1N} \\ z_{21} & z_{22} & \dots & z_{2N} \\ \vdots & & \ddots & \\ z_{N1} & z_{N2} & \dots & z_{NN} \end{bmatrix} \begin{bmatrix} I_1 \\ I_2 \\ \vdots \\ I_N \end{bmatrix}, \tag{2.150}$$

or in compact form as $$\mathbf{V} = \mathbf{Z}\mathbf{I} \tag{2.151}$$

$\mathbf{Z}$ is reciprocal if $z_{ij} = z_{ji}$. The z parameters defined here are more formally called port-based z parameters, as the voltage and current variables are port quantities.

Relating z and S parameters begins by relating the total voltage and current at the nth terminal plane to the traveling voltage and current waves. From Figure 2-16,

$$V_n = V_n^{+} + V_n^{-}, \quad \text{and} \quad I_n = I_n^{+} - I_n^{-}, \tag{2.152}$$

and in vector form

$$\begin{aligned} \mathbf{V} &= \mathbf{V}^{+} + \mathbf{V}^{-} & \mathbf{I} &= \mathbf{I}^{+} + \mathbf{I}^{-} \\ \mathbf{V}^{+} &= \mathbf{Z}_0^{*}\mathbf{I}^{+} & \mathbf{V}^{-} &= -\mathbf{Z}_0\mathbf{I}^{-}, \end{aligned} \tag{2.153}$$

where $\mathbf{Z}_0 = \mathrm{diag}(Z_{01}, Z_{02}, \dots, Z_{0N})$ (and z_{0n} can be complex). After some algebraic manipulation, the following relationships are obtained:

$$\mathbf{S}^{V} = [\mathbf{U} + \mathbf{Z}\mathbf{Z}_0^{-1}]^{-1}[\mathbf{Z}(\mathbf{Z}_0^{*})^{-1} - \mathbf{U}] \tag{2.154}$$

$$\mathbf{Z} = [\mathbf{U} + \mathbf{S}^{V}][\mathbf{Z}_0^{*\,-1} - \mathbf{Z}_0^{-1}(\mathbf{S}^{V})]^{-1}. \tag{2.155}$$

Note that $\mathbf{S}^V$ is the voltage scattering parameter matrix. These are related to the generalized scattering parameter matrix by Equation (2.123). For normalized S parameters the same real reference impedance is used at all ports ($Z_{0n} = Z_0, n = 1, \ldots, N$), then Equations (2.154) and (2.155) become

$$\mathbf{S} = [\mathbf{Z} + Z_0\mathbf{U}]^{-1} [\mathbf{Z} - Z_0\mathbf{U}] \quad \text{and} \quad \mathbf{Z} = Z_0 [\mathbf{U} + \mathbf{S}] [\mathbf{U} - \mathbf{S}]^{-1}. \tag{2.156}$$

2.4.8 Admittance Matrix Representation

In this section, N-port S parameters are related to N-port y parameters. The currents and voltages are related as

$$\begin{bmatrix} I_1 \\ I_2 \\ \vdots \\ I_N \end{bmatrix} = \begin{bmatrix} y_{11} & y_{12} & \ldots & y_{1N} \\ y_{21} & y_{22} & \ldots & y_{2N} \\ \vdots & & \ddots & \\ y_{N1} & y_{N2} & \ldots & y_{NN} \end{bmatrix} \begin{bmatrix} V_1 \\ V_2 \\ \vdots \\ V_N \end{bmatrix}, \tag{2.157}$$

or in compact form the port-based y parameters are

$$\mathbf{I} = \mathbf{Y}\mathbf{V}. \tag{2.158}$$

Using a similar approach to that in the previous subsection, the relationship between S and y parameters can be developed. The development will be done slightly differently and this development is applicable to generalized scattering parameters. First, consider the relationship of the total port voltage $\mathbf{V} = [V_1 \ldots V_n \ldots V_N]^{\mathrm{T}}$ and current $\mathbf{I} = [I_1 \ldots I_n \ldots I_N]^{\mathrm{T}}$ to forward- and backward-traveling voltage and current waves:

$$\mathbf{V} = \mathbf{V}^+ + \mathbf{V}^- \quad \text{and} \quad \mathbf{I} = \mathbf{I}^+ + \mathbf{I}^-, \tag{2.159}$$

where $\mathbf{I}^+ = \mathbf{Y}_0\mathbf{V}^+ = \mathbf{Y}_0^{1/2}\mathbf{a}$ and $\mathbf{I}^- = -\mathbf{Y}_0\mathbf{V}^- = -\mathbf{Y}_0^{1/2}\mathbf{b}$. (Each element of $\mathbf{Y_0}$, $Y_{0n} = 1/Z_{0n}$ and can be complex.) Using traveling waves, Equation (2.158) becomes

$$\mathbf{I}^+ + \mathbf{I}^- = \mathbf{Y}(\mathbf{V}^+ + \mathbf{V}^-) \tag{2.160}$$

$$\mathbf{Y}_0(\mathbf{V}^+ - \mathbf{V}^-) = \mathbf{Y}(\mathbf{V}^+ + \mathbf{V}^-) \tag{2.161}$$

$$\mathbf{Y}_0(\mathbf{1} - \mathbf{Y}_0^{-1/2}\mathbf{S}\mathbf{Y}_0^{1/2})\mathbf{V}^+ = \mathbf{Y}(\mathbf{1} + \mathbf{Y}_0^{-1/2}\mathbf{S}\mathbf{Y}_0^{1/2})\mathbf{V}^+, \tag{2.162}$$

and so the port y parameters in terms of the generalized scattering parameters are

$$\mathbf{Y} = \mathbf{Y}_0(\mathbf{1} - \mathbf{Y}_0^{-1/2}\,{}^G\mathbf{S}\mathbf{Y}_0^{1/2})(\mathbf{1} + \mathbf{Y}_0^{-1/2}\,{}^G\mathbf{S}\mathbf{Y}_0^{1/2})^{-1}. \tag{2.163}$$

Alternatively, Equation (2.161) can be rearranged as

$$(\mathbf{Y}_0 + \mathbf{Y})\mathbf{V}^- = (\mathbf{Y}_0 - \mathbf{Y})\mathbf{V}^+ \tag{2.164}$$

$$\mathbf{V}^- = (\mathbf{Y}_0 + \mathbf{Y})^{-1}(\mathbf{Y}_0 - \mathbf{Y})\mathbf{V}^+ \tag{2.165}$$

$$\mathbf{Y}_0^{-1/2}\mathbf{b} = (\mathbf{Y}_0 + \mathbf{Y})^{-1}(\mathbf{Y}_0 - \mathbf{Y})\mathbf{Y}_0^{-1/2}\mathbf{a}. \tag{2.166}$$

Comparing this to the definition of generalized S parameters in Equation (2.119) leads to

$${}^G\mathbf{S} = \mathbf{Y}_0^{1/2}(\mathbf{Y}_0 + \mathbf{Y})^{-1}(\mathbf{Y}_0 - \mathbf{Y})\mathbf{Y}_0^{-1/2}. \tag{2.167}$$

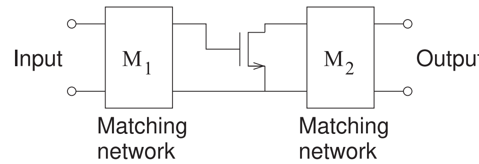

Figure 2-19: An amplifier with an active device and input (M_1) and output (M_2) matching networks. The biasing arrangement is not shown, but usually this is done with the appropriate choice of matching network topology.

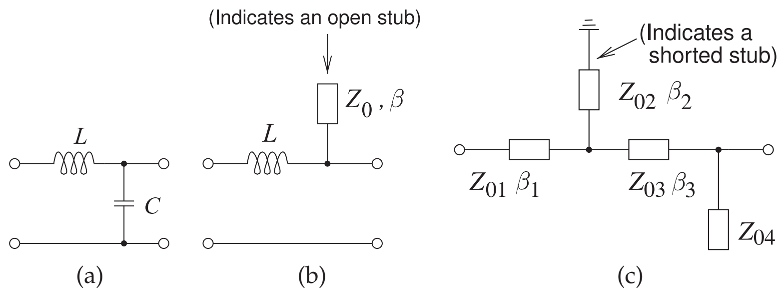

Figure 2-20: Three forms of matching networks with increasing use of transmission line sections.

For the usual case where all of the reference transmission lines have the same characteristic impedance $Z_0 = 1/Y_0$ (note $S = {}^N\mathbf{S}$),

$$\mathbf{Y} = Y_0(\mathbf{U} - \mathbf{S})(\mathbf{U} + \mathbf{S})^{-1} \quad \text{and} \quad \mathbf{S} = (\mathbf{Y}_0 + \mathbf{Y})^{-1}(\mathbf{Y}_0 - \mathbf{Y}). \tag{2.168}$$

2.5 Scattering Parameter Matrices of Common Two-Ports

RF and microwave circuits can generally be represented as interconnected two-ports, as most RF and microwave circuit designs involve cascaded functional blocks such as amplifiers, matching networks, filters, etc.[4] (see Figure 2-19). Thus there is great interest in various manipulations that can be performed on two-ports as well as the network parameters of common two-port circuit topologies. As an example, consider the matching networks in Figure 2-19. These are used to achieve maximum power transfer in an amplifier by acting as impedance transformers. Matching networks assume a variety of forms, as shown in Figure 2-20, and all can be viewed as two-port networks and a combination of simpler components. In this section, strategies are presented for developing the S parameters of two-ports.

Transmission Line

The traveling waves on a transmission line (Figure 2-21(a)) have a phase that depends on the electrical length, θ, of the line. The transmission line has a characteristic impedance, Z_0, and length, ℓ, which in general is different from

[4] This arrangement tends to maximize bandwidth, minimize losses, and maximize efficiency. Lower-frequency analog design utilizes more complex arrangements; for example, feedback high in the circuit hierarchy improves the reliability and robustness of design but comes at the cost of reduced bandwidth and lower power efficiency.

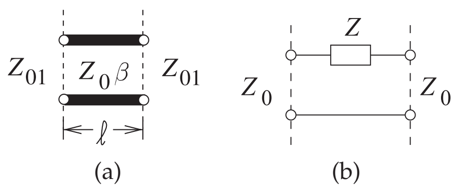

Figure 2-21: Two-ports: (a) section of transmission line; and (b) series element in the form of a two-port.

the system reference impedance, here Z_{01}. Thus

$$S_{11} = S_{22} = \frac{\Gamma(1 - e^{-2\jmath\theta})}{1 - \Gamma^2 e^{-2\jmath\theta}} \quad \text{and} \quad S_{21} = S_{12} = \frac{(1 - \Gamma^2)e^{-\jmath\theta}}{1 - \Gamma^2 e^{-2\jmath\theta}}, \tag{2.169}$$

where $\theta = \beta\ell$ and

$$\Gamma = \frac{Z_0 - Z_{01}}{Z_0 + Z_{01}}. \tag{2.170}$$

If the reference impedance is the same as the characteristic impedance of the line, i.e. $Z_{01} = Z_0$ and $\Gamma = 0$, the scattering parameters of the line are

$$\mathbf{S} = \begin{bmatrix} 0 & e^{-\jmath\theta} \\ e^{-\jmath\theta} & 0 \end{bmatrix}. \tag{2.171}$$

Shunt Element

The S parameters of the shunt element (Figure 2-15) were developed in Section 2.3.5. In a slightly different form these are

$$S_{11} = S_{22} = -\frac{\overline{y}}{(\overline{y} + 2)} \quad \text{and} \quad S_{12} = S_{21} = \frac{2}{(\overline{y} + 2)}, \tag{2.172}$$

where $\overline{y} = Y/Y_0$ is the admittance normalized to the system reference admittance ($Y_0 = 1/Z_0$).

Series Element

The S parameters of the series element (Figure 2-21(b)) are

$$S_{11} = S_{22} = \frac{\overline{z}}{(\overline{z} + 2)} \quad \text{and} \quad S_{12} = S_{21} = \frac{2}{(\overline{z} + 2)}, \tag{2.173}$$

where $\overline{z} = Z/Z_0$ is the normalized impedance.

2.6 T or Chain Scattering Parameters of Cascaded Two-Port Networks

The T parameters, also known as chain scattering parameters, are a cascadable form of scattering parameters. They are similar to regular S parameters and can be expressed in terms of the a and b root power waves or traveling voltage waves. Two two-port networks, A and B, in cascade are shown in Figure 2-22. Here (A) and (B) are used as superscripts to distinguish the parameters of each two-port network, but the subscripts A and B are used for matrix quantities. Since

$$a_2^{(A)} = b_1^{(B)} \quad \text{and} \quad b_2^{(A)} = a_1^{(B)}, \tag{2.174}$$

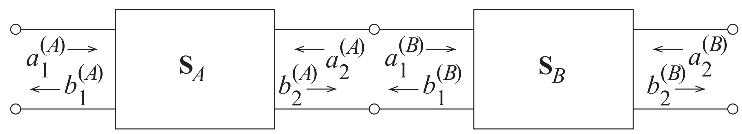

Figure 2-22: Two cascaded two-ports.

it is convenient to put the a and b parameters in cascadable form, leading to the following two-port chain matrix or T matrix representation (with respect to Figure 2-18):

$$\begin{bmatrix} a_1 \\ b_1 \end{bmatrix} = \begin{bmatrix} T_{11} & T_{12} \\ T_{21} & T_{22} \end{bmatrix} \begin{bmatrix} b_2 \\ a_2 \end{bmatrix}, \tag{2.175}$$

where the T matrix or chain scattering matrix is

$$\mathbf{T} = \begin{bmatrix} T_{11} & T_{12} \\ T_{21} & T_{22} \end{bmatrix}. \tag{2.176}$$

$\mathbf{T}$ is very similar to the scattering transfer matrix (${}^S\mathbf{T}$) of Section 2.3.7. The only difference is the ordering of the a and b components. You will come across both forms, so be careful that you understand which is being used. Both forms are used for the same function—cascading two-port networks. The relationships between $\mathbf{T}$ and $\mathbf{S}$ are given by

$$\mathbf{T} = \begin{bmatrix} S_{21}^{-1} & -S_{21}^{-1}S_{22} \\ S_{21}^{-1}S_{11} & S_{12} - S_{11}S_{21}^{-1}S_{22} \end{bmatrix} \tag{2.177}$$

$$\mathbf{S} = \begin{bmatrix} T_{21}T_{11}^{-1} & T_{22} - T_{21}T_{11}^{-1}T_{12} \\ T_{11}^{-1} & -T_{11}^{-1}T_{12} \end{bmatrix}. \tag{2.178}$$

For a two-port network, using Equations (2.174) and (2.175),

$$\begin{bmatrix} a_1^{(A)} \\ b_1^{(A)} \end{bmatrix} = \mathbf{T}_A \begin{bmatrix} b_2^{(A)} \\ a_2^{(A)} \end{bmatrix} \quad \text{and} \quad \begin{bmatrix} a_1^{(B)} \\ b_1^{(B)} \end{bmatrix} = \mathbf{T}_B \begin{bmatrix} b_2^{(B)} \\ a_2^{(B)} \end{bmatrix}, \tag{2.179}$$

thus

$$\begin{bmatrix} a_1^{(A)} \\ b_1^{(A)} \end{bmatrix} = \mathbf{T}_A\mathbf{T}_B \begin{bmatrix} b_2^{(B)} \\ a_2^{(B)} \end{bmatrix}. \tag{2.180}$$

For n cascaded two-port networks, Equation (2.180) generalizes to

$$\begin{bmatrix} a_1^{(1)} \\ b_1^{(1)} \end{bmatrix} = \mathbf{T}_1\mathbf{T}_2 \ldots \mathbf{T}_n \begin{bmatrix} b_2^{(n)} \\ a_2^{(n)} \end{bmatrix}, \tag{2.181}$$

and so the $\mathbf{T}$ matrix of the cascaded network is the matrix product of the $\mathbf{T}$ matrices of the individual two-ports.

Previously, in Section 2.3.7, the scattering transfer parameters were introduced. Both the chain scattering parameters and scattering transfer parameters are referred to as T parameters. Be careful to denote which form is being used.

EXAMPLE 2.6 Development of chain scattering parameters

Derive the T parameters of the two-port network to the right using a reference impedance Z_0.

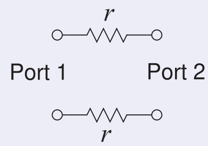

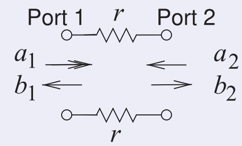

Solution:

Derivation of T_{11}

Terminate Port 2 in a matched load so that $a_2 = 0$. Then Equation (2.175) becomes $a_1 = T_{11} b_2$ and $b_1 = T_{21} b_2$ so

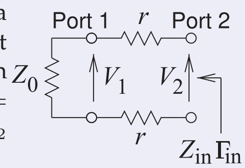

$$\Gamma_{in} = b_1/a_1 = T_{21}/T_{11}. \tag{2.182}$$

Now $Z_{in} = 2r + Z_0$, therefore

$$\Gamma_{in} = \frac{Z_{in} - Z_0}{Z_{in} + Z_0} = \frac{2r + Z_0 - Z_0}{2r + Z_0 + Z_0} = \frac{r}{r + Z_0}.$$

Thus

$$\Gamma_{in} = \frac{T_{21}}{T_{11}} = \frac{r}{r + Z_0}. \tag{2.183}$$

The next stage is relating b_2 to a_1 and since both ports have the same reference impedance a and b can be replaced by traveling voltages

$$V_1 = \left(V_1^+ + V_1^-\right) = V_1^+\left(1 + \Gamma_{in}\right) = V_1^+ \frac{2r + Z_0}{r + Z_0}.$$

Using voltage division (and since $V_2^+ = a_2 = 0$)

$$V_2 = V_2^- = \frac{Z_0}{2r + Z_0} V_1 = V_1^+ \frac{Z_0}{2r + Z_0}\frac{2r + Z_0}{r + Z_0}$$

$$V_2^- = V_1^+ \frac{Z_0}{r + Z_0}$$

$$T_{11} = \frac{V_1^+}{V_2^-} = \frac{a_1}{b_2} = \frac{r + Z_0}{Z_0}. \tag{2.184}$$

Derivation of T_{21}

Combining Equations (2.183) and (2.184)

$$T_{21} = \Gamma_{in} T_{11} = \frac{r}{r + Z_0}\frac{r + Z_0}{Z_0} = \frac{r}{Z_0} \tag{2.185}$$

Derivation of T_{22}

Terminate Port 2 in a matched load so that $a_1 = 0$. Then Equation (2.175) becomes

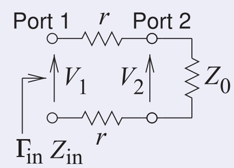

$$0 = T_{11} b_2 + T_{12} a_2$$

$$\Gamma_{in} = \frac{b_2}{a_2} = \frac{-T_{12}}{T_{11}} \rightarrow T_{12} = -T_{11}\Gamma_{in} \tag{2.186}$$

$$b_1 = T_{21} b_2 + T_{22} a_2$$

$$\frac{b_1}{a_2} = T_{21}\frac{b_2}{a_2} + T_{22}. \tag{2.187}$$

Now $Z_{in} = 2r + Z_0$ and so

$$\Gamma_{in} = \frac{2r + Z_0 - Z_0}{2r + Z_0 + Z_0} = \frac{r}{r + Z_0}. \tag{2.188}$$

Using voltage division

$$V_1 = V_1^- = \frac{Z_0}{2r + Z_0} V_2 = \frac{Z_0}{2r + Z_0} V_2^+\left(1 + \Gamma_{in}\right) = V_2^+ \frac{Z_0}{2r + Z_0}\frac{2r + Z_0}{r + Z_0} = V_2^+ \frac{Z_0}{r + Z_0}$$

$$\frac{V_1^-}{V_2^+} = \frac{b_1}{a_2} = \frac{Z_0}{r + Z_0}. \tag{2.189}$$

Substituting Equations (2.188) and (2.189) in Equation (2.187) and rearranging

$$T_{22} = \frac{Z_0}{r + Z_0} - T_{21}\frac{r}{r + Z_0}.$$

Combining this with Equation (2.185)

$$T_{22} = \frac{Z_0}{r + Z_0} - \frac{r}{Z_0}\frac{r}{r + Z_0} = \frac{Z_0^2 - r^2}{Z_0(r + Z_0)}. \tag{2.190}$$

Derivation of T_{12}

Combining Equations (2.184, 2.186 and 2.188)

$$T_{12} = -\frac{r + Z_0}{Z_0}\frac{r}{r + Z_0} = -\frac{r}{Z_0}. \tag{2.191}$$

Summary: The chain scattering matrix (T) parameters are given in Equations (2.184), (2.185), (2.190), and (2.191).

EXAMPLE 2.7 Cascading chain scattering parameters

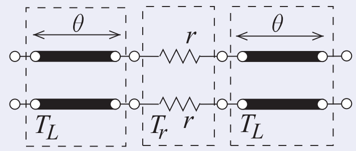

Develop the chain scattering parameters of the network to the right. Use a reference impedance $Z_{\text{REF}} = Z_0$, the characteristic impedance of the lines.

Solution:

The network comprises a transmission line of electrical length θ in cascade with a resistive network and another line of the same electrical length. From Equation (2.171) the scattering parameters of the transmission line are

$$\mathbf{S}_L = \begin{bmatrix} 0 & e^{-\jmath\theta} \\ e^{-\jmath\theta} & 0 \end{bmatrix}. \tag{2.192}$$

From Equation (2.177) the chain scattering matrix of the line is

$$\mathbf{T}_L = \begin{bmatrix} e^{\jmath\theta} & 0 \\ 0 & e^{-\jmath\theta} \end{bmatrix}. \tag{2.193}$$

From Example 2.6 the chain scattering matrix of the resistive network is

$$\mathbf{T}_r = \frac{1}{Z_0}\begin{bmatrix} gr + Z_0 & -r \\ r & (Z_0^2 - r^2)/(r + Z_0) \end{bmatrix}. \tag{2.194}$$

Yielding the chain scattering matrix of the cascade;

$$T_{LrL} = T_L T_r T_L$$
$$\frac{1}{Z_0}\begin{bmatrix} (r + Z_0)e^{2\jmath\theta} & -r \\ r & (Z_0^2 - r^2)/(r + Z_0)e^{-2\jmath\theta} \end{bmatrix}. \tag{2.195}$$

EXAMPLE 2.8 Input reflection coefficient of a terminated two-port.

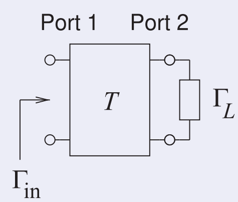

What is the input reflection coefficient in terms of chain scattering parameters of the terminated two-port to the right where the two-port is described by its chain scattering parameters.

Solution:

The chain scattering parameter relations are

$$\begin{bmatrix} a_1 \\ b_1 \end{bmatrix} = \begin{bmatrix} T_{11} & T_{12} \\ T_{21} & T_{22} \end{bmatrix}\begin{bmatrix} b_2 \\ a_2 \end{bmatrix}.$$

Expanding this matrix equation and using the substitution $a_2 = \Gamma_L b_2$

$$a_1 = T_{11}b_2 + T_{12}\Gamma_L b_2 \tag{2.196}$$
$$b_1 = T_{21}b_2 + T_{22}\Gamma_L b_2. \tag{2.197}$$

Multiplying Equation (2.196) by $(T_{21} + T_{22}\Gamma_L)$ and Equation (2.197) by $(T_{11} + T_{12}\Gamma_L)$ and then subtracting

$$(T_{21} + T_{22}\Gamma_L)a_1 = (T_{21} + T_{22}\Gamma_L)(T_{11}b_2 + T_{12}\Gamma_L)b_2$$
$$(T_{11} + T_{12}\Gamma_L)b_1 = (T_{11} + T_{12}\Gamma_L)(T_{21}b_2 + T_{22}\Gamma_L)b_2$$
$$(T_{21} + T_{22}\Gamma_L)a_1 = (T_{11} + T_{12}\Gamma_L)b_1.$$

Thus the input reflection coefficient is

$$\Gamma_{\text{in}} = \frac{b_1}{a_1} = \frac{T_{21} + T_{22}\gamma_L}{T_{11} + T_{12}\gamma_L}. \tag{2.198}$$

Now consider a transmission line of electrical length θ and characteristic impedance Z_0 (see the figure b) in cascade with the two-port.

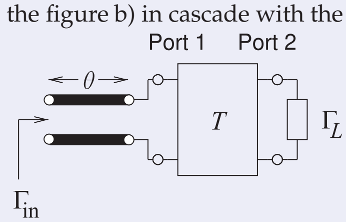

The input reflection coefficient now is found by first determining the total chain scattering matrix of the cascade:

$$^{T}\mathbf{T} = \mathbf{T_L T} = \begin{bmatrix} e^{\jmath\theta} & 0 \\ 0 & e^{-\jmath\theta} \end{bmatrix}\begin{bmatrix} T_{11} & T_{12} \\ T_{21} & T_{22} \end{bmatrix}$$
$$= \begin{bmatrix} T_{11}e^{\jmath\theta} & T_{12}e^{\jmath\theta} \\ T_{21}e^{-\jmath\theta} & T_{22}e^{-\jmath\theta} \end{bmatrix}\begin{bmatrix} ^{T}T_{11} & ^{T}T_{12} \\ ^{T}T_{21} & ^{T}T_{22} \end{bmatrix}.$$

Thus the input reflection coefficient is now

$$\Gamma_{\text{in}} = \frac{b_1}{a_1} = \frac{{}^{T}T_{21} + {}^{T}T_{22}\Gamma_L}{{}^{T}T_{11} + {}^{T}T_{12}\Gamma_L}$$
$$= \frac{T_{21}e^{-\jmath\theta} + T_{22}e^{-\jmath\theta}\Gamma_L}{T_{11}e^{\jmath\theta} + T_{12}e^{\jmath\theta}\Gamma_L}$$
$$= e^{-2\jmath\theta}\left(\frac{T_{21} + T_{22}\Gamma_L}{T_{11} + T_{12}\Gamma_L}\right). \quad (2.199)$$

If the load is now a short circuit $\Gamma_L = -1$ and the input reflection coefficient of the line and two-port cascade is

$$\Gamma_{\text{in}} = e^{-2\jmath\theta}\left(\frac{T_{21} - T_{22}}{T_{11} - T_{12}}\right). \quad (2.200)$$

2.6.1 Terminated Two-Port Network

A two-port with Port 2 terminated in a load with reflection coefficient Γ_L is shown in Figure 2-23 and $a_2 = \Gamma_L b_2$. Substituting this in Equation (2.175) leads to

$$a_1 = (T_{11} + T_{12}\Gamma_L)b_2 \quad \text{and} \quad b_1 = (T_{21} + T_{22}\Gamma_L)b_2,$$

eliminating b_2 results in

$$\Gamma_{\text{in}} = \frac{b_1}{a_1} = \frac{T_{21} + T_{22}\Gamma_L}{T_{11} + T_{12}\Gamma_L}. \quad (2.201)$$

2.7 Scattering Parameter Two-Port Relationships

2.7.1 Change in Reference Plane

It is often necessary during S parameter measurements of two-port devices to measure components at a position different from that actually desired. An example is shown in Figure 2-24(a). From direct measurement the S parameters are obtained, and thus the $\mathbf{T}$ matrix at Planes 1 and 2. However, $\mathbf{T}_{\text{DUT}}$ referenced to Planes 1′ and 2′ is required. Now,

$$\mathbf{T} = \mathbf{T}_{\theta_1}\mathbf{T}_{\text{DUT}}\mathbf{T}_{\theta_2}, \quad (2.202)$$

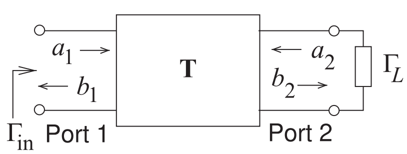

Figure 2-23: Terminated two-port network.

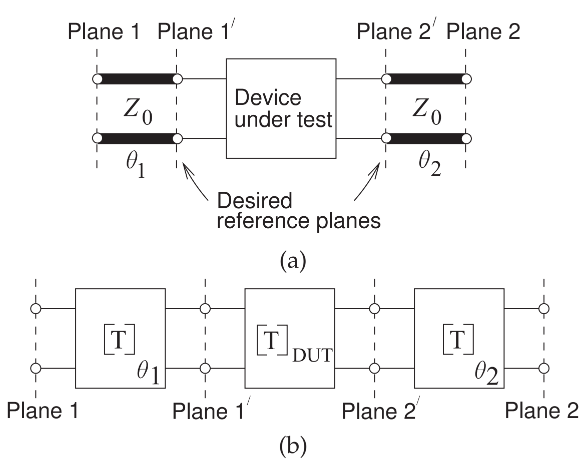

Figure 2-24: Two-port measurement setup: (a) a two-port comprising a device under test (DUT) and transmission line sections that create a reference plane at Planes 1 and 2; and (b) representation as cascaded two-port networks.

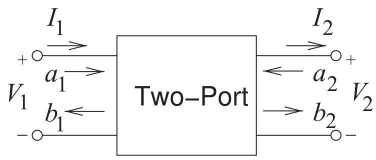

Figure 2-25: Two-port with parameters suitable for defining S and $ABCD$ parameters.

and so $$\mathbf{T}_{\text{DUT}} = \mathbf{T}_{\theta_1}^{-1}\mathbf{T}\mathbf{T}_{\theta_2}^{-1}. \tag{2.203}$$

A section of line with electrical length θ and port impedances equal to its characteristic impedance has

$$\mathbf{S} = \begin{bmatrix} 0 & \mathrm{e}^{-\jmath\theta} \\ \mathrm{e}^{-\jmath\theta} & 0 \end{bmatrix} \quad (2.204) \qquad \text{and } \mathbf{T}_\theta = \begin{bmatrix} \mathrm{e}^{\jmath\theta} & 0 \\ 0 & \mathrm{e}^{-\jmath\theta} \end{bmatrix}. \quad (2.205)$$

Therefore Equation (2.203) becomes

$$\mathbf{T}_{\text{DUT}} = \begin{bmatrix} T_{11}\mathrm{e}^{-\jmath(\theta_1+\theta_2)} & T_{12}\mathrm{e}^{-\jmath(\theta_1-\theta_2)} \\ T_{21}\mathrm{e}^{\jmath(\theta_1-\theta_2)} & T_{22}\mathrm{e}^{\jmath(\theta_1+\theta_2)} \end{bmatrix}, \tag{2.206}$$

and then the desired S parameters of the DUT are obtained as

$$\mathbf{S}_{\text{DUT}} = \begin{bmatrix} S_{11}\mathrm{e}^{\jmath 2\theta_1} & S_{12}\mathrm{e}^{\jmath(\theta_1+\theta_2)} \\ S_{21}\mathrm{e}^{\jmath(\theta_1+\theta_2)} & S_{22}\mathrm{e}^{\jmath 2\theta_2} \end{bmatrix}. \tag{2.207}$$

2.7.2 Conversion Between S and $ABCD$ Parameters

Figure 2-25 can be used to relate the parameters of the two views of the network. If both ports have the same reference impedance Z_0, then

$$\begin{bmatrix} V_1 \\ I_1 \end{bmatrix} = \begin{bmatrix} A & B \\ C & D \end{bmatrix} \begin{bmatrix} V_2 \\ I_2 \end{bmatrix} \quad \text{and} \quad \begin{bmatrix} b_1 \\ b_2 \end{bmatrix} = \begin{bmatrix} S_{11} & S_{12} \\ S_{21} & S_{22} \end{bmatrix} \begin{bmatrix} a_1 \\ a_2 \end{bmatrix}.$$

The S parameters are then expressed as

$$\begin{aligned} S_{11} &= \frac{A + B/Z_0 - CZ_0 - D}{\triangle} & S_{12} &= \frac{2(AD - BC)}{\triangle} \\ S_{21} &= \frac{2}{\triangle} & S_{22} &= \frac{-A + B/Z_0 - CZ_0 + D}{\triangle}, \end{aligned} \tag{2.208}$$

where $$\triangle = A + B/Z_0 + CZ_0 + D. \tag{2.209}$$

The $ABCD$ parameters can be expressed in terms of the S parameters as

$$A = \frac{(1+S_{11})(1-S_{22}) + S_{12}S_{21}}{2S_{21}} \tag{2.210}$$

$$B = Z_0\frac{(1+S_{11})(1+S_{22}) - S_{12}S_{21}}{2S_{21}} \tag{2.211}$$

$$C = \frac{1}{Z_0}\frac{(1-S_{11})(1-S_{22}) - S_{12}S_{21}}{2S_{21}} \tag{2.212}$$

$$D = \frac{(1-S_{11})(1+S_{22}) + S_{12}S_{21}}{2S_{21}}. \tag{2.213}$$

2.8 Return Loss, Substitution Loss, and Insertion Loss

2.8.1 Return Loss

Return loss, also known as **reflection loss**, is a measure of the fraction of power that is not delivered by a source to a load. If the power incident on a load is P_i and the power reflected by the load is P_r, then the return loss in decibels is [6, 7]

$$\mathrm{RL}_{\mathrm{dB}} = 10 \log \frac{P_i}{P_r}. \tag{2.214}$$

The better the load is matched to the source, the lower the reflected power and hence the higher the return loss. RL is a positive quantity if the reflected power is less than the incident power. If the load has a complex reflection coefficient ρ, then

$$\mathrm{RL}_{\mathrm{dB}} = 10 \log \left| \frac{1}{\rho^2} \right| = -20 \log |\rho| \,. \tag{2.215}$$

That is, the return loss is the negative of the input reflection coefficient expressed in decibels [8].

When generalized to a terminated two ports, the return loss is defined with respect to the input reflection coefficient of the terminated two port [9]. The two port in Figure 2-26 has the input reflection coefficient

$$\Gamma_{\mathrm{in}} = S_{11} + \frac{\Gamma_L S_{12} S_{21}}{(1 - \Gamma_L S_{22})}, \tag{2.216}$$

where Γ_L is the reflection coefficient of the load. Thus the return loss of a terminated two-port is

$$\mathrm{RL}_{\mathrm{dB}} = -20 \log |\Gamma_{\mathrm{in}}| = -20 \log \left| S_{11} + \frac{\Gamma_L S_{12} S_{21}}{(1 - \Gamma_L S_{22})} \right|. \tag{2.217}$$

If the load is matched, i.e. $Z_L = Z_0^*$ (the system reference impedance), then

$$\mathrm{RL}_{\mathrm{dB}} = -20 \log |S_{11}| \,. \tag{2.218}$$

This return loss is also called the input return loss since the reflection coefficient is calculated at Port 1. The output return loss is calculated looking into Port 2 of the two-port, where now the termination at Port 1 is just the source impedance.

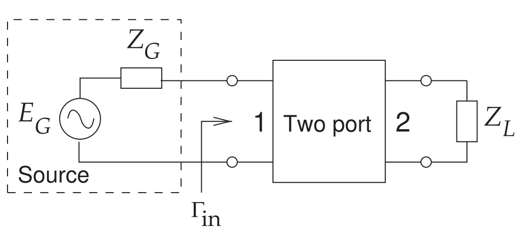

Figure 2-26: Terminated two-port used to define return loss.

2.8.2 Substitution Loss and Insertion Loss

The substitution loss is the ratio of the power, ${}^{i}P_L$, delivered to the load by an initial two-port identified by the leading superscript 'i', and the power delivered to the load, ${}^{f}P_L$, with a substituted final two-port identified by the leading superscript 'f'. In terms of generalized scattering parameters with reference impedances Z_{01} at Port 1 and Z_{02} at Port 2 the substitution loss in decibels is (using the results of Example 3.2 and noting that Γ_S is referred to Z_{01} and Γ_L is referred to Z_{02})

$$L_S|_{\mathrm{dB}} = \frac{{}^{i}P_L}{{}^{f}P_L} = 10\log\left|\frac{{}^{i}S_{21}}{{}^{f}S_{21}}\frac{\left[(1-{}^{f}S_{11}\Gamma_S)(1-{}^{f}S_{22}\Gamma_L)-{}^{f}S_{12}{}^{f}S_{21}\Gamma_S\Gamma_L\right]}{\left[(1-{}^{i}S_{11}\Gamma_S)(1-{}^{i}S_{22}\Gamma_L)-{}^{i}S_{12}{}^{i}S_{21}\Gamma_S\Gamma_L\right]}\right|^2. \tag{2.219}$$

Insertion loss is a special case of substitution loss with particular types of initial two-port networks. There are a number of special cases to consider.

Insertion Loss with an Ideal Adaptor

Comparing the power delivered to the load with an inserted two-port with that delivered with an ideal adaptor is the commonly accepted definition of insertion loss [10]. That is, 'insertion loss' without qualifications is the same as 'insertion loss with an ideal adaptor.' An ideal adaptor (as the initial two-port network) transforms from the Port 1 reference impedance, Z_{01}, to the Port 2 reference impedance, Z_{02}. In terms of generalized S parameters the ideal adaptor has ${}^{i}\left({}^{G}S_{11}\right) = 0 = {}^{i}\left({}^{G}S_{22}\right)$ (for no reflection), ${}^{i}\left({}^{G}S_{12}\right){}^{i}\left({}^{G}S_{21}\right) = 1$ (for no loss in the adaptor and there is no phase shift), and ${}^{i}\left({}^{G}S_{12}\right) = {}^{i}\left({}^{G}S_{21}\right)Z_{01}/Z_{02}$ (for reciprocity). (If $Z_{01} = Z_{02}$ this ideal adaptor is the same as a direct connection.) Insertion loss in decibels is, using Equation (2.219):

$$\mathrm{IL}|_{\mathrm{dB}} = 10\log\left\{\frac{Z_{02}}{Z_{01}}\left|\frac{\left[1-{}^{f}\left({}^{G}S_{11}\right)\Gamma_S\right]\left[1-{}^{f}\left({}^{G}S_{22}\right)\Gamma_L\right]-{}^{f}\left({}^{G}S_{12}\right){}^{f}\left({}^{G}S_{21}\right)\Gamma_S\Gamma_L}{{}^{f}\left({}^{G}S_{12}\right)(1-\Gamma_S\Gamma)}\right|^2\right\} \tag{2.220}$$

Attenuation is defined as the insertion loss without source and load reflections ($\Gamma_S = 0 = \Gamma_L$) [10], and Equation (2.220) becomes

$$A|_{\mathrm{dB}} = 10\log\left(\frac{Z_{02}}{Z_{01}}\frac{1}{\left|{}^{G}S_{21}\right|^2}\right) \quad (= \mathrm{IL}|_{\mathrm{dB}} \text{ with } \Gamma_S = 0 = \Gamma_L). \tag{2.221}$$

where ${}^{G}S_{21}$ is that of the final two-port.

Insertion Loss with Direct Connection

With normalized S parameters, i.e. $Z_{01} = Z_{02}$, the insertion loss with an initial direct connection is as given in Equation (2.220). With different reference impedances at each port, the initial direct connection 'i', from Example 2.4, ${}^{i}\left({}^{G}S_{11}\right) = (Z_{02}-Z_{01})/(Z_{02}+Z_{01})$, ${}^{i}\left({}^{G}S_{22}\right) = -{}^{i}\left({}^{G}S_{11}\right)$, ${}^{i}\left({}^{G}S_{21}\right) = \left[1+{}^{i}\left({}^{G}S_{11}\right)\right] \times \sqrt{\Re\{Z_{02}\}}/\sqrt{\Re\{Z_{01}\}}$, and ${}^{i}\left({}^{G}S_{12}\right) =$

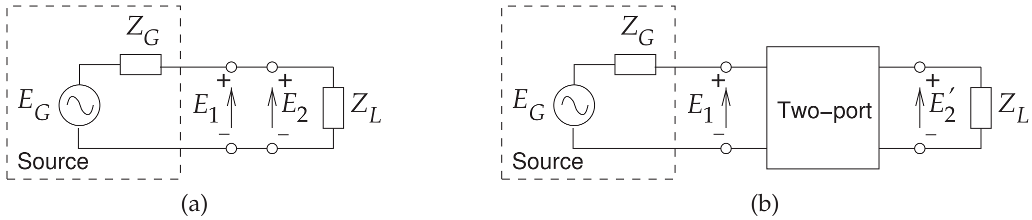

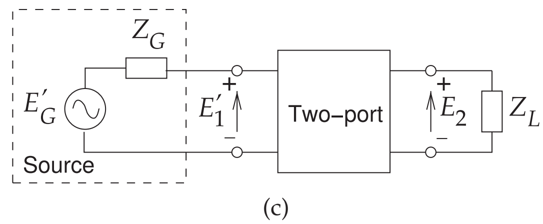

Figure 2-27: Two-port insertion and definition of variables for defining insertion loss: (a) source and load before insertion; (b) insertion of two-port network with source level unchanged; and (c) insertion of two-port network with source level adjusted to maintain a constant voltage across the load.

$\left[1 + {}^{i}\left({}^{G}S_{22}\right)\right] \sqrt{\Re\{Z_{01}\}}/\sqrt{\Re\{Z_{02}\}}$. These S parameters of the initial two-port network are substituted in Equation (2.219) to determine insertion loss with a direct connection.

2.8.3 Measurement of Insertion Loss

If the S parameters of a two-port network can be measured it is simple to calculate the insertion loss of the two-port. However there are situations where the S parameters cannot be measured and this includes where there is not a port connection (e.g., the air side of an antenna) and the system reference impedances differ at the two ports. In this section methods for measuring insertion loss in such difficult situations is described. If S parameter measurements are not available the insertion loss of a two-port network is defined as the ratio, in decibels, of voltages immediately beyond the point of insertion, before and after insertion [6, 11]. Referring to Figure 2-27(a and b), insertion loss is expressed in decibels as

$$\mathrm{IL_{dB}} = 20 \log \left| \frac{E_2}{E_2'} \right|, \tag{2.222}$$

where E_2 is the voltage across the load (Z_L) before insertion of the two-port and E_2' is the voltage across the load (Z_L) after insertion of the two-port. The power delivered to the load is proportional to the square of the magnitude of the voltage across the load, so this definition is equivalent to that described in section 2.8.2 where

$$\mathrm{IL_{dB}} = 10 \log \frac{P_L}{P_T}, \tag{2.223}$$

where P_L is the power delivered to the load before the insertion of the two-port and P_T is the power delivered to the load following insertion.

EXAMPLE 2.9 Insertion loss of a two-port in a different reference system

A 50 Ω attenuator has an attenuation of 3 dB and a return loss of 20 dB. If the attenuator is used in a 75 Ω system what is the insertion loss of the attenuator?

Solution:

The insertion loss can be calculated using the insertion loss formula in Equation (2.219). To apply this the 50 Ω S parameters of the attenuator are needed and then the load and source reflection coefficients, Γ_L and Γ_S respectively, which will be the reflection coefficients of the 75 Ω load and source impedances referred to 50 Ω. Also note that $Z_{01} = Z_{02} = 50\ \Omega$. Since there are two reference systems the leading superscripts 50 and 75 will be used to distinguish them.

Step 1. Find Γ_S and Γ_L in the 50 Ω system: $\Gamma_S = \Gamma_L = (55 - 50)/(55 + 50) = 0.2000$

Step 2. Find the S parameters in a 50 Ω system. (case 1, assume $\angle S_{11} = \angle S_{21} = 0°$)

It is known that ${}^{50}\mathrm{RL}|_{\mathrm{dB}} = 20$ dB and ${}^{50}\mathrm{IL}|_{\mathrm{dB}} = 3$ dB. Also an attenuator is symmetrical so that ${}^{50}S_{11} = {}^{50}S_{22}$ and ${}^{50}S_{12} = {}^{50}S_{21}$. Using Equations (2.218) and (2.221)

$$|{}^{50}S_{11}| = |{}^{50}S_{22}| = 10^{-{}^{50}\mathrm{RL}|_{\mathrm{dB}}/20} = 10^{-20/20} = 0.1000$$

$$\text{and} \quad |{}^{50}S_{12}| = |{}^{50}S_{21}| = 10^{-{}^{50}\mathrm{IL}|_{\mathrm{dB}}/20} = 10^{-3/20} = 0.7080.$$

The phases of the S parameters are not known. Assume first (use the leading subscript '1') that the phases are 0° and consider alternatives later and then the S parameter matrix is

$${}_1\mathbf{S} = \begin{bmatrix} {}^{50}_{1}S_{11} & {}^{50}_{1}S_{12} \\ {}^{50}_{1}S_{21} & {}^{50}_{1}S_{22} \end{bmatrix} = \begin{bmatrix} 0.1000 & 0.7080 \\ 0.7080 & 0.1000 \end{bmatrix}. \tag{2.224}$$

From Equation (2.220)

$${}^{75}_{1}\mathrm{IL}_{\mathrm{dB}} = 10 \log \left[\frac{50}{50} \left| \frac{(1 - 0.1 \cdot 0.2)\,(1 - 0.1 \cdot 0.2) - 0.7080 \cdot 0.7080 \cdot 0.2 \cdot 0.2}{0.7080\,(1 - 0.2 \cdot 0.2)} \right|^2 \right] = 2.82 \text{ dB}. \tag{2.225}$$

Step 3 Four phase assumptions for S_{11} and S_{22}

Case 1	$\angle S_{11} = \angle S_{22} = 0°$, $\angle S_{21} = \angle S_{12} = 0°$	${}^{75}_{1}\mathrm{IL}_{\mathrm{dB}} = 2.82$ dB
Case 2	$\angle S_{11} = \angle S_{22} = 0°$, $\angle S_{21} = \angle S_{12} = 180°$	${}^{75}_{2}\mathrm{IL}_{\mathrm{dB}} = 2.82$ dB
Case 3	$\angle S_{11} = \angle S_{22} = 180°$, $\angle S_{21} = \angle S_{12} = 0°$	${}^{75}_{3}\mathrm{IL}_{\mathrm{dB}} = 3.53$ dB
Case 4	$\angle S_{11} = \angle S_{22} = 180°$, $\angle S_{21} = \angle S_{12} = 180°$	${}^{75}_{4}\mathrm{IL}_{\mathrm{dB}} = 3.53$ dB

Thus just knowing the return loss and insertion loss in one reference system is not enough to know the insertion loss in another system without knowing the phases of the S parameters.

EXAMPLE 2.10 Insertion loss calculation using change of reference impedance

A 50 Ω attenuator has an attenuation of 3 dB and a return loss of 20 dB. If the attenuator is used in a 75 Ω system what is the insertion loss of the attenuator?

Solution:

This is alternative to the method used in Example 2.9. Using the S parameters of the attenuator in Equation (2.224), in a 75 Ω system the S parameters are found using Equation (2.138) and noting that $\Gamma_{75} = 0.2$ is the reflection coefficient of 75 Ω in a 50 Ω system:

$$ {}^{75}\mathbf{S} = \begin{bmatrix} {}^{75}S_{11} & {}^{75}S_{12} \\ {}^{75}S_{21} & {}^{75}S_{22} \end{bmatrix} = \begin{bmatrix} {}^{50}_{1}S_{11} - \Gamma_{75} & {}^{50}_{1}S_{12} \\ {}^{50}_{1}S_{21} & {}^{50}_{1}S_{22} - \Gamma_{75} \end{bmatrix} \begin{bmatrix} 1 - \Gamma_{75}\,{}^{50}_{1}S_{11} & -\Gamma_{75}\,{}^{50}_{1}S_{12} \\ -\Gamma_{75}\,{}^{50}_{1}S_{21} & 1 - \Gamma_{75}\,{}^{50}_{1}S_{22} \end{bmatrix}^{-1} $$

$$ = \begin{bmatrix} -0.1 & 0.7080 \\ 0.7080 & -0.1 \end{bmatrix} \begin{bmatrix} 0.9800 & -0.1416 \\ -0.1416 & 0.9800 \end{bmatrix}^{-1} = \begin{bmatrix} 0.002379 & 0.7227 \\ 0.7227 & 0.002379 \end{bmatrix}. \quad (2.226) $$

In the 75 Ω system the load and source are matched and using Equation (2.220)

$$ {}^{75}_{1}\mathrm{IL}_{\mathrm{dB}} = 10 \log \frac{1}{|{}^{75}S_{21}|^2} = 10 \log \frac{1}{|0.7227|^2} = 2.82 \text{ dB}. \quad (2.227) $$

which is in agreement with the calculation in Example 2.9, see Equation (2.225).

2.8.4 Minimum Transducer Loss, Intrinsic Attenuation

Another situation often required is determining the minimum possible loss of a two-port. This is obtained with lossless two-port networks, M_1 and M_2 at the input and output of the two-port of interest, M_3. M_1 and M_2 are adjusted to obtained the minimum possible loss of M_3. This is not the same as designing M_1 and M_2 to obtain matching. The **minimum insertion loss**, also called the intrinsic attenuation, or minimum transducer loss in dB is [12] (the derivation is involved),

$$ L_{\mathrm{TM}}|_{\mathrm{dB}} = 10 \log \left[\frac{Z_{02}}{Z_{01}} \frac{|1 - S_{22}\Gamma_{\mathrm{TM}}|^2 - |(S_{12}S_{21} - S_{11}S_{22})\Gamma_{\mathrm{TM}} + S_{11}|^2}{|S_{21}|^2 (1 - |\Gamma_{\mathrm{TM}}|^2)} \right] \quad (2.228) $$

where the S parameters are of M_3 Z_{01} and Z_{02} are the real reference impedances at ports 1 and 2 respectively, and

$$ \Gamma_{\mathrm{TM}} = \frac{B}{2A} \left(1 \pm \sqrt{1 - \frac{2|A|}{B}} \right), \quad (2.229) $$

where

$$ A = S_{22} + S_{11}^{*} (S_{12}S_{21} - S_{11}S_{22}) \quad (2.230) $$

and

$$ B = 1 - |S_{11}|^2 + |S_{22}|^2 - |S_{12}S_{21} - S_{11}S_{22}|^2. \quad (2.231) $$

The intrinsic attenuation is a useful metric when a device is being developed and has not yet been optimally matched.

Other insertion loss concepts are **comparison loss**, **mismatch loss**, and **conjugate mismatch loss**, see [10].

2.9 Scattering Parameters and Directional Couplers

Directional couplers were described in Section 5.8 of [13] but described without the use of S parameters. A directional coupler with ports defined as in Figure 2-28, and with the ports matched (so that $S_{11} = 0 = S_{22} = S_{33} = S_{44}$), has the following scattering parameter matrix:

$$\mathbf{S} = \begin{bmatrix} 0 & T & 1/C & 1/I \\ T & 0 & 1/I & 1/C \\ 1/C & 1/I & 0 & T \\ 1/I & 1/C & T & 0 \end{bmatrix}. \tag{2.232}$$

There are many types of directional couplers, and the phases of the traveling waves at the ports will not necessarily be in phase as Equation (2.232) implies. When the phase difference between traveling waves entering at Port 1 and leaving at Port 2 is $90°$, Equation (2.232) becomes

$$\mathbf{S} = \begin{bmatrix} 0 & -\jmath T & 1/C & 1/I \\ -\jmath T & 0 & 1/I & 1/C \\ 1/C & 1/I & 0 & -\jmath T \\ 1/I & 1/C & -\jmath T & 0 \end{bmatrix}. \tag{2.233}$$

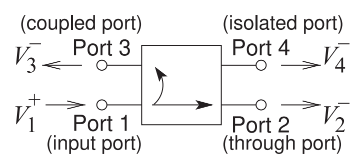

Figure 2-28: Schematic of a directional coupler.

EXAMPLE 2.11 Identifying Ports of a Directional Coupler

A directional coupler has the following S parameters:

$$S = \begin{bmatrix} 0 & 0.9 & 0.001 & 0.1 \\ 0.9 & 0 & 0.1 & 0.001 \\ 0.001 & 0.1 & 0 & 0.9 \\ 0.1 & 0.001 & 0.9 & 0 \end{bmatrix}.$$

(a) What are the through (i.e., transmission) paths? Identify two paths. That is, identify the pairs of ports at the ends of the through paths.
First note that the assignment of ports to a directional coupler is arbitrary. So the S parameters need to be considered to figure out how the ports are related. The S parameters relate the forward-traveling waves to the backward-traveling waves and this leads to the required understanding, thus

$$\begin{bmatrix} V_1^- \\ V_2^- \\ V_3^- \\ V_4^- \end{bmatrix} = S \begin{bmatrix} V_1^+ \\ V_2^+ \\ V_3^+ \\ V_4^+ \end{bmatrix} = \begin{bmatrix} 0 & 0.9 & 0.001 & 0.1 \\ 0.9 & 0 & 0.1 & 0.001 \\ 0.001 & 0.1 & 0 & 0.9 \\ 0.1 & 0.001 & 0.9 & 0 \end{bmatrix} \begin{bmatrix} V_1^+ \\ V_2^+ \\ V_3^+ \\ V_4^+ \end{bmatrix}.$$

Writing the S parameters out this way makes it easier to identify the largest backward-traveling waves for each of the inputs at Ports 1, 2, 3, and 4. The backward-traveling wave will leave the directional coupler and the inputs will be forward-traveling waves. Consider Port 1, the largest backward-traveling wave is at Port 2, and so Ports 1 and 2 define one of the through paths. The other through path is between Ports 3 and 4.
So the through paths are 1–2 and 3–4.

(b) What is the coupled port for the signal entering Port 1?

The coupled port is identified by the port with the largest backward-traveling signal not including the port at the other end of the through path. For Port 1 the coupled port is Port 4.

(c) What is the coupling factor?

$$C = \frac{V_1^+}{V_4^-} = \frac{1}{0.1} = 10 = 20\ \text{dB}.$$

(d) What is the isolated port for the signal entering Port 1?
The isolated port is Port 3. The backward-traveling wave at this port is the smallest given an input at Port 1.

(e) What is the isolation factor?

$$I = \frac{V_1^+}{V_3^-} = \frac{1}{0.001} = 1000 = 60\ \text{dB}.$$

(f) What is the directivity factor?
The directivity factor indicates how much stronger the signal is at the coupled port compared to the isolated port for a signal at the input. For an input at Port 1, the directivity factor is

$$D = \frac{V_4^-}{V_3^-} = \frac{0.1}{0.001} = 100 = 40\ \text{dB}.$$

As a check $D = I/C = 1000/10 = 100$.

(g) Draw a schematic of the directional coupler.
There are four ways to draw it depending on which port is chosen to be the input port (see Figure 2-29).

2.10 Summary

There are several network parameters used with RF and microwave circuits. Which is used depends on which makes the task of visualizing circuit operation more clear, which makes analyzing circuits more convenient, and which makes design easier.

Scattering parameters are parameters that are almost exclusively used by RF and microwave engineers. They describe power flow and traveling waves and are essential to describing distributed circuits. Much of RF and microwave engineering is concerned with managing the signal-to-noise power ratio and with power efficiency. It is therefore natural to work with parameters that directly relate to power flow. RF and microwave design is characterized by conceptual insight and it is essential to use parameters

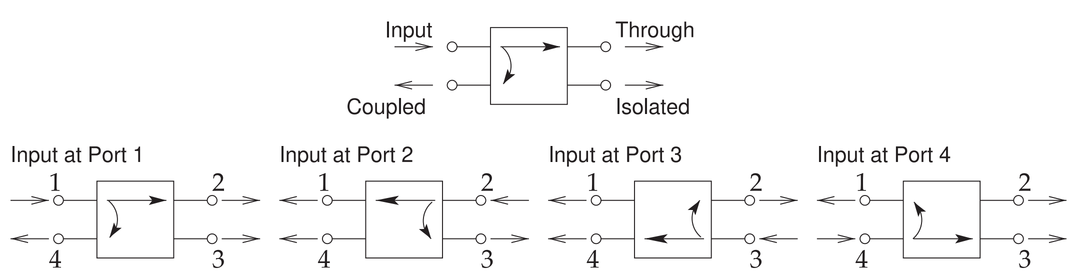

Figure 2-29: Directional coupler schematic drawn with each of the four possible input ports.

and graphical representations that are close to the physical world. Scattering parameters have very natural graphical representations, as will be seen in the next chapter.

The next most important network parameters considered in this chapter are the $ABCD$ parameters. The special significance of these parameters in microwave engineering is that they can be used to relate a distributed circuit to a lumped-element circuit. Many RF designs begin as lumped-element prototypes that are eventually transformed into electrically equivalent distributed structures. This equivalence process nearly always involves $ABCD$ parameters.

2.11 References

[1] N. Marcuvitz, *Waveguide Handbook*. McGraw-Hill, 1955.

[2] R. Collins, *Foundations for Microwave Engineering*. McGraw Hill, 1966.

[3] D. M. Kerns and R. W. Beatty, *Basic theory of waveguide junctions and introductory microwave network analysis*. Pergamon Press New York, 1967.

[4] R. B. Marks and D. F. Williams, "A general waveguide circuit theory," *Journal of Research-National Institute of Standards and Technology*, vol. 97, pp. 533–533, Sep.–Oct. 1992.

[5] D. Williams and B. Alpert, "Causality and waveguide circuit theory," *IEEE Trans. on Microwave Theory and Techniques*, vol. 49, no. 4, pp. 615–623, Apr. 2001.

[6] "Telecommunications: Glossary of Telecommunication Terms," Federal Standard 1037C, U.S. General Services Administration Information Technology Service, Aug. 7, 1996.

[7] T. S. Bird, "Definition and misuse of return loss [report of the trans. editor-in-chief]," *IEEE Antennas and Propagation Magazine*, vol. 51, no. 2, pp. 166–167, Apr. 2009.

[8] IEEE, *IEEE Standard Dictionary of Electrical and Electronic Engineering Terms*, 4th ed. IEEE Press, 1988.

[9] T. Otoshi, "Maximum and minimum return losses from a passive two-port network terminated with a mismatched load," *IEEE Trans. on Microwave Theory and Techniques*, vol. 42, no. 5, pp. 787–792, May 1994.

[10] R. Beatty, "Insertion loss concepts," *Proc. of the IEEE*, vol. 52, no. 6, pp. 663–671, Jun. 1964.

[11] "MIL-STD-220C: Test method standard, method of insertion loss measurement."

[12] R. W. Beatty, "Intrinsic attenuation," *IEEE Transactions on Microwave Theory and Techniques*, vol. 11, no. 3, pp. 179–182, 1963.

[13] M. Steer, *Microwave and RF Design, Transmission Lines*, 3rd ed. North Carolina State University, 2019.

2.12 Exercises

1. A load has a reflection coefficient of $0.5 - \jmath 0.1$ in a 75 Ω reference system. What is the reflection coefficient in a 50 Ω reference system?

2. The 50 Ω S parameters of a two-port are $S_{11} = 0.5 + \jmath 0.5$, $S_{12} = 0.95 + \jmath 0.25$, $S_{21} = 0.15 - \jmath 0.05$, and $S_{22} = 0.5 - \jmath 0.5$. Port 1 is connected to a 50 Ω source with an available power of 1 W and Port 2 is terminated in 50 Ω. What is the power reflected from Port 1?

3. Derive the two-port 50 Ω S parameters for the resistive circuit below.

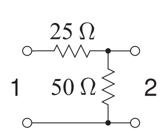

4. Derive the two-port 50 Ω S parameters at 1 GHz for the circuit below.

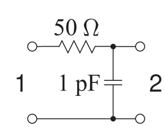

5. Derive the two-port 50 Ω S parameters at 1 GHz for the circuit below.

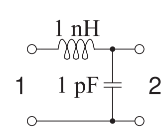

6. Derive the two-port S parameters of a shunt 25 Ω resistor in a 50 Ω reference system using the method presented in Section 2.3.5.

7. Derive the two-port S parameters of a series

25 Ω resistor in a 100 Ω reference system using the method presented in Section 2.3.5.

8. A two-port consists of a π resistor network as shown. Derive the scattering parameters referenced to 50 Ω using the method in Section 2.3.5.

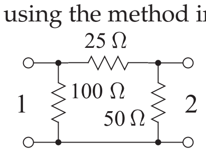

9. A two-port consists of a T resistor network as shown. Derive the scattering parameters referenced to 1 Ω using the method in 2.3.5.

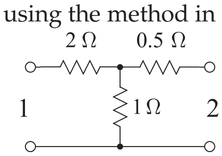

10. Derive the 50 Ω S parameters of the following.

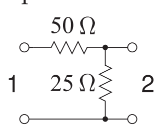

11. Derive the 50 Ω S parameters of the following.

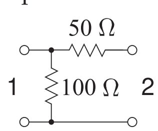

12. Derive the 100 Ω S parameters of the following.

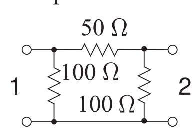

13. The scattering parameters of a certain two-port are $S_{11} = 0.5 + \jmath 0.5$, $S_{12} = 0.95 + \jmath 0.25$, $S_{21} = 0.15 - \jmath 0.05$, and $S_{22} = 0.5 - \jmath 0.5$. The system reference impedance is 50 Ω.
   (a) Is the two-port reciprocal? Explain.
   (b) Consider that Port 1 is connected to a 50 Ω source with an available power of 1 W. What is the power delivered to a 50 Ω load placed at Port 2?
   (c) What is the reflection coefficient of the load required for maximum power transfer at Port 2?

14. In characterizing a two-port, power could only be applied at Port 1. The signal reflected was measured and the signal at a 50 Ω load at Port 2 was also measured. This yielded two S parameters referenced to 50 Ω: $S_{11} = 0.3 - \jmath 0.4$ and $S_{21} = 0.5$.
   (a) If the network is reciprocal, what is S_{12}?
   (b) Is the two-port lossless?
   (c) What is the power delivered into the 50 Ω load at Port 2 when the available power at Port 1 is 0 dBm?

15. The S parameters of a two-port are $S_{11} = 0.25$, $S_{12} = 0$, $S_{21} = 1.2$, and $S_{22} = 0.5$. The system reference impedance is 50 Ω and $Z_G = 50$ Ω. The power available from the source is 1 mW. $Z_L = 25$ Ω.

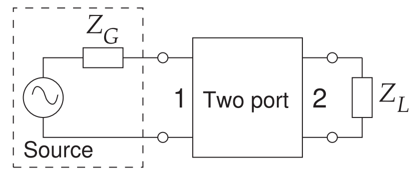

   (a) Is the two-port reciprocal and why?
   (b) What is the voltage of the source?
   (c) What is the power reflected from Port 1?
   (d) Determine the z parameters of the two-port.
   (e) Using z parameters, what is the power dissipated by the load at Port 2?

16. The scattering parameters of a two-port network are $S_{11} = 0.25$, $S_{21} = 2.$, $S_{21} = 0.1$, and $S_{22} = 0.5$ and the reference impedance is 50 Ω. What are the scattering transfer (T) parameters of the two-port?

17. A matched lossless transmission line has a length of one-quarter wavelength. What are the scattering parameters of the two-port?

18. Consider a two-port comprising a 100 Ω resistor connected in series between the ports.
   (a) Write down the S parameters of the two-port using a 50 Ω reference impedance.
   (b) From the scattering parameters derive the $ABCD$ parameters of the two-port.

19. Consider a two-port comprising a 25 Ω resistor connected in shunt.
   (a) Write down the scattering parameters of the two-port using a 50 Ω reference impedance.
   (b) From the scattering parameters derive the $ABCD$ parameters of the two-port.

20. What are the scattering transfer T parameters of a two port with the scattering parameters $S_{11} = 0 = S_{22}$ and $S_{12} = -\jmath = S_{21}$?

21. The scattering parameters of a two-port amplifier referred to 50 Ω are $S_{11} = 0.5$, $S_{21} = 2$, $S_{12} = 0.1$, and $S_{22} = -0.01$. What are the generalized scattering parameters of the two-port network if the reference impedance at Port 1 is 100 Ω and at Port 2 is 10 Ω?

22. A 50 Ω, 10 dB attenuator is inserted in a 75 Ω system. (That is, the attenuator is a two-port

network and using a 50 Ω reference the S-parameters of the attenuator are $S_{11} = 0 = S_{22}$ and the insertion loss of the two-port in the 50 Ω system is 10 dB. Now consider the same two-port in a 75 Ω system.)

(a) What is the transmission coefficient in the 75 Ω system?
(b) What is the attenuation (i.e., the insertion loss) in decibels in the 75 Ω system?
(c) What is the input reflection coefficient at Port 1 including the 75 Ω at Port 2?

23. A two-port has the 50-Ω scattering parameters $S_{11} = 0.1$; $S_{12} = 0.9 = S_{21}$; $S_{22} = 0.2$. The 50-Ω source at port 1 has an available power of 1 W. (This is the power that would be delivered to a 50 Ω termination at the source.)
    (a) What is the power delivered to a 50 Ω load at port 2?
    (b) What are the generalized scattering parameters with a 50 Ω reference at port 1 and a 75 Ω reference at port 2?
    (c) Using the generalized scattering parameters, calculate the power delivered to the 50 Ω load at port 2.

24. A two-port is matched to a source with a Thevenin impedance of 50 Ω connected at Port 1 and a load of 25 Ω at Port 2. If the two-port is represented by generalized scattering parameters, what should the normalization impedances at the ports be for $S_{11} = 0 = S_{22}$?

25. A two-port is terminated at Port 2 in 50 Ω. At Port 1 is a source with a Thevenin equivalent impedance of 75 Ω. The generalized scattering parameters of the two-port are $S_{11} = 0$, $S_{21} = 2.$, $S_{12} = 0.1$, and $S_{22} = 0.5$. The reference impedances are 75 Ω at Port 1 and 50 Ω at Port 2. If the Thevenin equivalent source has a peak voltage of 1 V, write down the root power waves at each port.

26. A two-port is terminated at Port 2 in 10 Ω. At Port 1 is a source with a Thevenin equivalent impedance of 100 Ω. The generalized scattering parameters of the two-port are $S_{11} = 0.2$, $S_{21} = 0.5$, $S_{12} = 0.1$, and $S_{22} = 0.3$. The reference impedances are 100 Ω at Port 1 and 10 Ω at Port 2. If the Thevenin equivalent source has a peak voltage of 50 V, what are a_1, b_1, a_2, and b_2?

27. The scattering parameters of a two-port network are $S_{11} = 0.6$, $S_{21} = 0.8$, $S_{12} = 0.5$, and $S_{22} = 0.3$ and the reference impedance is 50 Ω. At Port 1 a 50 Ω transmission line with an electrical length of 90° is connected and at Port 2 a 50 Ω transmission line with an electrical length of 180° is connected. What are the scattering parameters of the cascaded system (transmission line–original two-port–transmission line)?

28. A connector has the scattering parameters $S_{11} = 0.05$, $S_{21} = 0.9$, $S_{12} = 0.9$, and $S_{22} = 0.04$ and the reference impedance is 50 Ω. What is the return loss in dB of the connector at Port 1 in a 50 Ω system?

29. The scattering parameters of an amplifier are $S_{11} = 0.5$, $S_{21} = 2.$, $S_{12} = 0.1$, and $S_{22} = -0.2$ and the reference impedance is 50 Ω. If the amplifier is terminated at Port 2 in a resistance of 25 Ω, what is the return loss in dB at Port 1?

30. A two-port network has the scattering parameters $S_{11} = -0.5$, $S_{21} = 0.9$, $S_{12} = 0.8$, and $S_{22} = 0.04$ and the reference impedance is 50 Ω.
    (a) What is the return loss in dB of the connector at Port 1 in a 50 Ω system?
    (b) Is the two-port reciprocal and why?

31. A two-port network has the scattering parameters $S_{11} = -0.2$, $S_{21} = 0.8$, $S_{12} = 0.7$, and $S_{22} = 0.5$ and the reference impedance is 75 Ω.
    (a) What is the return loss in dB of the connector at Port 1 in a 75 Ω system?
    (b) Is the two-port reciprocal and why?

32. A cable has the scattering parameters $S_{11} = 0.1$, $S_{21} = 0.7$, $S_{12} = 0.7$, and $S_{22} = 0.1$. At Port 2 is a 55 Ω load and the S parameters and reflection coefficients are referred to 50 Ω.
    (a) What is the load's reflection coefficient?
    (b) What is the input reflection coefficient of the terminated cable?
    (c) What is the return loss, at Port 1 and in dB, of the cable terminated in the load?

33. A cable has the 50 Ω scattering parameters $S_{11} = 0.05$, $S_{21} = 0.5$, $S_{12} = 0.5$, and $S_{22} = 0.05$. What is the insertion loss in dB of the cable if the source at Port 1 has a 50 Ω Thevenin impedance and the termination at Port 2 is 50 Ω?

34. A 1 m long cable has the 50 Ω scattering parameters $S_{11} = 0.1$, $S_{21} = 0.7$, $S_{12} = 0.7$, and $S_{22} = 0.1$. The cable is used in a 55 Ω system.
    (a) What is the return loss in dB of the cable in the 55 Ω system? (Hint see Section 2.3.4 and consider finding Z_{in}.]
    (b) What is the insertion loss in dB of the cable in the 55 Ω system? Follow the procedure in Example 2.9
    (c) What is the return loss in dB of the cable in a 50 Ω system?
    (d) What is the insertion loss in dB of the cable in a 50 Ω system?

35. A 1 m long cable has the 50 Ω scattering parameters $S_{11} = 0.1$, $S_{21} = 0.7$, $S_{12} = 0.7$, and $S_{22} = 0.1$. The cable is used in a 55 Ω system. Follow the procedure in Example 2.10.
    (a) What is the return loss in dB of the cable in the 55 Ω system?
    (b) What is the insertion loss in dB of the cable in the 55 Ω system?
36. A 10 m long cable has the 50 Ω scattering parameters $S_{11} = -0.1$, $S_{21} = 0.5$, $S_{12} = 0.5$, and $S_{22} = -0.1$. The cable is used in a 75 Ω system. Use the change of S parameter reference impedance method [Parallels Example 2.10]. Express your answers in decibels.
    (a) What is the return loss of the cable in the 75 Ω system?
    (b) What is the insertion loss of the cable in the 75 Ω system?
37. A 1 m long cable has the 50 Ω scattering parameters $S_{11} = 0.05$, $S_{21} = 0.5$, $S_{12} = 0.5$, and $S_{22} = 0.05$. The Thevenin equivalent impedance of the source and terminating load impedances of the cable are 50 Ω.
    (a) What is the return loss in dB of the cable?
    (b) What is the insertion lossin dB of the cable?
38. A cable in a 50 Ω system has the S parameters $S_{11} = 0.1$, $S_{21} = 0.7$, $S_{12} = 0.7$, and $S_{22} = 0.1$. The available power at Port 1 is 0 dBm and at Port 2 is a 55 Ω load. Γ is reflection coefficient and a_n and b_n are the root power waves at the nth port..
    (a) What is the load's Γ?
    (b) What is a_1 (see Equation (2.117)?
    (c) What is b_2?
    (d) What is a_2?
    (e) What is the power, in dBm, delivered to the load?
    (f) What is the power, in dBm, delivered to the load if the cable is removed and replaced by a direct connection?
    (g) Hence what is the insertion loss, in dB, of the cable?
39. A lossy directional coupler has the following 50 Ω S parameters:

$$S = \begin{bmatrix} 0 & -0.95\jmath & 0.005 & 0.1 \\ -0.95\jmath & 0 & 0.1 & 0.005 \\ 0.005 & 0.1 & 0 & -0.95\jmath \\ 0.1 & 0.005 & -0.95\jmath & 0 \end{bmatrix}.$$

    (a) What are the through (transmission) paths (identify two paths)? That is, identify the pairs of ports at the ends of the through paths.
    (b) What is the coupling in decibels?
    (c) What is the isolation in decibels?
    (d) What is the directivity in decibels?
40. A directional coupler has the following characteristics: coupling factor $C = 20$, transmission factor 0.9, and directivity factor 25 dB. Also, the coupler is matched so that $S_{11} = 0 = S_{22} = S_{33} = S_{44}$.
    (a) What is the isolation factor in decibels?
    (b) Determine the power dissipated in the directional coupler if the input power to Port 1 is 1 W.
41. A lossy directional coupler has the following 50 Ω S parameters:

$$S = \begin{bmatrix} 0 & 0.25 & -0.9\jmath & 0.01 \\ 0.25 & 0 & 0.01 & -0.9\jmath \\ -0.9\jmath & 0.01 & 0 & 0.25 \\ 0.01 & -0.9\jmath & 0.25 & 0 \end{bmatrix}.$$

    (a) Which port is the input port (there could be more than one answer)?
    (b) What is the coupling in decibels?
    (c) What is the isolation in decibels?
    (d) What is the directivity factor in decibels?
    (e) Draw the signal flow graph of the directional coupler.
42. A directional coupler using coupled lines has a coupling factor of 3.38, a transmission factor of $-\jmath 0.955$, and infinite directivity and isolation. The input port is Port 2 and the through port is Port 2. Write down the 4×4 S parameter matrix of the coupler.

2.12.1 Exercises by Section

†challenging

§2.3 1, 2, 3†, 4†, 5†, 6†, 7†, 8†, 9†, 10, 11, 12, 13†, 14†, 15†, 16, 17†, 18†, 19†, 20, 21, 22†

§2.4 23†, 24, 25†, 26†

§2.6 27

§2.8 28, 29, 30, 31, 32, 33, 34†, 35, 36, 37, 38

§2.9 39†, 40†, 41†, 42†

2.12.2 Answers to Selected Exercises

1 $0.638 - \jmath 0.079$

5 $\begin{bmatrix} .096\angle{-115^\circ} & .995\angle{-12.6^\circ} \\ .995\angle{-12.6^\circ} & .097\angle{-91^\circ} \end{bmatrix}$

9 $S_{21} = 0.2222$

13(d) $50 + \jmath 100\ \Omega$

22(c) -0.1807

25 $b_2 = 0.1155$

28 26 dB

34(b) 2.99 dB

40(b) 187 mW

41(d) 28 dB

CHAPTER 3

Graphical Network Analysis

3.1 Introduction

The network parameters that directly describe reflected and transmitted power flow in circuits are scattering (S) parameters. This chapter introduces two widely used graphical techniques for describing and solving problems using S parameters. The first graphical technique is signal flow graph analysis (SFG) and is a graphical way of representing equations and variables. Simplifying an SFG is the same as solving simultaneous equations and the equations can be kept in symbolic form. The second graphical representation is an annotated polar plot of S parameters called a Smith chart. This is one of the most powerful tools in RF and microwave engineering and is used to present measured results, to conceptualize designs, and to intuitively solve problems involving distributed networks.

3.2 Signal Flow Graph

SFGs are convenient ways to graphically represent systems of simultaneous linear equations [1, 2]. SFGs are used in many disciplines, but they are particularly useful with RF and microwave circuits.

An SFG represents a linear operation on an input. Consider the inductor shown in Figure 3-1(a), where the circuit quantities are v and i, and these are related by the impedance of the inductor sL. The SFG representation of this relation is given in Figure 3-1(b), with the operation performed written beside a directed edge. The operation here is simple, multiplying an input quantity by a scale factor. The edge is directed from the excitation node to the response node. The algebraic relationship between v and i is, in the Laplace domain,

$$v = sLi, \tag{3.1}$$

and this is exactly how the SFG of Figure 3-1(b) is interpreted. Several linear equations are represented in SFG form in Table 3-1.

3.2.1 SFG Representation of Mathematical Relations

In this section the basic rules for manipulating SFGs are presented. Think back to when you first started working with circuits. The great abstraction came about when the physical world was represented graphically as connections of circuit elements. Provided that a few simple rules were followed, the graphical representation enabled recognition of circuit topologies and the selection of appropriate solution strategies (e.g., applying the voltage divider rule). When it comes to working with S parameters and interconnections of multiport networks, SFGs serve much the same purpose. As well, SFG analysis enables the development of symbolic expressions. Only a portion of SFG theory is considered here—the aspects relevant to manipulating scattering parameter descriptions. Balabanian [3], Abrahams and Coverly [4], and Di Stefano et al. [5] provide a more detailed and general treatment.

3.2.2 SFG Representation of Scattering Parameters

Scattering parameters relate incident and reflected waves:

$$\mathbf{b} = \mathbf{S}\mathbf{a}, \tag{3.2}$$

where $\mathbf{a}$ and $\mathbf{b}$ are vectors and their ith elements refer to the incident and reflected waves, respectively. These relationships can be represented by SFGs. Consider the two-port in Figure 3-2(a) described by the equations

$$b_1 = S_{11}a_1 + S_{12}a_2 \qquad (3.3) \qquad\qquad b_2 = S_{21}a_1 + S_{22}a_2, \qquad (3.4)$$

which are represented in SFG form in Figure 3-2(b).

3.2.3 Simplification and Reduction of SFGs

The power of SFG analysis is that an SFG can be formulated by building up the set of equations describing a network by connecting together the SFGs of sections. Pattern recognition can be used to identify patterns that can be

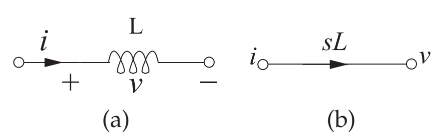

Figure 3-1: An inductor represented as: (a) a two-terminal element; and (b) its signal flow graph.

Table 3-1: Mathematical relations in the form of signal flow graphs with **edges** connecting **nodes**. Edges and nodes are used in graph theory, a superset of SFG theory. An edge is also called a **branch**.

(a)	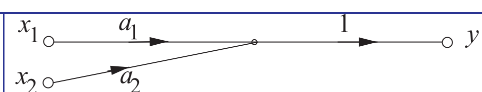	$y = a_1x_1 + a_2x_2$
(b)	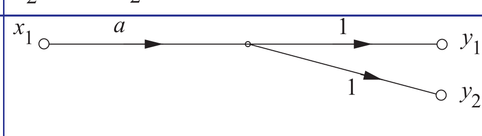	$y_1 = ax_1$ $y_2 = ax_1$
(c)	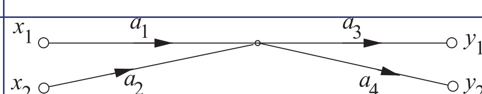	$y_1 = a_3(a_1x_1 + a_2x_2)$ $y_2 = a_4(a_1x_1 + a_2x_2)$

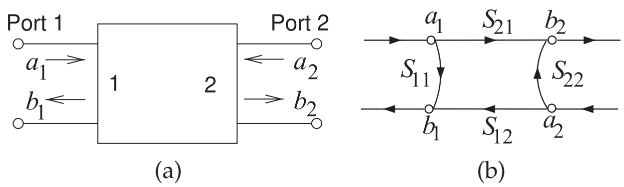

Figure 3-2: Two-port represented as (a) a two-port network with incident and reflected waves; and (b) its SFG representation.

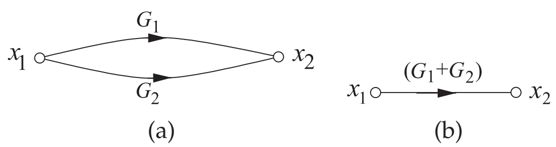

Figure 3-3: Signal flow graph representation of addition.

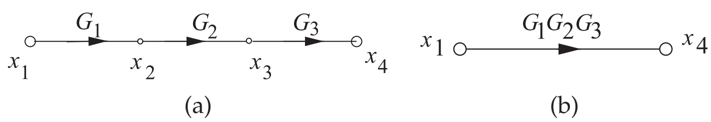

Figure 3-4: Cascade reduction of SFG: (a) three cascaded blocks; and (b) reduced form.

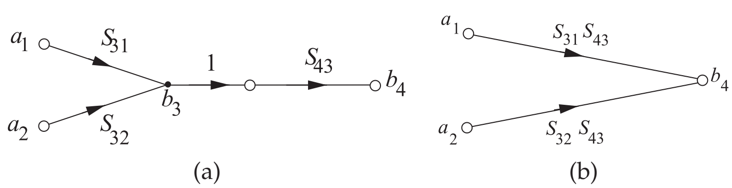

Figure 3-5: Signal flow graph simplification eliminating a variable.

reduced and simplified to arrive at a simple relationship between system input and output. Humans are extraordinarily good at pattern recognition.

Addition

Figure 3-3 depicts SFG addition. Figures 3-3(a and b) denote

$$x_2 = G_1 x_1 + G_2 x_1. \tag{3.5}$$

Multiplication

Consider the three cascaded blocks represented by the SFG of Figure 3-4(a). Here the output of the first block, x_2, is described by $x_2 = G_1 x_1$. Now x_2 is the input to the second block with output $x_3 = G_2 x_2$, and so on. The total response is the product of the individual responses (see Figure 3-4(b)):

$$x_4 = G_1 G_2 G_3 x_1. \tag{3.6}$$

Commutation

The rules that govern the simplification of SFGs use the fact that each graph represents a set of simultaneous equations. Consider the removal of the internal node, b_3, in Figure 3-5(a). Here

$$b_3 = S_{31} a_1 + S_{32} a_2 \quad \text{and} \quad b_4 = S_{43} b_3. \tag{3.7}$$

Node b_3 is called a mixed node (being both input and output) and can be eliminated, so

$$b_4 = S_{31} S_{43} a_1 + S_{32} S_{43} a_2, \tag{3.8}$$

which has the SFG of Figure 3-5(b). In Figure 3-5(b) the node representing the variable b_3 has been eliminated. Thus elimination of a node corresponds to

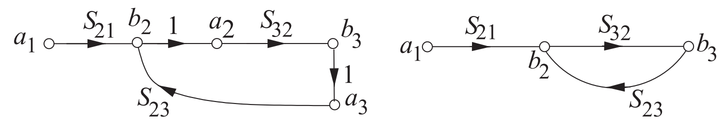

(a) (b)

Figure 3-6: Signal flow graphs having a self-loop: (a) original SFG; and (b) after eliminating a_2.

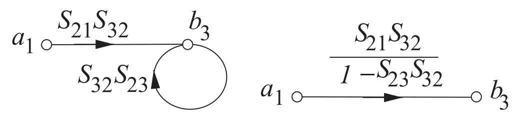

(a) (b)

Figure 3-7: Signal flow graph of (a) a self-loop; and (b) with the loop eliminated.

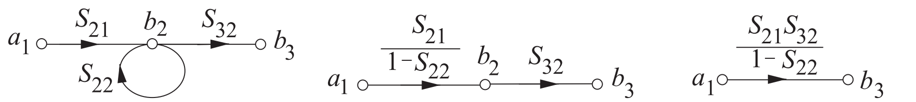

(a) Embedded loop (b) Loop eliminated (c) Variable elimination

Figure 3-8: Signal flow graph with loop.

the elimination of a variable in the simultaneous. It is sufficient to recognize the SFG pattern shown in Figure 3-5(a) and replace it with the SFG of Figure 3-5(b) to achieve SFG reduction.

Self-loop

Recognizing a self-loop and eliminating it is the best example yet of pattern identification and direct application of SFG reduction strategies. Consider the SFG of Figure 3-6(a), which has a self-loop, which describes The equations for this graph are

$$b_3 = S_{32}a_2, \quad S_{23}a_2 = b_2, \quad b_2 = S_{21}a_1 + S_{23}a_3, \quad a_3 = b_3. \tag{3.9}$$

Thus $$b_3 = S_{32}S_{21}a_1 + S_{32}S_{23}b_3 \quad \text{and} \quad (1 - S_{32})\, b_3 = S_{32}S_{21}a_1, \tag{3.10}$$

where the variable b_2 has been eliminated. The graph of Equation (3.10) is shown in Figure 3-7(a). The loop attached to node b_3 is called a self-loop. Such loops are not particularly convenient and can be removed by writing Equation (3.10) in the form

$$b_3 = \frac{S_{21}S_{32}}{1 - S_{23}S_{32}} a_1, \tag{3.11}$$

and the SFG for this equation is shown in Figure 3-7(b). The rule for removing self-loops follows from the manner in which Figure 3-7(a) was transformed into Figure 3-7(b). As an example, Figure 3-8(a) becomes Figure 3-8(b) and this can be reduced to the SFG of Figure 3-8(c).

As a further example, consider the more difficult multiple-loop case shown in Figure 3-9(a). This may be redrawn as Figure 3-9(b). The two self-loops are added and then the graph reduces to that in Figure 3-9(c).

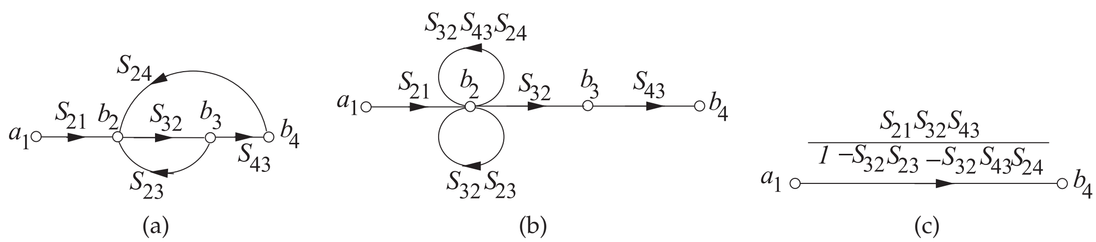

Figure 3-9: Signal flow graph with multiple loops.

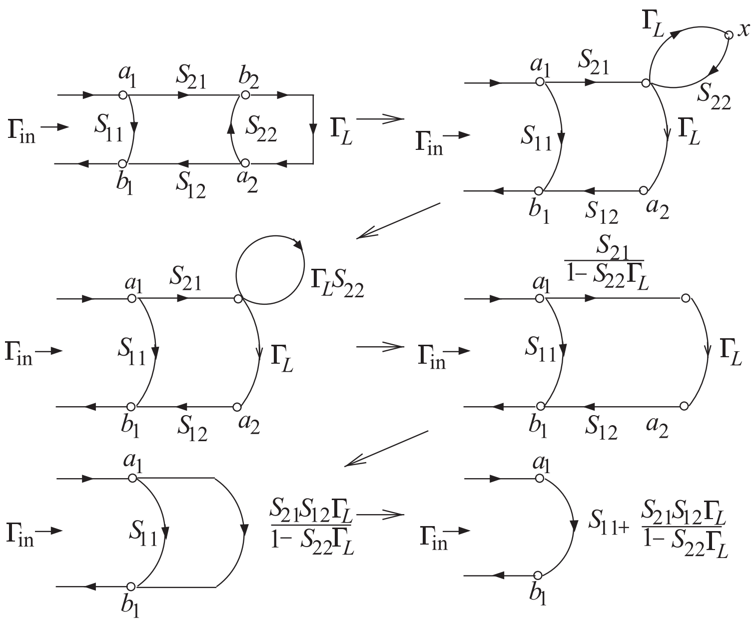

Figure 3-10: Sequence of graphical manipulations in Example 3.1 reducing a terminated two-port to a reflection only.

EXAMPLE 3.1 Signal Flow Graph

Draw the SFG of a two-port with a load (at Port 2) having a voltage reflection coefficient of Γ_L, and at Port 1 a source has a reflection coefficient of Γ_S. Using SFG analysis, derive an expression for the input reflection coefficient looking into the two-port at Port 1.

Solution:

The two-port is shown to the right with the load attached. The input reflection coefficient is $\Gamma_{\rm in} = b_1/a_1$ and the properties of the source here have no impact.

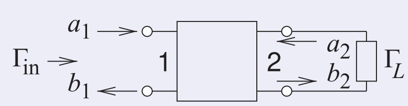

The sequence of SFG manipulations is shown in Figure 3-10 beginning with the SFG in the top left-hand corner. So the input reflection coefficient is

$$\Gamma_{\rm in} = \frac{b_1}{a_1} = S_{11} + \frac{S_{21}S_{12}\Gamma_L}{1 - S_{22}\Gamma_L}. \tag{3.12}$$

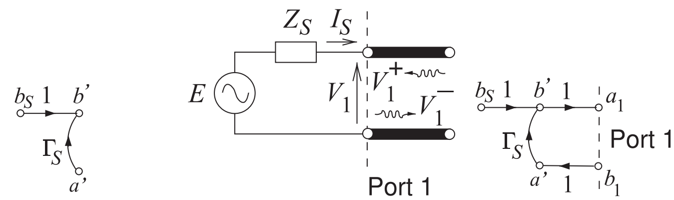

Figure 3-11: Development of the signal flow graph model of a source. The model in (a) is for a real reference impedance Z_0.

(a) SFG model of a source $b_S = \sqrt{Z_0}E/(Z_S + Z_0)$ (b) Transmission line model (c) SFG model used in development

3.2.4 SFG Model of a Source

The SFG model, referenced to a possibly complex impedance Z_0, of a source with a Thevenin equivalent voltage E and impedance Z_S is shown in Figure 3-11(a). In developing this model the circuit shown in Figure 3-11(b) is used where the transmission line of infinitesimal length separates the forward and backward-traveling voltage waves, V_1^+ and V_1^- for a system reference impedance of Z_0, the characteristic impedance of the transmission line. The SFG model used with the transmission line-augmented source is shown in Figure 3-11(c). The SFG model of Figure 3-11(c) describes

$$a_1 = b_s + \Gamma_S b_1. \tag{3.13}$$

where the source reflection coefficient $\Gamma_S = (Z_S - Z_0)/(Z_S + Z_0)$. The circuit equations for Figure 3-11(b) are

$$V_1 = E - I_S Z_S = V_1^+ + V_1^- \quad \text{and} \quad I_S = \frac{V_1^+}{Z_0} - \frac{V_1^-}{Z_0}. \tag{3.14}$$

Now, the traveling wave voltages are related to the a and b root power waves as (see Equation (3.15))

$$a_1 = \frac{V_1^+}{\sqrt{\Re\{Z_0\}}} \quad \text{and} \quad b_1 = \frac{V_1^-}{\sqrt{\Re\{Z_0\}}}. \tag{3.15}$$

Then combining Equations (3.14) and (3.15) yields

$$\begin{aligned}
E &= V_1^+ \frac{Z_S + Z_0}{Z_0} - V_1^- \frac{Z_S - Z_0}{Z_0} \\
\frac{Z_0}{\sqrt{\Re\{Z_0\}}} \frac{1}{Z_S + Z_0} E &= \frac{V_1^+}{\sqrt{\Re\{Z_0\}}} \left(\frac{Z_S + Z_0}{Z_S + Z_0}\right) - \frac{V_1^-}{\sqrt{\Re\{Z_0\}}} \left(\frac{Z_S - Z_0}{Z_S + Z_0}\right) \\
\frac{Z_0}{\sqrt{\Re\{Z_0\}}} \frac{1}{Z_S + Z_0} E &= a_1 - b_1 \Gamma_S.
\end{aligned} \tag{3.16}$$

Comparing Equations (3.13) and (3.16) it is seen that

$$b_s = \frac{Z_0}{\sqrt{\Re\{Z_0\}}} \frac{1}{Z_S + Z_0} E. \tag{3.17}$$

Thus the SFG model of a source is as shown in Figure 3-11(a) where the model is shown for a real Z_0.

EXAMPLE 3.2 Power Delivered to a Load and Substitution Loss

This example illustrates the method for determining powers using signal flow graph analysis with generalized S parameters having reference impedances Z_{01} at Port 1 and Z_{02} at Port 2. This is then used to determine substitution loss. The substitution loss is the ratio of the power delivered to a load with an initial two-port, to the power delivered with the substituted final two-port network. The SFG elements are shown on the right with Γ_S referred to Z_{01} and Γ_L referred to Z_{02}.

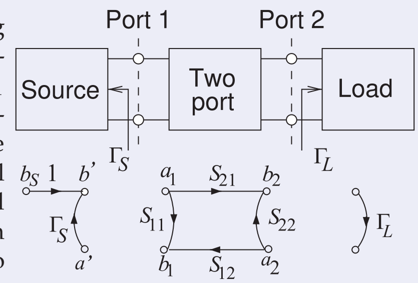

Solution:

The SFG manipulations that determine the power delivered to the load are shown in Figure 3-12 where

$$\alpha = \frac{S_{21}}{1 - S_{22}\Gamma_L}, \qquad \beta = \frac{1}{1 - \Gamma_S\left(S_{11} + S_{12}\Gamma_L\alpha\right)} \tag{3.18}$$

and
$$\begin{aligned}
b_2 = b_S\alpha\beta &= b_S \frac{S_{21}}{(1 - S_{22}\Gamma_L)} \frac{1}{\{1 - \Gamma_S\left[S_{11} + S_{12}S_{21}\Gamma_L/(1 - S_{22}\Gamma_L)\right]\}} \\
&= b_S \frac{S_{21}}{(1 - S_{22}\Gamma_L)} \frac{(1 - S_{22}\Gamma_L)}{[(1 - S_{22}\Gamma_L) - S_{11}\Gamma_S(1 - S_{22}\Gamma_L) + S_{12}S_{21}\Gamma_S\Gamma_L]} \\
&= b_S \frac{S_{21}}{1 - S_{22}\Gamma_L - S_{11}\Gamma_S + S_{11}S_{22}\Gamma_S\Gamma_L + S_{12}S_{21}\Gamma_S\Gamma_L} \\
&= b_S \frac{S_{21}}{(1 - S_{11}\Gamma_S)(1 - S_{22}\Gamma_L) - S_{12}S_{21}\Gamma_S\Gamma_L}
\end{aligned} \tag{3.19}$$

Then the power delivered to the load is (using Equation (2.117))

$$P_L = \tfrac{1}{2}|b_2|^2\left(1 - |\Gamma_L|^2\right) = \frac{\tfrac{1}{2}\left|b_S S_{21}\right|^2\left(1 - |\Gamma_L|^2\right)}{\left|(1 - S_{11}\Gamma_S)(1 - S_{22}\Gamma_L) - S_{12}S_{21}\Gamma_S\Gamma_L\right|^2} \tag{3.20}$$

The **substitution loss**, L_S, is the ratio of the power delivered to the load by an initial two-port identified by the leading superscript 'i', and the power delivered to the load with a final two port identified by the leading superscript 'f'. In decibels

$$L_S|_{\mathrm{dB}} = 10\log\left|\frac{{}^iP_L}{{}^fP_L}\right| = 10\log\left|\frac{{}^iS_{21}}{{}^fS_{21}}\frac{\left[(1 - {}^fS_{11}\Gamma_S)(1 - {}^fS_{22}\Gamma_L) - {}^fS_{12}{}^fS_{21}\Gamma_S\Gamma_L\right]}{\left[(1 - {}^iS_{11}\Gamma_S)(1 - {}^iS_{22}\Gamma_L) - {}^iS_{12}{}^iS_{21}\Gamma_S\Gamma_L\right]}\right|^2 \tag{3.21}$$

Substitution loss is used in deriving formulas for insertion loss, see Section 2.8.2.

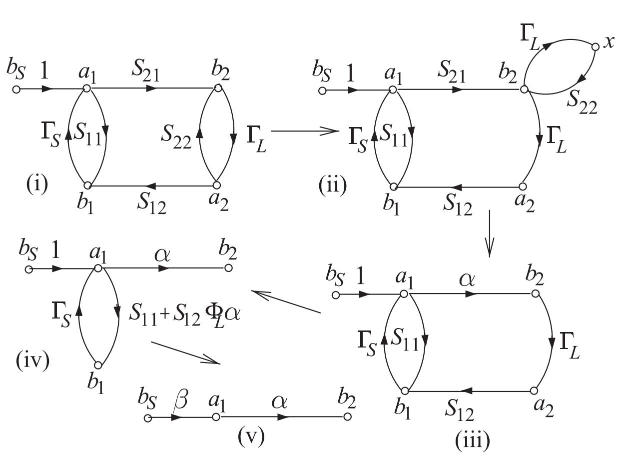

Figure 3-12: SFG manipulations in developing the power delivered to a load with a two-port network between source and load.

3.2.5 Mason's Rule

Mason's rule is a general procedure for reducing SFGs with multiple loops and is a systematic procedure for the reduction of SFGs to a single branch. Mason [6] derived the formula with the aim of developing a general method for the computer analysis of electrical circuits. First, a number of topology definitions must be introduced.

A path begins at one node and traverses a number of successive edges in the direction of the arrows to arrive at the final node or sink. In SFG analysis, a path is a forward path, as the successive edges are traversed in the direction of the arrows. An open path encounters the same node only once, and a closed path (or a loop) ends on the same node at which it is started. The product of the transmittances of all edges in a loop is called the loop transmittance. Two paths, open or closed, are said to be non-touching paths if they have no nodes in common. Similarly, disjoint loops are loops that have no nodes in common.

Mason's rule:
If T represents the overall graph transfer function and T_k represents the transfer function of the kth forward path from source to sink, then

$$T = \frac{1}{\lambda}\sum_k T_k \lambda_k, \tag{3.22}$$

where λ is the determinant of the matrix of coefficients of the equations represented by the SFG (usually called the determinant of the graph) and λ_k is the determinant of that part of the graph (subgraph) that does not touch the kth forward path. The determinant is given by

$$\lambda = 1 - \sum_j P_{j1} + \sum_j P_{j2} - \sum_j P_{j3} + \ldots, \tag{3.23}$$

where the first summation in Equation (3.23) is the sum of the loop transfer functions of all the loops in the graph. In the second summation, the products of the transfer functions of all pairs of non-touching loops are added. In the third summation, the products of the transfer functions of disjoint loops taken three at a time are added, and so on. Mason's rule can be quite difficult to apply, but any problem that Mason's rule can solve can also be solved using multiple applications of SFG manipulations described previously.

EXAMPLE 3.3 Application of Mason's Rule

Use Mason's rule to reduce the SFG shown in Figure 3-13(a). Here, input node a_1 is the excitation and the output node b_4 is the response. The transmittance T is equal to b_4/a_1.

Solution:

First, consider the determinant of the flow graph. Since all the loops have at least one node in common, the expression for the determinant reduces to

$$\lambda = 1 - \sum_j P_{j1}. \tag{3.24}$$

There are three loops identified in Figure 3-13(b) with transmittances A = $S_{21}S_{32}S_{13}$, B = $S_{32}S_{43}S_{24}$, and C = $S_{21}S_{32}S_{43}S_{14}$. Thus the sum of the loop transmittances is

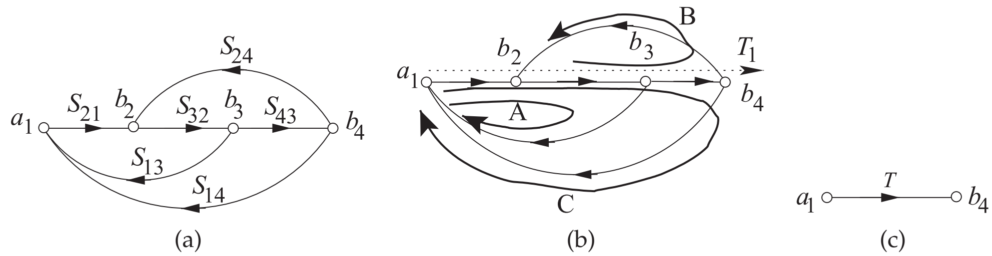

Figure 3-13: Signal flow graph used in Example 3.3 applying Mason's rule: (a) SFG; (b) annotation identifying loops and through-path; and (c) final reduction.

$$\sum_j P_{j1} = S_{21}S_{32}S_{13} + S_{32}S_{43}S_{24} + S_{21}S_{32}S_{43}S_{14} \tag{3.25}$$

and the determinant is given by

$$\lambda = 1 - S_{21}S_{32}S_{13} - S_{32}S_{43}S_{24} - S_{21}S_{32}S_{43}S_{14}. \tag{3.26}$$

This rule works well with the human ability to recognize patterns, in this case loops. There is only one forward path, identified in Figure 3-13(b), from source a_1 to sink b_4, given by

$$T_1 = S_{21}S_{32}S_{43}. \tag{3.27}$$

Since all the loops of the graph have nodes that touch T_1, then $\lambda_1 = 1$ and

$$\sum_k T_k\lambda_k = T_1\lambda_1 = S_{21}S_{32}S_{43}. \tag{3.28}$$

Thus $$\frac{b_4}{a_1} = T = \frac{S_{21}S_{32}S_{43}}{1 - S_{21}S_{32}S_{13} - S_{32}S_{43}S_{24} - S_{21}S_{32}S_{43}S_{14}}. \tag{3.29}$$

This can be represented by a single edge from a_1 to b_4 as shown in Figure 3-13(c).

3.2.6 Summary

SFG reduction can be used with numerical values but the real power comes from the ability to develop symbolic expressions. In RF and Microwave engineering these expressions nearly always involve scattering parameters but they can be used with any sets of equations. Design is best undertaken by developing symbolic solutions as these enable optimization to be performed and insights gained as to the significance of parameters.

3.3 Polar Representations of Scattering Parameters

Scattering parameters are most naturally represented in polar form with the square of the magnitude relating to power flow. In this section a greater rationale for representing S parameters on a polar plot is presented and this serves as the basis for a more complicated representation of S parameters on a Smith chart to be described in the next section.

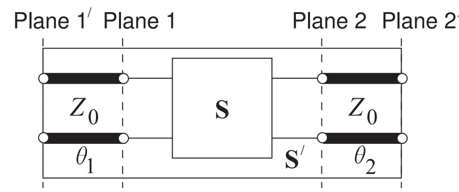

Figure 3-14: A two-port with scattering parameter matrix **S** augmented by lines at each port with the line at Port n having the reference characteristic impedance at that port, i.e. Z_{0n} and with electrical length (in radians) of θ_n. The scattering parameter matrix of the augmented two-port is $\mathbf{S}'$.

3.3.1 Shift of Reference Planes as a S Parameter Rotation

A polar plot is a natural way to present S parameters graphically. In general S parameters are referenced to different characteristic impedances Z_{0n} at each port. Adding additional lengths of the lines at each port rotates the S parameters. Consider the two-port in Figure 3-14. Here the original two-port with scattering parameter matrix **S** is augmented by lines at each port with each having a characteristic impedance equal to the reference impedance. The S parameter matrix of the augmented two-port, $\mathbf{S}'$, are the same as the original S parameter matrix but phase-shifted. That is

$$\mathbf{S}' = \begin{bmatrix} S'_{11} & S'_{12} \\ S'_{21} & S'_{22} \end{bmatrix} = \begin{bmatrix} S_{11}\mathrm{e}^{-\jmath 2\theta 1} & S_{12}\mathrm{e}^{-\jmath(\theta 1+\theta 2)} \\ S_{21}\mathrm{e}^{-\jmath(\theta 1+\theta 2)} & S_{22}\mathrm{e}^{-\jmath 2\theta 2} \end{bmatrix}. \tag{3.30}$$

The shift in reference planes simply rotates the S parameters. This is one of the main reasons why S parameters are commonly plotted on a polar plot.

3.3.2 Polar Plot of Reflection Coefficient

The polar plot of reflection coefficient is simply the polar plot of a complex number. Figure 3-15 is used in plotting reflection coefficients and is a polar plot that has a radius of one. So a reflection coefficient with a magnitude of one is on the unit circle. The center of the polar plot is zero so the reflection coefficient of a matched load, which is zero, is plotted at the center of the circle. Plotting a reflection coefficient on the polar plot enables convenient interpretation of the properties of a reflection. The graph has additional notation that enables easy plotting of an S parameter on the graph. Conversely, the magnitude and phase of an S parameter can be easily read from the graph. The horizontal label going from 0 to 1 is used in determining magnitude. The notation arranged on the outer perimeter of the polar plot is used to read off angle information. Notice the additional notation "ANGLE OF REFLECTION COEFFICIENT IN DEGREES" and the scale relates to the actual angle of the polar plot. Verify that the $90°$ point is just where one would expect it to be.

Figure 3-16 annotates the polar plot of reflection coefficient with real and imaginary axes and shows the location of the short circuit and open circuit points. Note that the reflection coefficient of an inductive impedance is in the top half of the polar plot while the reflection coefficient of a capacitive impedance is in the bottom half of the polar plot.

The nomograph shown in Figure 3-17 aids in interpretation of polar reflection coefficient plots. The nomograph relates the reflection coefficient (RFL. COEFFICIENT), ρ (ρ was originally used instead of Γ and is still used with the Smith chart); the return loss (RTN. LOSS) (in decibels); and the standing wave ratio (SWR); and the standing wave ratio (in decibels) as $20\ \log(\mathrm{SWR})$. When printed together with the reflection coefficient polar plot (Figures 3-15 and 3-17 combined) the nomograph is scaled properly, but

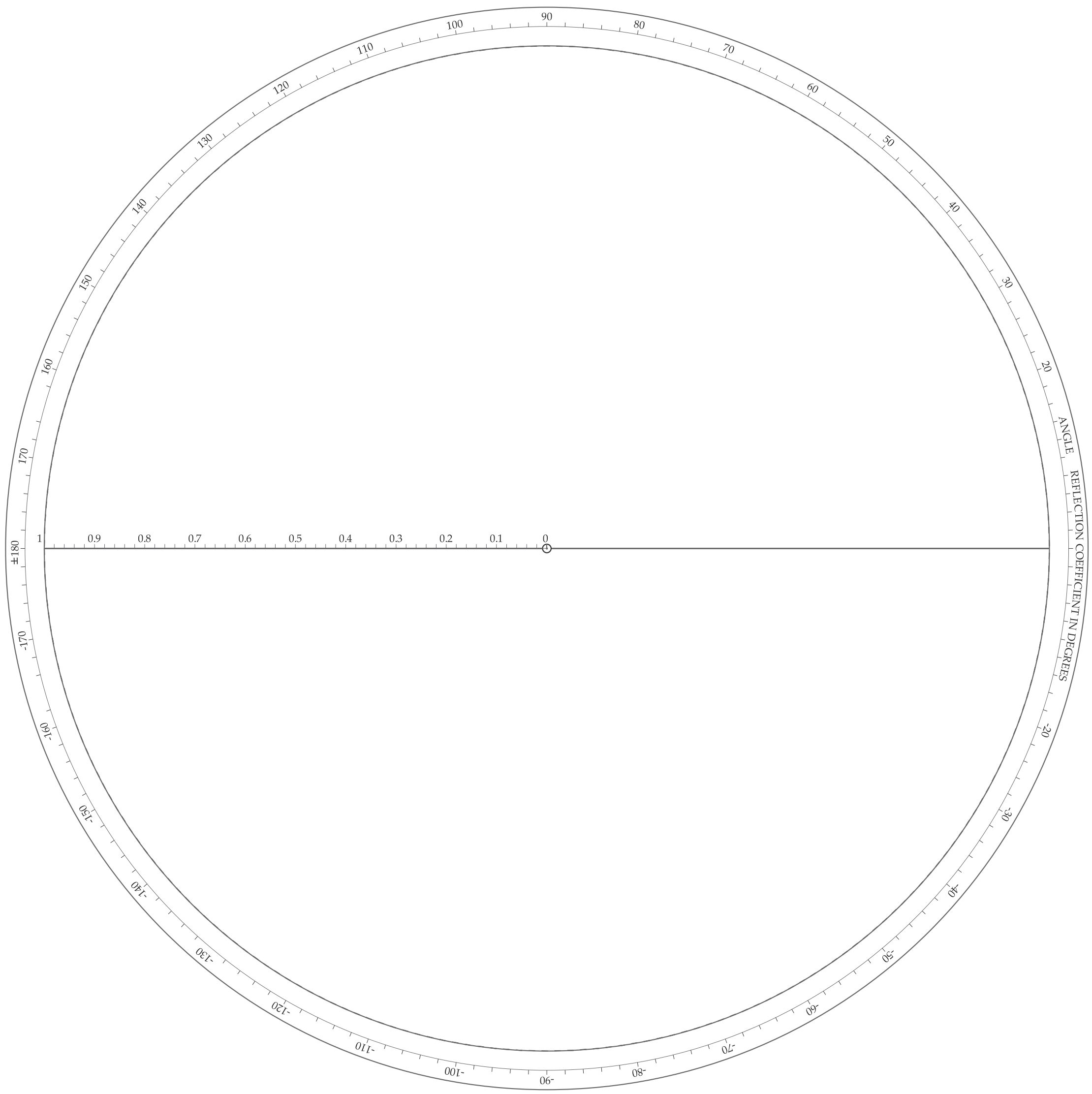

Figure 3-15: Polar chart for plotting reflection coefficient and transmission coefficient.

it is expanded here so that it can be read more easily. So with the aid of a compass with one point on the zero point of the polar plot and the other at the reflection coefficient (as plotted on the polar plot), the magnitude of the reflection coefficient is captured. The compass can then be brought down to the nomograph to read ρ, the return loss, and VSWR directly.

3.3.3 Summary

This section introduced the plotting of reflection coefficients as a complex number on a polar plot. The use of angle and magnitude scales make it easy to plot a complex number in magnitude-angle form but it is also easy to plot or read-off the complex number in real-imaginary form. Nomographs also enable return loss and SWR to be developed without calculation. The

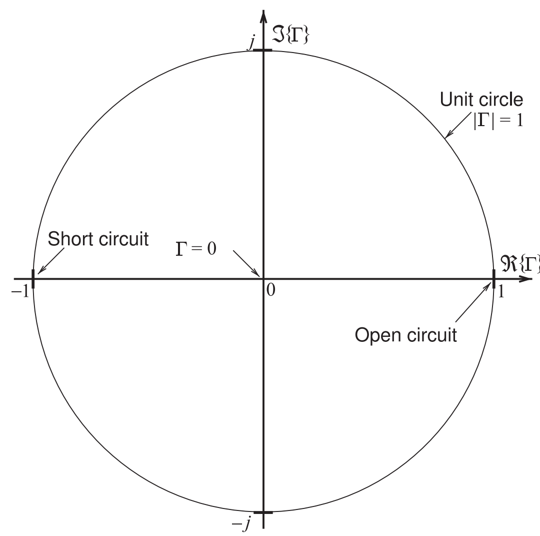

Figure 3-16: Annotated polar plot of reflection coefficient with real, $\Re$, and imaginary, $\Im$, axes. The short circuit $\Gamma = -1$ and open circuit $\Gamma = +1$ are indicated. The reflection coefficient is referenced to a reference impedance Z_{REF}. Thus an impedance Z_L has the reflection coefficient $\Gamma = (Z_L - Z_{\text{REF}})/(Z_L + Z_{\text{REF}}))$. An interesting observation is that the angle of Γ when Z_L is inductive, i.e. has a positive reactance, has a positive angle between $0°$ and $180°$ and so Γ is in the top half of the polar plot. Similarly the angle of Γ when Z_L is capacitive, i.e. has a negative reactance, has a negative angle between $0°$ and $-180°$ and so Γ is in the bottom half of the polar plot.

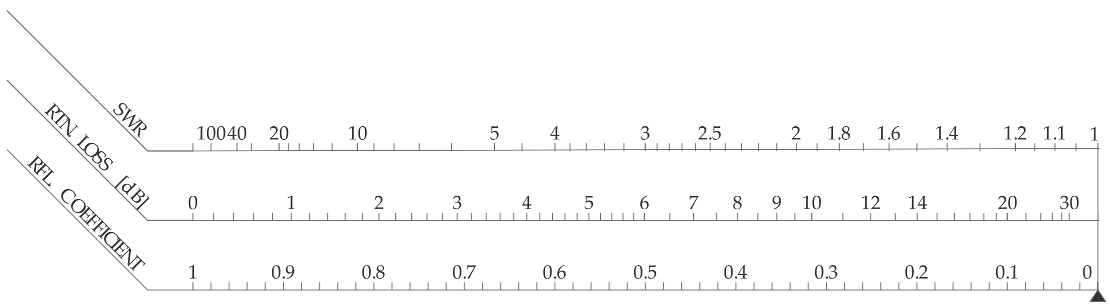

Figure 3-17: Nomograph relating the reflection coefficient (RFL. COEFFICIENT), ρ; the return loss (RTN. LOSS) (in decibels); and the standing wave ratio (SWR).

transmission coefficient can be plotted on the same polar plot, i.e. Figure 3-15, as the polar plot is the representation of a complex number.

3.4 Smith Chart

The Smith chart is a powerful graphical tool used in the design of microwave circuits. Mastering the Smith chart is essential to entering the world of RF and microwave circuit design as all practitioners use this as if it is well understood by others. It takes effort to master but fundamentally it is quite simple combining a polar plot used for plotting S parameters directly, curves that enable normalized impedances and admittances to be plotted directly, and scales that enable electrical lengths in terms of wavelengths and degrees to be read off. The chart has many numbers printed in quite small font and with signs dropped as there is not room.

The Smith chart was invented by Phillip Smith and presented in close to its current form in 1937, see [7–10]. Once nomographs and graphical calculators were common engineering tools mainly because of limited computing resources. Only a few have survived in electrical engineering usage, with Smith charts being overwhelmingly the most important.

This section first presents the impedance Smith chart and then the admittance Smith chart before introducing a combined Smith chart which is the form needed in design. The Smith chart presents a large amount of information in a confined space and interpretation, such as applying appropriate signs, is required to extract values. The Smith chart is a 'back-of-the-envelope' tool that designers use to sketch out designs.

3.4.1 Impedance Smith Chart

The reflection coefficient, Γ, is related to a load, Z_L, by

$$\Gamma = \frac{Z_L - Z_{\mathrm{REF}}}{Z_L + Z_{\mathrm{REF}}}, \tag{3.31}$$

where Z_{REF} is the system reference impedance. With normalized load impedance $z_l = r + \jmath x = Z_L/Z_{\mathrm{REF}}$, this becomes

$$\Gamma = \frac{r + \jmath x - 1}{r + \jmath x + 1}. \tag{3.32}$$

Commonly in network design reactive elements are added either in shunt or in series to an existing network. If a reactive element is added in series then the input reactance, x, is changed while the input resistance, r, is held constant. So superimposing the loci of Γ (on the S parameter polar plot) with fixed values of r, but varying values of x (x varying from $-\infty$ to ∞), proves useful, as will be seen. Another loci of Γ with fixed values of x and varying values of r (r varying from 0 to ∞) is also useful. The combination of the reflection/transmission polar plots, the nomographs, and the r and x loci is called the impedance Smith chart, see Figure 3-18. This is still a polar plot of reflection coefficient and the arcs and circles of constant and resistance enable easy conversion between reflection coefficient and impedance.

The full impedance Smith chart shown in Figure 3-18 is daunting so discussion will begin with the less dense form of the impedance Smith chart shown in Figure 3-19(a) which is annotated in Figure 3-19(b). Referring to Figure 3-19(b), the unit circle corresponds to a reflection coefficient magnitude of one and hence a pure reactance. Note that there are lines of constant resistance and arcs of constant reactance. All points in the top half of the Smith chart have positive reactances and so all reflection coefficient points plotted in the top half of the Smith chart indicate inductive impedances. All points in the bottom half of the Smith chart have negative reactances and so all reflection coefficient points plotted in the bottom half of the Smith chart indicate capacitive impedances. The horizontal line across the middle of the Smith chart indicates pure resistance.

A point on the unit circle indicate that the resistance of the point is zero, while a reflection coefficient point inside the unit circle indicates a finite positive resistance.

One big difference between the less dense form of the impedance Smith chart, Figure 3-19(a), and the full impedance Smith chart of Figure 3-18 is that the signs of the reactances are missing in the full impedance Smith chart. This is simply because there is not enough room and the user must add the appropriate sign when reading the chart. Thus it is essential that the user keep the annotations in Figure 3-19(b) in mind. Yet another factor that makes it difficult to develop essential Smith chart skills.

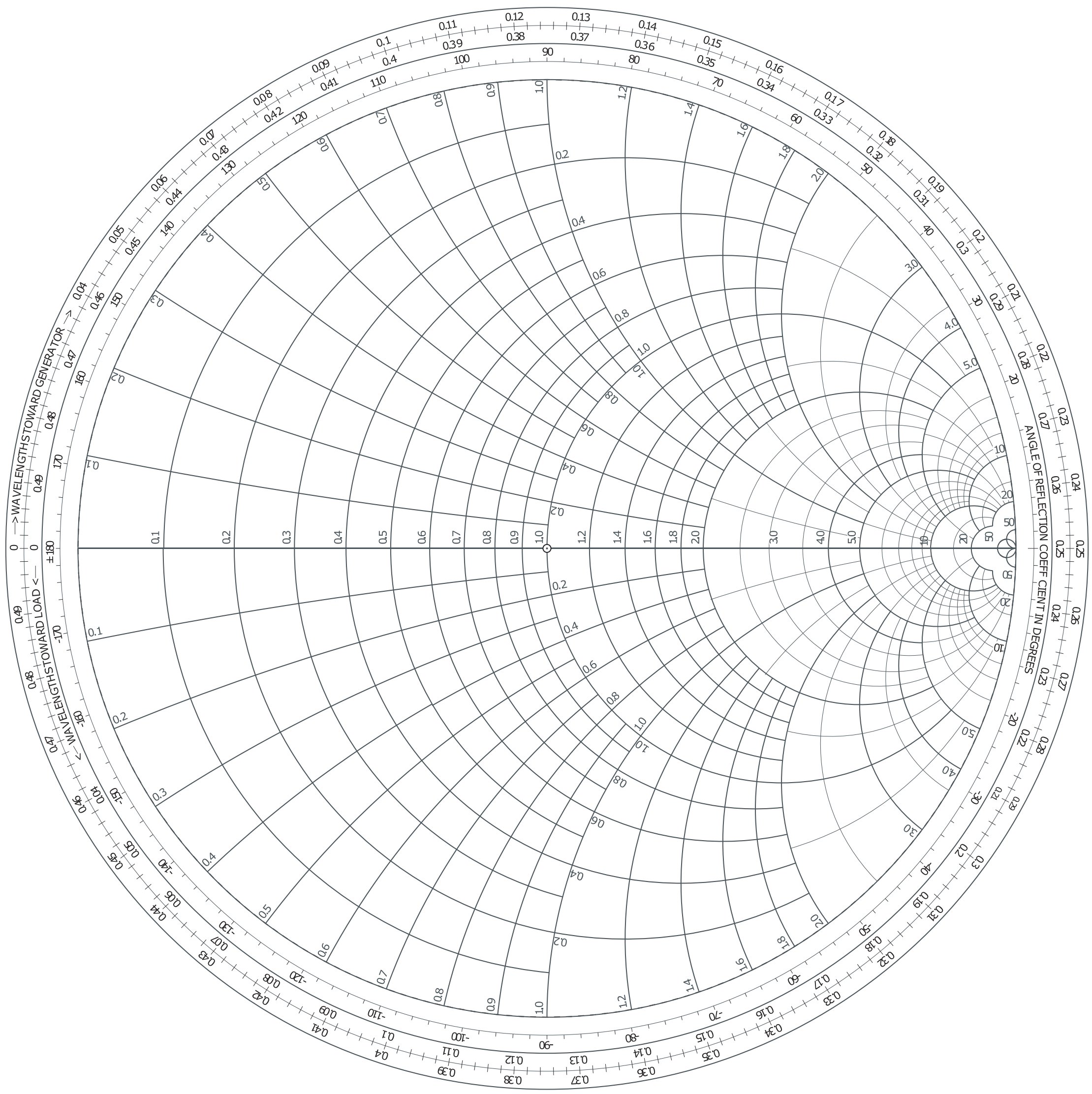

Figure 3-18: Impedance Smith chart. Also called a normalized Smith chart since resistances and reactances have been normalized to the system reference impedance Z_{REF}: $z = Z/Z_{\mathrm{REF}}$.
A point plotted on the Smith chart represents a complex number A. The magnitude of A is obtained by measuring the distance from the origin of the polar plot (the same as the origin of the Smith chart in the center of the unit circle) to point A, say using a ruler, and comparing that to the measurement of the radius of the unit circle which corresponds to a complex number with a magnitude of 1. The angle in degrees of the complex number A is read from the innermost circular scale. The technique used is to draw a straight line from the origin through point A out to the circular scale.

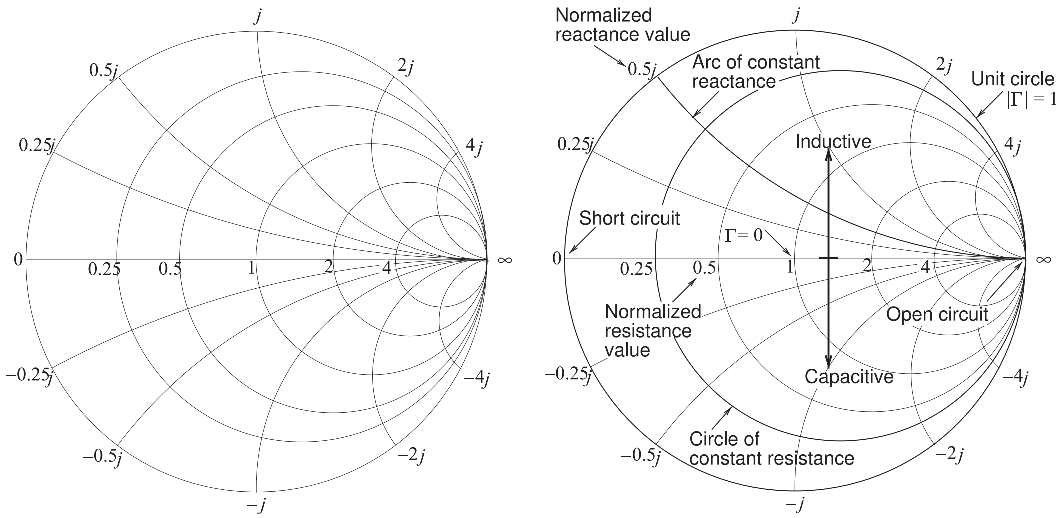

(a) Impedance Smith chart (b) Annotated impedance Smith chart

Figure 3-19: Normalized impedance Smith charts.

EXAMPLE 3.4 Impedance Plotting

Plot the normalized impedances $z_A = 1 - 2\jmath$ and $z_B = 0.3 + 0.6\jmath$ on an impedance Smith chart.

Solution:

The impedance $z_A = 1 - 2\jmath$ is plotted as Point A to the right. To plot this, first identify the circle of constant normalized resistance $r = 1$, and then identify the arc of constant normalized reactance $x = -2$. The intersection of the circle and arc locates z_A at point A. The reader is encouraged to do this with the full impedance Smith chart as shown in Figure 3-18. Recall that signs of reactances are missing on the full chart. As an exercise read off the reflection coefficient (the answer is $0.5 - \jmath 0.5 = 0.707\angle -45°$).

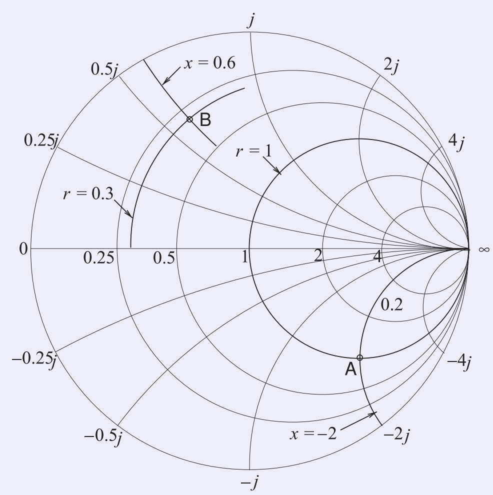

The impedance $z_B = 0.3 + 0.6\jmath$ is plotted as Point B which is at the intersection of the circle $r = 0.3$ and the arc $x = +0.6$. Interpolation is required to identify the required circle and arc. The reader should do this with the full impedance Smith chart. As an exercise read off the reflection coefficient (the answer is $-0.268 + \jmath 0.585 = 0.644\angle 115°$).

EXAMPLE 3.5 Impedance Synthesis

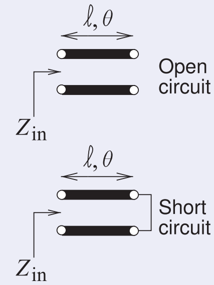

Use a length of terminated transmission line to realize an impedance of $Z_{\text{in}} = \jmath 140\ \Omega$.

Solution:
The impedance to be synthesized is reactive so the termination must also be lossless. The simplest termination is either a short circuit or an open circuit. Both cases will be considered. Choose a transmission line with a characteristic impedance, Z_0, of $100\ \Omega$ so that the desired normalized input impedance is $\jmath 140\ \Omega/Z_0 = 1.4\jmath$, plotted as point B in Figure 3-20.

First, the short-circuit case. In Figure 3-20, consider the path AB. The termination is a short circuit and the impedance of this load is Point A with a reference length of $\ell_A = 0\ \lambda$ (from the outermost circular scale). The corresponding reflection coefficient reference angle from the scale is $\theta_A = 180^\circ$ (from the innermost circular scale labeled 'WAVELENGTHS TOWARDS THE GENERATOR' which is the same as 'wavelengths away from the load'). As the line length increases, the input impedance of the terminated line follows the clockwise path to Point B where the normalized input impedance is $\jmath 1.4$. (To verify your understanding that the locus of the refection coefficient rotates in the clockwise direction, i.e. increasingly negative angle, as the line length increases see Section 2.3.3 of [11].) At Point B the reference line length $\ell_B = 0.1515\ \lambda$ and the corresponding reflection coefficient reference angle from the scale is $\theta_B = 71.2^\circ$. The reflection coefficient angle and length in terms of wavelengths were read directly off the Smith chart and care needs to be taken that the right sign and correct scale are used. A good strategy is to correlate the scales with the easily remembered properties at the open-circuit and short-circuit points. Here the line length is

$$\ell = \ell_B - \ell_A = 0.1515\lambda - 0\lambda = 0.1515\lambda, \tag{3.33}$$

and the electrical length is half of the difference in the reflection coefficient angles,

$$\theta = \tfrac{1}{2}\,|\theta_B - \theta_A| = \tfrac{1}{2}\,|71.2^\circ - 180^\circ| = 54.4^\circ, \tag{3.34}$$

corresponding to a length of $(54.4^\circ/360^\circ)\lambda = 0.1511\lambda$ (the discrepancy with the previously determine line length of 0.1515λ is small). This is as close as could be expected from using the scales. So the length of the stub with a short-circuit termination is 0.1515λ.

For the open-circuited stub, the path begins at the infinite impedance point $\Gamma = +1$ and rotates clockwise to Point A (this is a 90° or 0.25λ rotation) before continuing on to Point B. For the open-circuited stub,

$$\ell = 0.1515\lambda + 0.25\lambda = 0.4015\lambda. \tag{3.35}$$

3.4.2 Admittance Smith Chart

The admittance Smith chart has loci for discrete constant susceptances ranging from $-\infty$ to ∞, and for discrete constant conductance ranging from 0 to ∞, see Figure 3-21. A less dense form is shown in Figure 3-22(a). This chart looks like the flipped version of the impedance Smith chart but it is the same polar plot of a reflection coefficient so that the positions of the open and short circuit remain the same as do the capacitive and inductive halves of the Smith chart. In the full version of the admittance Smith chart, Figure 3-21, signs have been dropped as there is not room for them. Thus interpreting admittances from the chart requires that the user separately determine the signs of susceptances. The less dense version, Figure 3-22(a), retains the signs making it easier to follow some of the discussions and examples. It is important that the user readily understand the annotations on the less dense form of the Smith chart, see Figure 3-22(b).

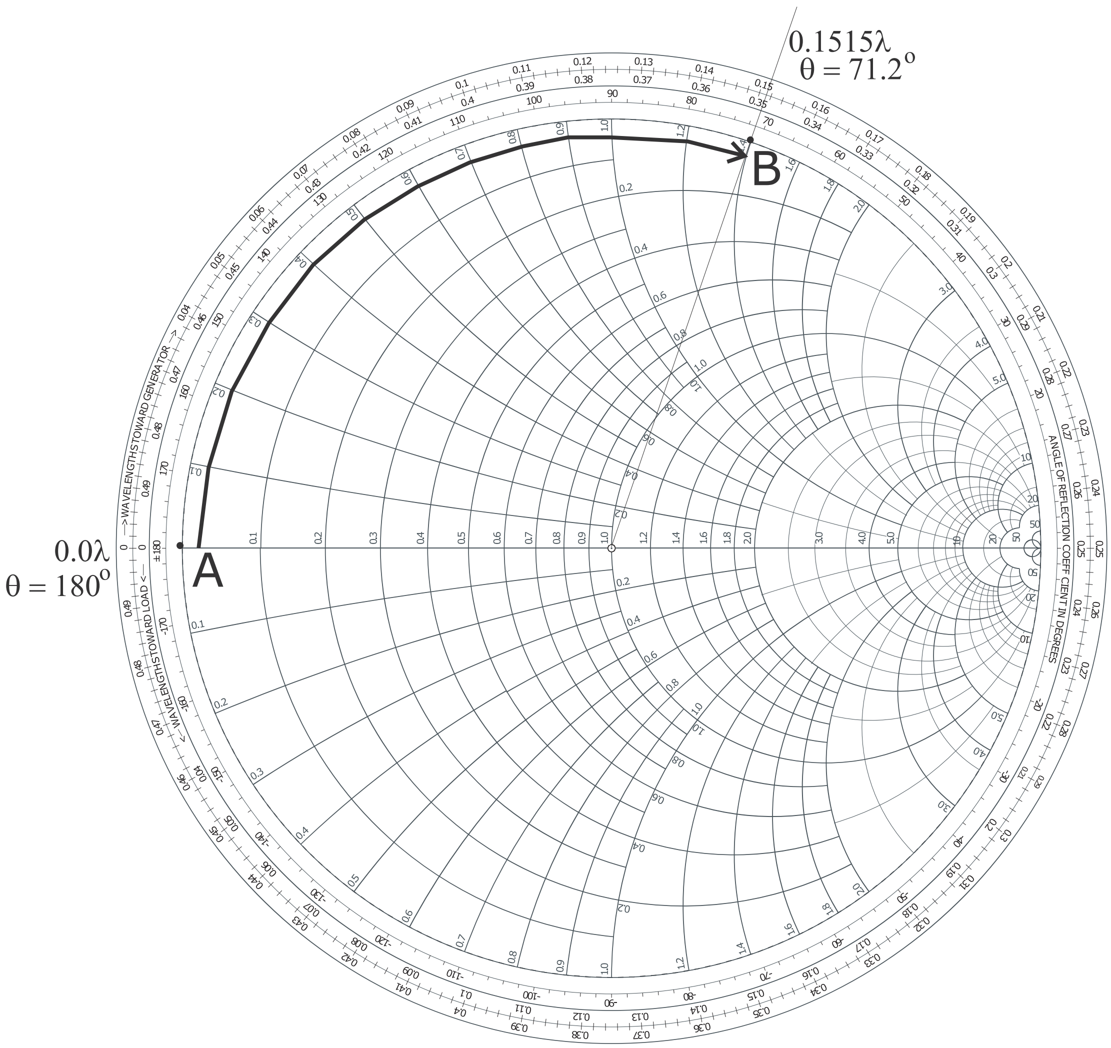

Figure 3-20: Design of a short-circuit stub with a normalized input impedance of $\jmath 1.4$. The path AB is actually on the unit circle but has been displaced here to avoid covering numbers. The electrical length in wavelengths has been read from the outermost circular scale, and the angle, θ, in degrees refers to the angle of the polar plot (and is twice the electrical length).

3.4.3 Combined Smith Chart

The combination of the reflection/transmission polar plots, nomographs, and the impedance and admittance Smith chart leads to the combined Smith chart (see Figure 3-23). This color Smith chart is the preferred version for use in design and the separate impedance and admittance versions of the Smith chart are rarely used. The combined Smith charts is rich with information and care is required to identify the lines that correspond to admittances (specifically lines of constant normalized conductance and constant normalized susceptances), and the lines that correspond to impedances (constant normalized resistances and constant normalized

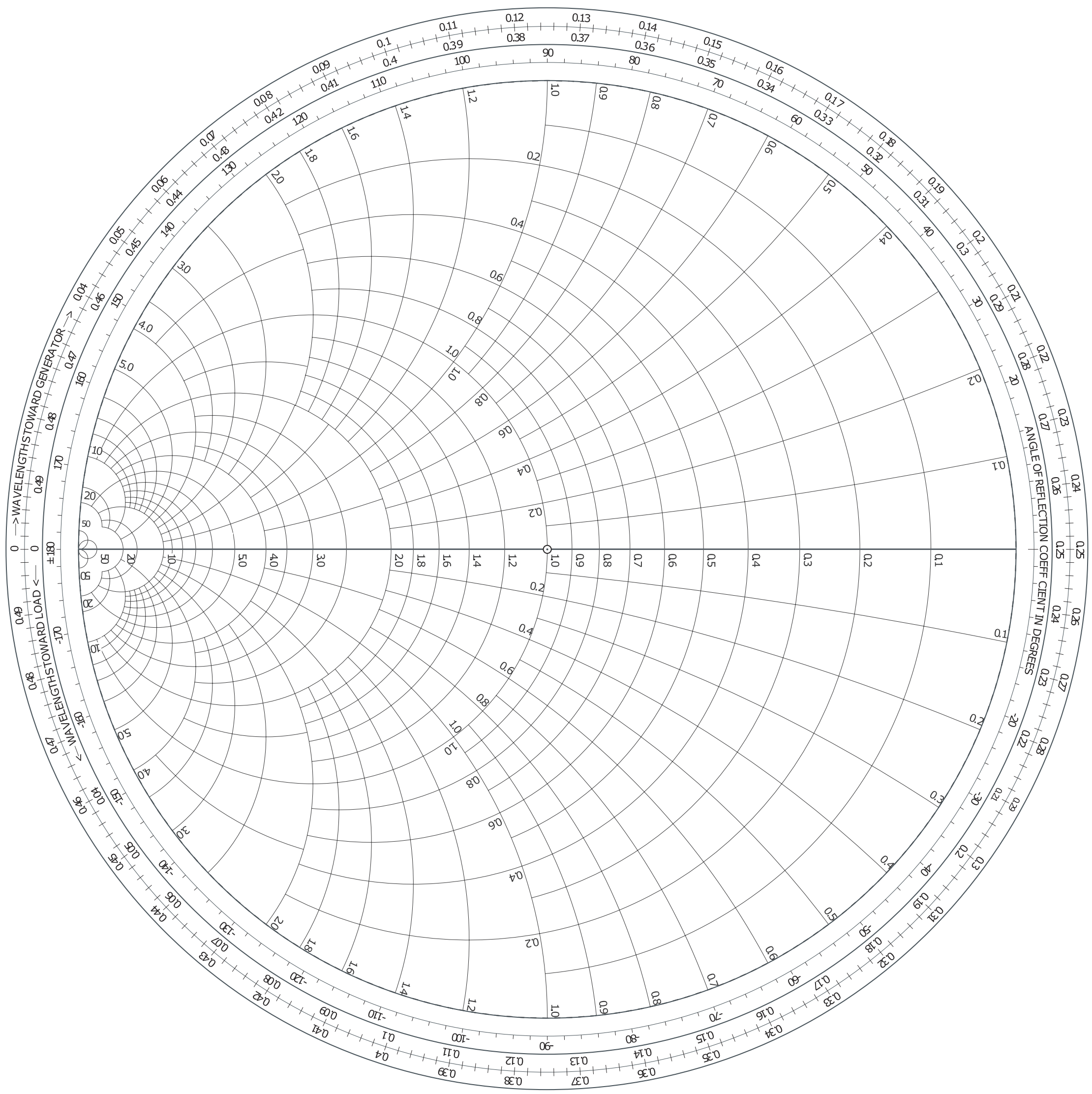

Figure 3-21: Admittance Smith chart.

reactances). The signs of the reactances and susceptible are missing and left to the user to add them depending on whether a reflection coefficient point is capacitive (in the lower half of the Smith chart and hence susceptances are positive and reactances are negative) or whether a point is inductive (in the upper half of the Smith chart and hence susceptances are negative and reactances are positive). A less dense version of the combined Smith chart, with the addition of signs, is shown in Figure 3-24(a).

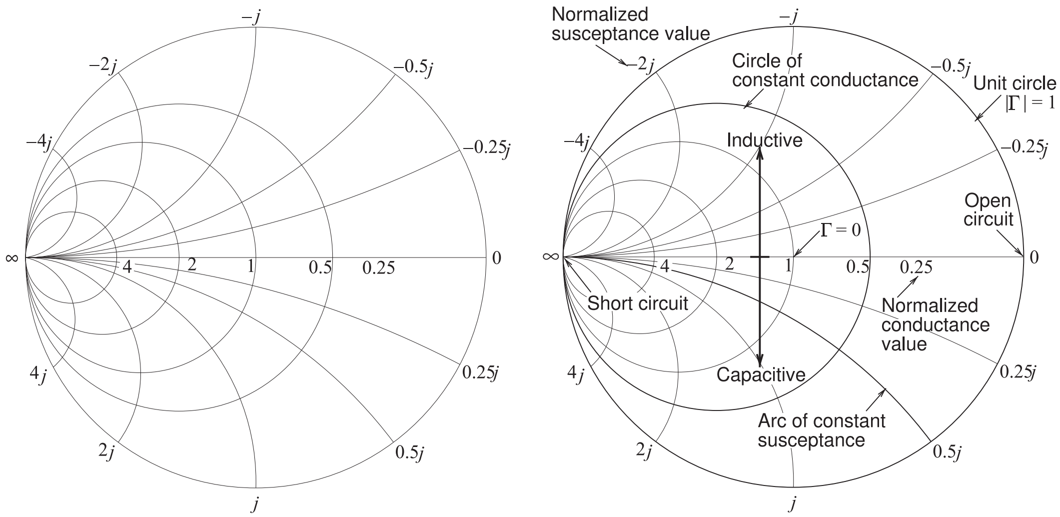

(a) Admittance Smith chart (b) Annotated admittance Smith chart

Figure 3-22: Normalized admittance Smith chart.

EXAMPLE 3.6 Impedance to Admittance Conversion

Use a Smith chart to convert the impedance $z = 1 - 2\jmath$ to an admittance.

Solution:

The impedance $z = 1-2\jmath$ is plotted as Point A in Figure 3-24(b). To read the admittance from the chart, the lines of constant conductance and constant susceptance must be interpolated from the arcs and circles provided. The interpolations are shown in the figure, indicating a conductance of 0.2 and a susceptance of $0.4\jmath$. Thus

$$y = 0.2 + 0.4\jmath.$$

(This agrees with the calculation: $y = 1/z = 1/(1 - 2\jmath) = 0.2 + 0.4\jmath$.)

Adding Reactance and Susceptance

A good amount of microwave design, such as designing a matching network for maximum power transfer, involves beginning with a load impedance plotted on a Smith chart and inserting series and shunt reactances, and transmission lines, to transform the impedance to another value. The preferred view of the design process is that of a reflection coefficient that gradually evolves from one value to another. That is, in the case of a series reactance, the effect is that of a reflection coefficient gradually changing as the reactances increase from zero to its actual value. The path traced out by the gradually evolving reflection coefficient value is called a locus. The loci of common circuit elements added to various loads are shown in Figure 3-25. For each locus the load is at the start of the arrow with the value of the element increasing from zero to its actual final value at the arrow head.

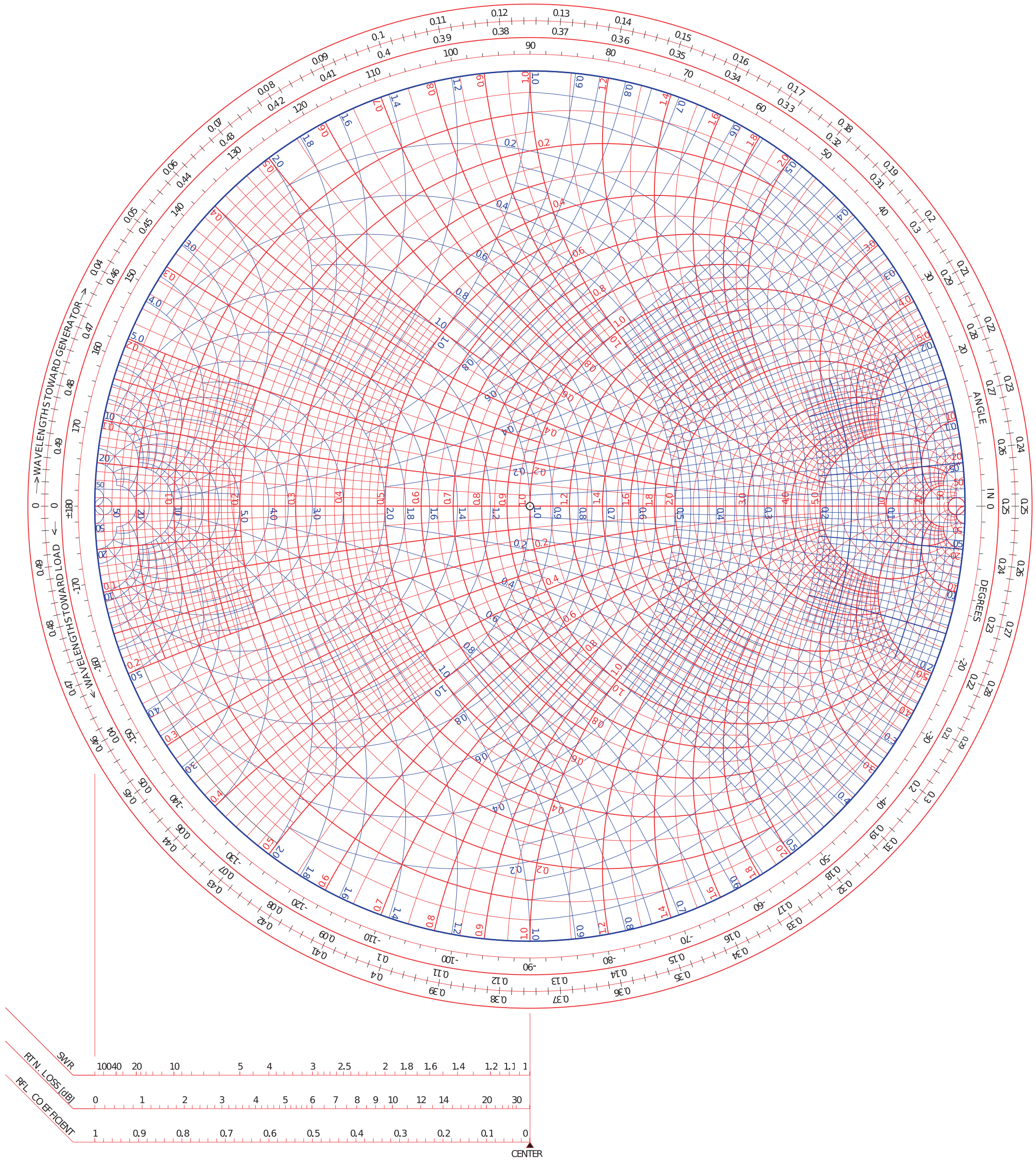

Figure 3-23: Normalized combined Smith chart combining impedance and admittance Smith charts.

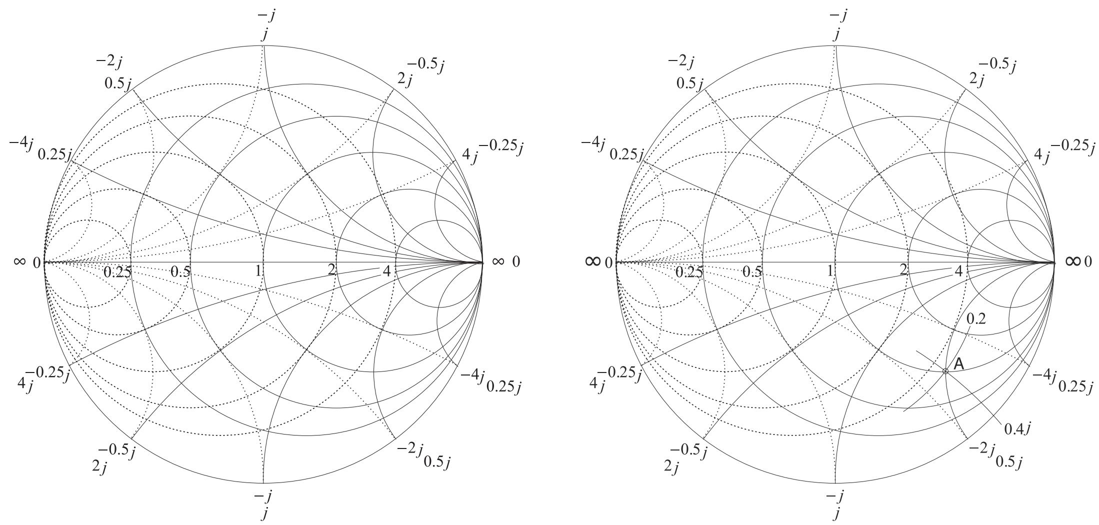

(a) Combined impedance and admittance Smith chart (b) Smith chart used in Example 3.11

Figure 3-24: Combined impedance and admittance Smith chart.

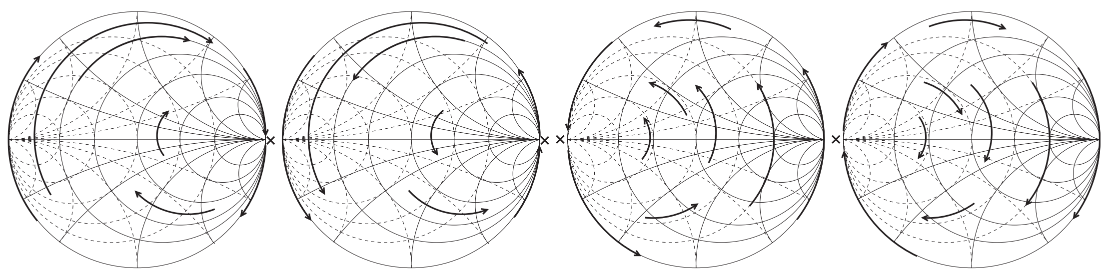

$x \to$ more positive
(a) Series L

$x \to$ more negative
(b) Series C

$b \to$ more negative
(c) Shunt L

$b \to$ more positive
(d) Shunt C

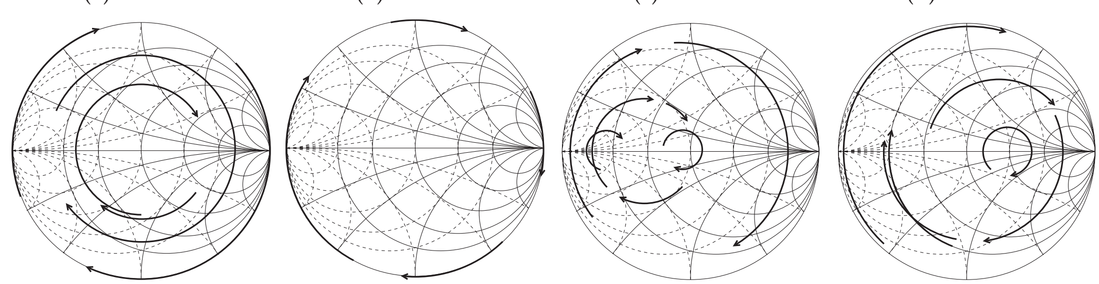

ℓ increasing
(e) Transmission line
$Z_0 = Z_{\mathrm{REF}}$

ℓ increasing
(f) Line with reactive load, Z_0 has any value

ℓ increasing
(g) Transmission line
$Z_0 < Z_{\mathrm{REF}}$

ℓ increasing
(h) Transmission line
$Z_0 > Z_{\mathrm{REF}}$

Figure 3-25: Reflection coefficient locus of a load augmented by elements as indicated. The original load is at the start of the arrowed arc. In (a) and (b) the locus is with respect to increasing $|x|$ (normalized reactance magnitude), in (c) and (d) the locus is with respect to increasing $|b|$ (normalized susceptance magnitude), and in (e)–(h) with respect to increasing length ℓ. In (e)–(h) the loci are parts of circles centered on the $x = 0$ line. x indicates that the locus cannot cross infinity (open circuit for (a) and (b), short circuit for (c) and (d)).

3.4.4 Smith Chart Manipulations

Microwave design often proceeds by taking a known load and transforming it into another impedance, perhaps for maximum power transfer. Smith charts are used to show these manipulations. In design the manipulations required are not known up front and the Smith chart enables identification of those required. Except for particular situations, lossless elements such as reactances and transmission lines are used. The few situations where resistances are introduced include introducing stability in oscillators and amplifiers, and deliberately reduce signals levels. Most of the time introducing resistances unnecessarily increases noise and reduces signal levels thus reducing critical signal-to-noise ratios.

The circuit in Figure 3-26 will be used to illustrate the representation of manipulations on a Smith chart. The most common view is to consider that the Smith chart is a plot of the reflection coefficient at various stages in the circuit, i.e., Γ_A, Γ_B, Γ_C, Γ_D, and Γ_{IN}. Additionally the load, Z_L, is plotted and reactances, susceptances, or transmission lines transform the reflection coefficient from one stage to the next. Yet another concept is the idea that the effect of an element is regarded as gradually increasing from a negligible value up to the final actual value and in so doing tracing out a locus which ends in an arrow head. This is the approach nearly all RF and microwave engineers use. The manipulations corresponding to the circuit are illustrated in Figure 3-27. The individual steps are identified in Figure 3-28. The first few steps are confined to the top half of the Smith chart which is repeated on a larger scale in Figure 3-29 for the first three steps.

Step 1 L, a, b, c, d, e, f
The first step is to plot the load Z_L on a Smith chart and this is the Point L in Figures 3-27–3-29. The reference impedance Z_{REF} is chosen to be $50\ \Omega$, the same as the characteristic impedance of the transmission line in the circuit. The Smith chart is now known as a 50-Ω Smith chart. This is a common choice because then the locus of reflection coefficient variation introduced by the line will be a circle centered at the origin of the Smith chart. To plot L derive the normalized load impedance $z_L = Z_L/Z_{\mathrm{REF}} = 0.3 + \jmath 0.6$ (future numerical values are given in Figure 3-26).

To plot z_L the normalized resistance circle for 0.3 and the normalized

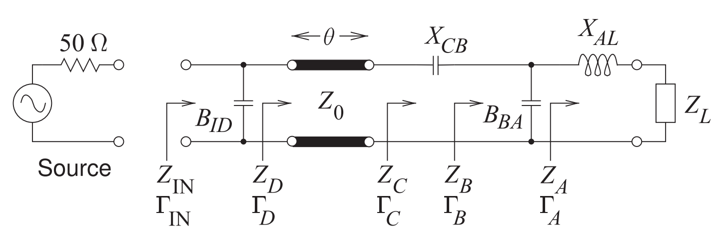

Circuit elements	Normalized	Derived values	
$Z_L = 15 + \jmath 30\ \Omega$	$z_L = 0.3 + \jmath 0.6$	$\Gamma_L = 0.644\angle 115°$	$z_A = 0.300 + \jmath 1.200$
$X_{AL} = 30\ \Omega$	$x_{AL} = 0.600$	$\Gamma_A = 0.785\angle 115°$	$y_A = 0.196 - \jmath 0.784$
$B_{BA} = 4.6$ mS	$b_{BA} = 0.230$	$\Gamma_B = 0.741\angle 59°$	$y_B = 0.196 - \jmath 0.554$
$X_{CB} = -180\ \Omega$	$x_{CB} = -3.600$	$\Gamma_C = 0.805\angle -50°$	$z_B = 0.567 + \jmath 1.603$
$Z_0 = 50\ \Omega$	$Z_0 = 1$	$\Gamma_D = 0.805\angle 144°$	$z_C = 0.567 - \jmath 1.997$
$\theta = 83°$	$\theta = 83°$	$\Gamma_{\mathrm{IN}} = 0$	$y_D = 0.998 - \jmath 2.71$
$B_{ID} = 54.2$ mS	$b_{ID} = 2.71$		$z_{\mathrm{IN}} = 1$, $y_{\mathrm{IN}} = 1$

Figure 3-26: Circuit used in illustrating Smith chart manipulations. $Z_{\mathrm{REF}} = 50\ \Omega$, $Y_{\mathrm{REF}} = 1/Z_{\mathrm{REF}} = 20$ mS, $z = Z/Z_{\mathrm{REF}}$, $y = Y/Y_{\mathrm{REF}}$, $Z_{\mathrm{IN}} = Z_{\mathrm{REF}} = 50\ \Omega$. In the circuit B indicates susceptance and X indicates reactance.

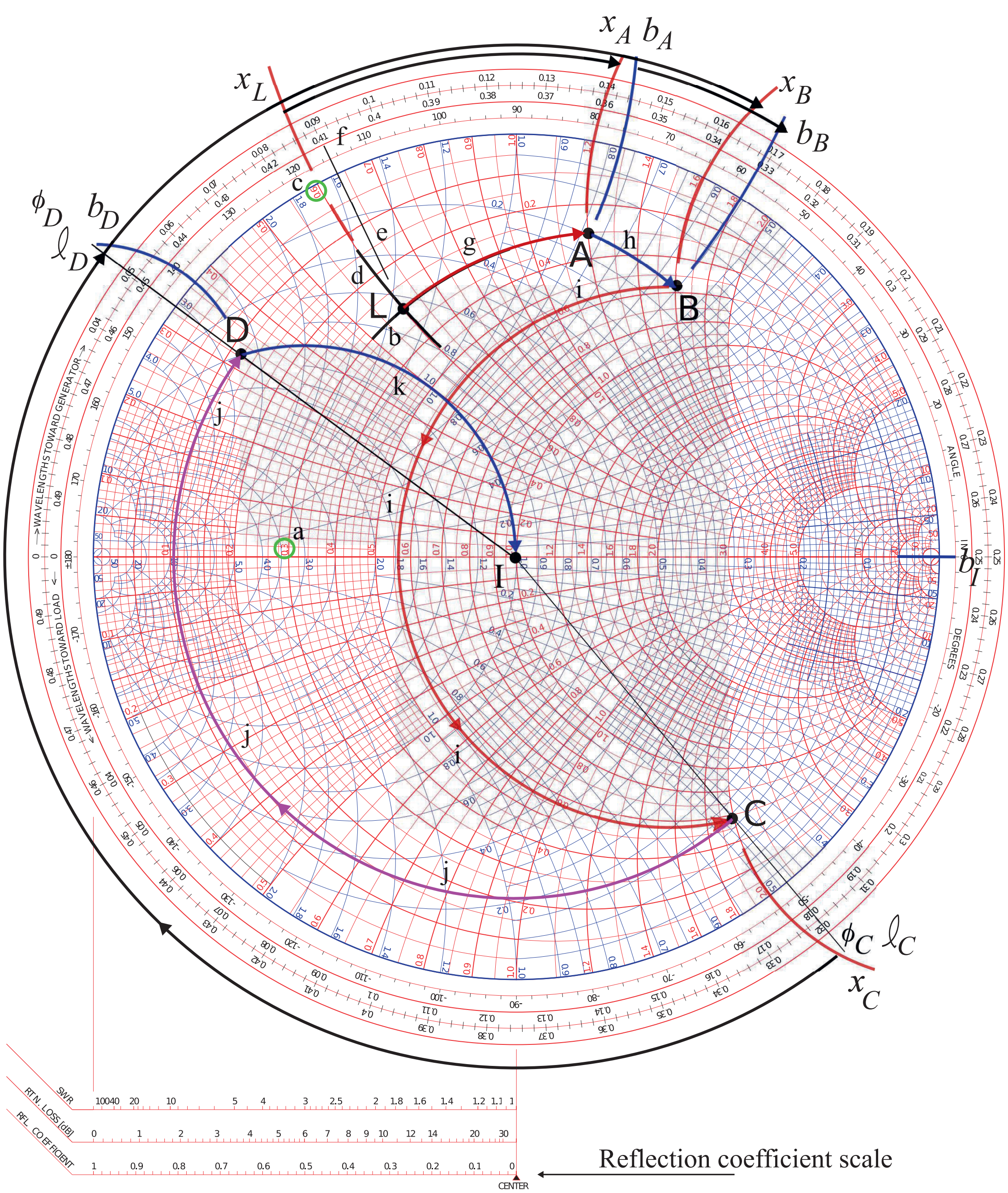

Figure 3-27: Smith chart manipulations corresponding to the circuit in Figure 3-26 with circuit elements added one at a time beginning with the load impedance at Point L.

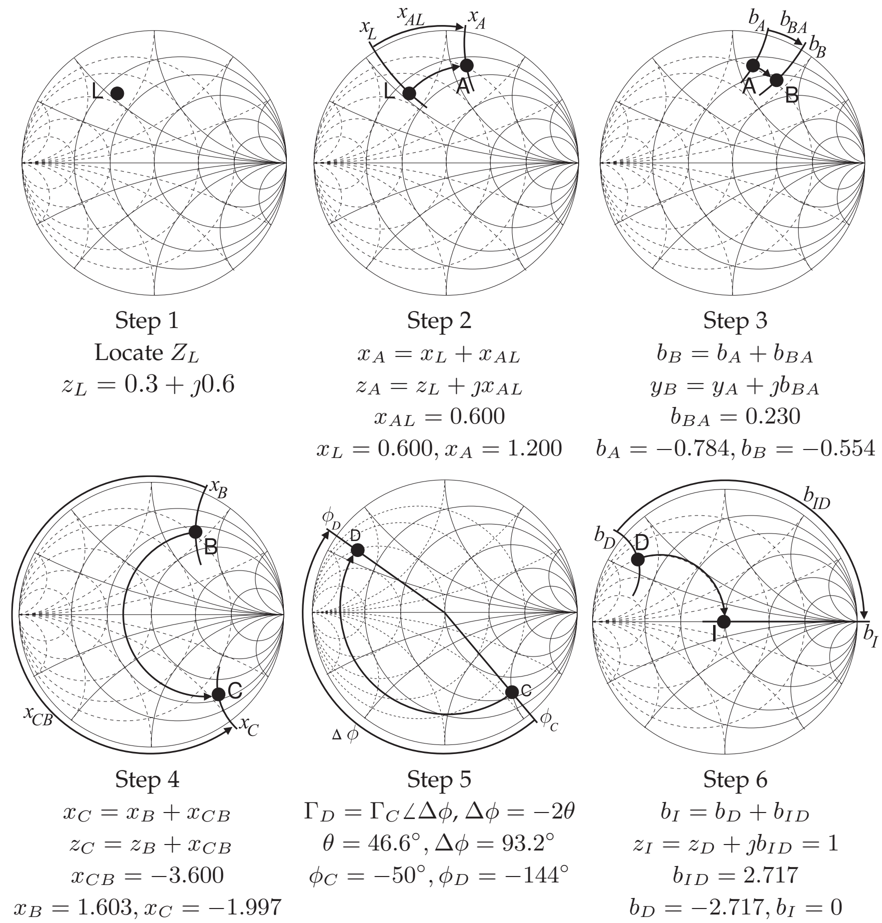

Figure 3-28: Steps in the Smith chart manipulations shown in Figures 3-27 and 3-29.

reactance arc for $+0.3$ must be located. The resistance circle is identified from the scale on the horizontal axis of the Smith chart, see the circled value labeled 'a'. Locating the $+0.3$ reactance arc is not as direct as the signs of reactance are missing on the Smith chart. Referring back to Figure 3-19 it is noted that an inductive impedance is in the top half of the Smith chart and so positive reactances are in the top half. Thus the $+0.3$ reactance arc is in the top half of the Smith chart and the correct arc is identified by 'c'. From the curves identified by 'a' and 'c' the arcs 'b' and 'd' are drawn with the impedance z_L, i.e. point L, at the intersection of the arcs.

It is instructive to determine Γ_L, the reflection coefficient at L. On the Smith chart the reflection coefficient vector Γ_L is drawn from the origin to the point L. Γ_L is evaluated by separately determining its magnitude and angle. To determine the magnitude measure the length of the $\Gamma_L|$ vector either using a ruler, a compass, or marking the edge of a piece of paper. Then this length can be compared against the reflection coefficient scale shown at the bottom of Figure 3-27 yielding $|\Gamma_L| = 0.644$. The angle of Γ_L is read by extending the Γ_L vector out to the inner most circular scale on the Smith chart. This extension is labeled as e. The angle is read at point 'f' as 115°. Thus $\Gamma_L = 0.644\angle 115^\circ$.

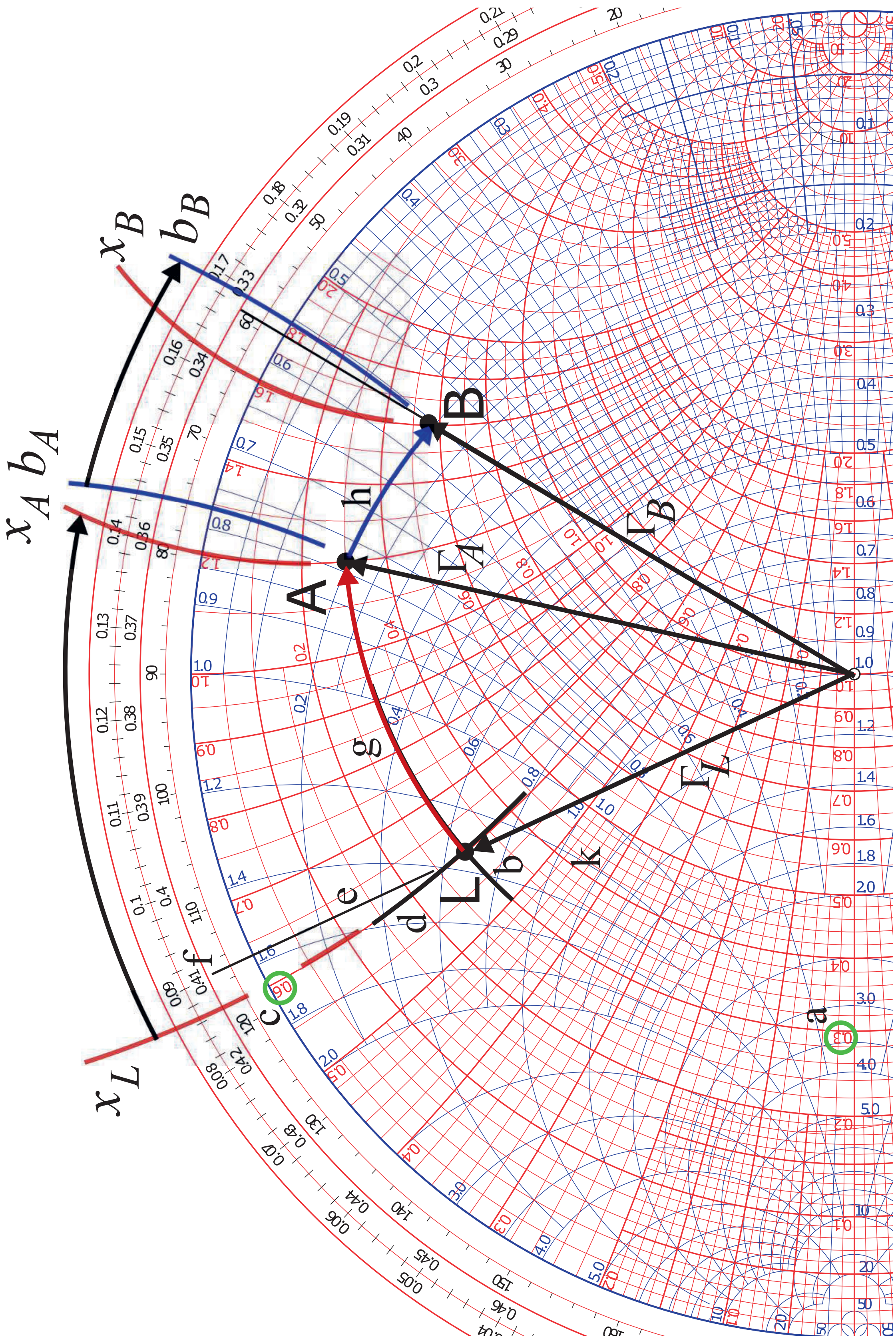

Figure 3-29: The first three steps in the Smith chart manipulations in Figure 3-27.

Step 2 Add the series reactance X_{AL}, path L to A, g
In step 2 an inductor with reactance X_{AL} is in series with Z_L and the reflection coefficient transitions from point L to point A. Now $x_L = \Im\{z_L\} = 0.6$. To this $x_{AL} = 0.6$ is added so that the normalized reactance at A is $x_A = x_L + x_{AL} = 0.6 + 0.6 = 1.2$. The locus of this operation is the arc, 'g', extending from L with gradually increasing series reactance until the full value x_{AL}, at the arrowhead of the locus, is obtained. The procedure is to identify the arc of $x_A = +1.2$ reactance and then follow the circle of constant resistance (since the resistance is not changing) up to this arc. This operation traces out the locus 'g'.

Step 3 Add the shunt susceptance B_{BA}, path A to B, h
In step 3 a capacitor with susceptance X_{BA} is in shunt with Z_A and the reflection coefficient transitions from point A to point B. The locus of this operation follows a circle of constant conductance with only they susceptance changing. The final value must be calculated as $b_B = b_A + b_{BA}$. The susceptance b_B is read from the graph as -0.784. This value is read by following the arc of constant susceptance out to the unit circle where a value of 0.784 is read. Note that the arc must be interpolated and that the user must realize that the susceptance is negative in the top half of the Smith chart so the susceptance must be negative even though a minus sign is not shown on the Smith chart. Thus the correct reading for x_A is -0.784. Now $b_{BA} = +0.230$ so the locus, 'h', of the transition follows the circle of constant conductance ending at the (interpolated arc) with susceptance $b_B = b_a + b_{BA} = -0.784 + 0.230 = -0.554$.

Step 4 Add the series reactance X_{CB}, path B to C, i
In step 4 a capacitor with reactance X_{CB} is in series with Z_B and the reflection coefficient transitions from point B to point C. Now x_B is read from the graph as $+1.603$. To this add $x_{CB} = -3.600$ so that the normalized reactance at C is $x_C = x_B + x_{CB} = 1.603 + (-3.600) = -1.997$. The locus from B to C, path 'i', begins at B and follows a circle of constant resistance up to the arc with normalized reactance $x_C = -1.997$. This reactance arc is in the bottom half of the Smith chart as reactances are negative there even though the signs are missing on the labels of the reactance arcs in the bottom half of the chart. The locus of this operation is the arc, 'g', from L with gradually increasing series reactance until the full value z_{CB}, at the arrowhead of the locus, is obtained. The procedure is to identify the arc of $x_C = -1.997$ reactance and then follow the circle of constant resistance (since the resistance is not changing) up to this arc. This traces out the locus 'i'.

Step 5 Insert the transmission line, path C to D, j
Step 5 illustrates a different type of manipulation as now there is a transmission line and the reflection coefficient transitions from Γ_C, i.e. point C to the input reflection coefficient of the line Γ_D. The locus of this transition must be clockwise, i.e. having increasingly negative angle (as discussed in Section 2.3.3 of [11]). The electrical length of the transmission line is $\theta = 83°$ and the reflection coefficient changes by the negative of twice this amount, $\phi_{DC} = -2\theta = -166°$. The locus is drawn in Figure 3-27 with the transmission line gradually increasing in length tracing out a circle which, since $Z_0 = Z_{\mathrm{REF}}$, is centered at the origin of the Smith cart. The procedure is to find the scale value of the angle at point C which is read by drawing a line from the origin through C intersecting the reflection coefficient angle scale

(the innermost circular scale) yielding $\phi_C = -50.4°$ and so $\phi_D = \phi_C + \phi_{DC} = -50.4° - 166° + 360°) = +143.6°$. The locus from C to D is drawn by first drawing a line from the origin to the $\phi_D = -143.6°$ point on the angle scale. Then point D will be at the intersection of this line and a circle of constant radius drawn through C. The locus is shown as path 'j' in Figure 3-27.

Step 6 Add the shunt susceptance B_{ID}, path D to I, k
The final step is to add the shunt capacitor with susceptance B_{ID} to Z_D. Following the previous procedure b_D is read as -2.71 to which $b_{ID} = 2.71$ is added so that $b_I = 0$ which is just the horizontal line across the middle of the Smith chart. This line corresponds to zero reactance and zero susceptance. The locus, path 'k', extends from D to I following the circle of constant conductance. The final result is that $z_{\text{IN}} = 1.00$ and $Z_{\text{IN}} = z_{\text{IN}} \cdot Z_0 = 50\ \Omega$.

Summary

The Smith chart manipulations considered here modified the reflection coefficient of a load by adding shunt and series reactive elements. The final result of the circuit manipulations is that the input impedance is $Z_{\text{IN}} = 50\ \Omega$. If the source has a Thevenin source impedance of $50\ \Omega$ then there is maximum power transfer to the circuit. Since all of the elements in the circuit manipulations are lossless this means that there is maximum power transfer from the source to the load Z_L. Of course fewer circuit manipulations could have been used to achieve this result. Note that manipulations resulting from adding series and/or shunt resistances were not considered. It is rare that this would be desired as that simply means that power is absorbed in the resistance and additional noise is added to the circuit.

EXAMPLE 3.7 Reflection Coefficient of a Shorted Microstrip Line on a Smith Chart

AWR Design Environment Project File: RFDesign_Shorted_Microstrip_Line_Smith.emp

The example in Section 3.5.2 of [11] calculated the input reflection coefficient, Γ, of the shorted microstrip line on alumina substrate shown in Figure 3-30. The line had low loss and so Γ was always close to 1. The microstrip line was designed to be 50 Ω and the locus of Γ with respect to frequency of the low loss line is plotted on a 50-Ω Smith chart in Figure 3-31(a). Plotting Γ on a 50-Ω Smith chart indicates that the reflection coefficient was calculated with respect to 50 Ω. At a very low frequency, 0.1 GHz is the lowest frequency here, the locus of the reflection coefficient is very close to $\Gamma = -1$, identifying a short circuit. As the electrical length increases, in this case the frequency increases as the physical length of the line is fixed, the locus of the reflection coefficient moves clockwise, hugging the unity reflection coefficient circle. At the highest frequency, 30 GHz, the reflection coefficient is less than 1 and the locus starts moving in from the unity circle. It is interesting to see what happens with a high-loss line, and this is achieved by changing the loss tangent, $\tan\delta$, of the substrate from 0.001 to 0.1. The locus of the reflection coefficient of the high-loss line is shown in Figure 3-31(b). Loss increases as the electrical length of the line increases and the locus of the reflection coefficient traces out a clockwise inward spiral.

Figure 3-30: A 50 Ω shorted gold microstrip line with width w = 500 μm, length ℓ = 1 cm on a 600 μm thick alumina substrate with relative permittivity ε_r = 9.8 and loss tangent $\tan\delta = 0.001$.

3.4.5 An Alternative Admittance Chart

Design often requires switching between admittance and impedance. So it is convenient to use the colored combined Smith chart shown in Figure 3-23. Monochrome charts were once the only ones available and an impedance Smith chart was used for admittance-based calculations provided that reflection coefficients are rotated by $180°$. This form of the Smith chart is not used now.

3.4.6 Expanded Smith Chart

Another form of the Smith chart is the expanded Smith chart shown in Figure 3-32. This is used to plot reflection coefficients of loads with a negative resistance that have a reflection coefficient magnitude greater than one. An oscillator, for example, presents a negative resistance to a resonator. It is also used to plot transmission parameters that have a magnitude greater than one, such as the forward transmission parameter, S_{21}, of a transistor.

3.4.7 Summary

The Smith chart is the most powerful of tools used in RF and Microwave Design. Design using Smith charts will be considered in other chapters but at this stage the reader should be totally conversant with the techniques described in this section.

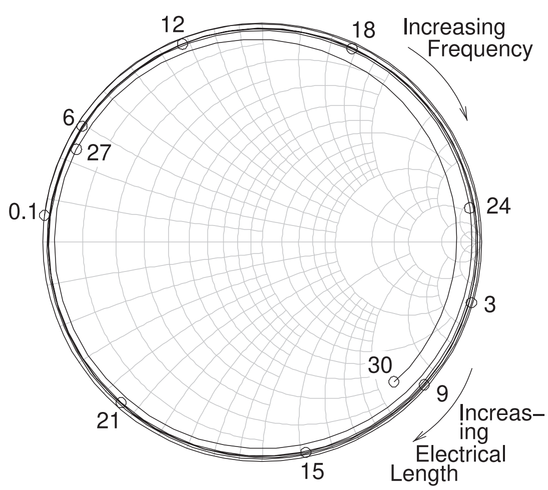

(a) $\tan\delta = 0.001$

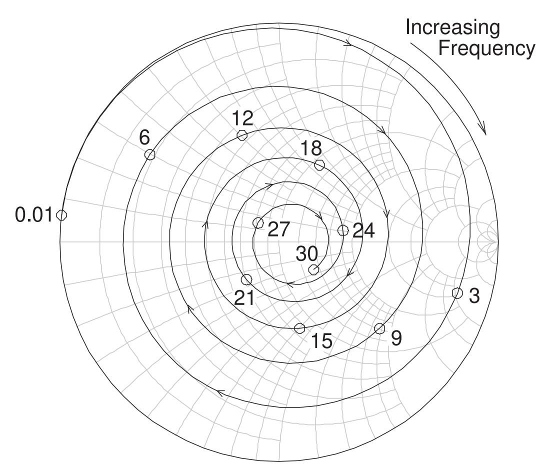

(b) $\tan\delta = 0.1$

Figure 3-31: Smith chart plot of the reflection coefficient of the shorted 1 cm-long microstrip line in Figure 3-30: (a) a low-loss substrate with $\tan\delta = 0.001$; and (b) a high-loss substrate with $\tan\delta = 0.1$. Frequencies are marked in gigahertz.

3.5 Transmission Lines and Smith Charts

The locus of a transmission line on a Smith chart is a circle. When the characteristic impedance of the line is equal to the system reference impedance this circle is centered at the origin of the Smith chart. The main purpose of this section is to consider the situation where the characteristic impedance and the system reference impedance differ.

3.5.1 Bilinear Transform

Mathematically the input reflection coefficient of a terminated transmission line of characteristic impedance Z_{02} is referenced to a system impedance Z_{01}. The mathematics describing this is based on the bilinear transform. The generalized bilinear transform of two complex numbers z and w is

$$w = \frac{Az + B}{Cz + D}, \tag{3.36}$$

where A, B, C, and D are constants[1] that may themselves be complex. This is of interest in dealing with reflection coefficients where w and z are reflection coefficients and A, B, C, and D describe the two-port network connected to a load with a complex reflection coefficient z, and w is the reflection coefficient looking into the network. The special property of the bilinear transform is that a circle in the complex plane (here the locus of z) is mapped onto another circle (here the locus of w) in the complex plane. (This is shown in Section 1.A.14 of [11].)

[1] These are not the cascadable $ABCD$ parameters, but simply the coefficients commonly used with bilinear transforms.

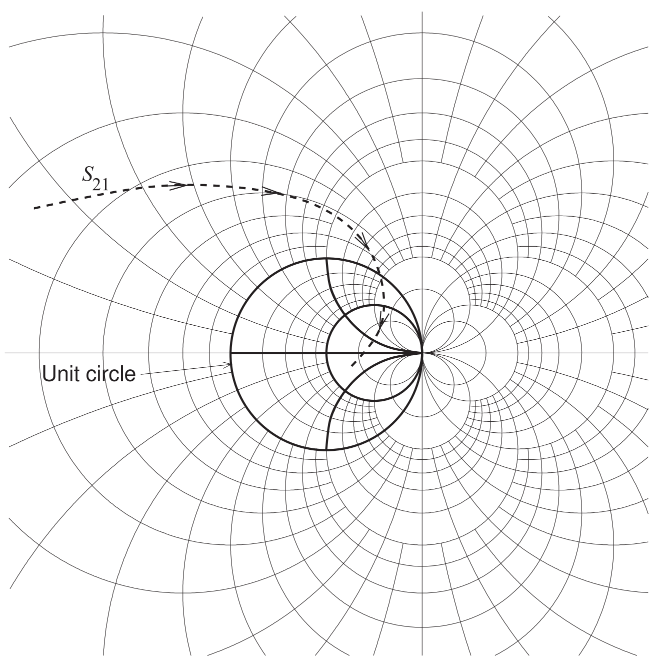

Figure 3-32: Expanded Smith chart used to plot scattering parameters with a magnitude greater than 1. The forward transmission parameter, S_{21}, of a transistor is shown with the arrows in the direction of increasing frequency. The unit circle of a conventional Smith chart is shown

3.5.2 Reference Impedance Change as a Bilinear Transform

In Figure 3-33 a fixed load terminates a transmission line of characteristic impedance Z_{01} and the input reflection coefficient is Γ_{in}. As will be shown, the locus of Γ_{in}, normalized to any system impedance, is a circle on the complex plane as the electrical length of the line increases. The electrical length of the line increases as the frequency increases with the physical length of the line held constant, or as the physical length of the line increases with the frequency held constant.

From Equation ((2.60)) of [11] the reflection coefficient of a load Z_L referenced to Z_{01} is

$$\Gamma_{L,Z01} = \frac{Z_L - Z_{01}}{Z_L + Z_{01}} \tag{3.37}$$

and the input reflection coefficient referenced to Z_{01} is

$$\Gamma_{\text{in},Z01} = \Gamma_{L,Z01} \text{e}^{-\jmath 2\theta}, \tag{3.38}$$

where $\theta = \beta\ell$ is the electrical length of the line. As θ increases from zero, $\Gamma_{\text{in},Z01}$ plotted on a polar chart traces out a circle rotating in the clockwise direction. The important result that will be developed in this section is that when the input reflection coefficient is referenced to another impedance, the new reflection coefficient will also trace out a circle. The development of $\Gamma_{\text{in},Z02}$ (the input reflection coefficient referred to Z_{02}) begins by calculating the input impedance of the line (in Figure 3-33):

$$Z_{\text{in}} = Z_{01} \frac{1 + \Gamma_{\text{in},Z01}}{1 - \Gamma_{\text{in},Z01}} \tag{3.39}$$

so that the reflection coefficient referenced to Z_{02} is

$$\begin{aligned} \Gamma_{\text{in},Z02} &= \frac{Z_{\text{in}} - Z_{02}}{Z_{\text{in}} + Z_{02}} = \frac{(Z_{\text{in}} - Z_{02})(1 - \Gamma_{\text{in},Z01})}{(Z_{\text{in}} + Z_{02})(1 - \Gamma_{\text{in},Z01})} \\ &= \frac{(Z_{01} + Z_{02})\Gamma_{\text{in},Z01} + (Z_{01} - Z_{02})}{(Z_{01} - Z_{02})\Gamma_{\text{in},Z01} + (Z_{01} + Z_{02})} \\ &= \frac{\Gamma_{\text{in},Z01} + B}{B\Gamma_{\text{in},Z01} + 1} = \frac{A\Gamma_{\text{in},Z01} + B}{C\Gamma_{\text{in},Z01} + D}. \end{aligned} \tag{3.40}$$

This mapping has the form of a bilinear transform (Equation (3.36)) with

$$A = 1 = D, \quad B = \frac{Z_{01} - Z_{02}}{Z_{01} + Z_{02}} = C. \tag{3.41}$$

Since Equation (3.40) is a general bilinear transform, if the locus of $\Gamma_{\text{in},Z01}$ is a circle, then the locus of $\Gamma_{\text{in},Z02}$ is also a circle.

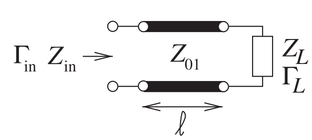

Figure 3-33: Transmission line of characteristic impedance Z_{01} terminated in a load with a reflection coefficient Γ_L.

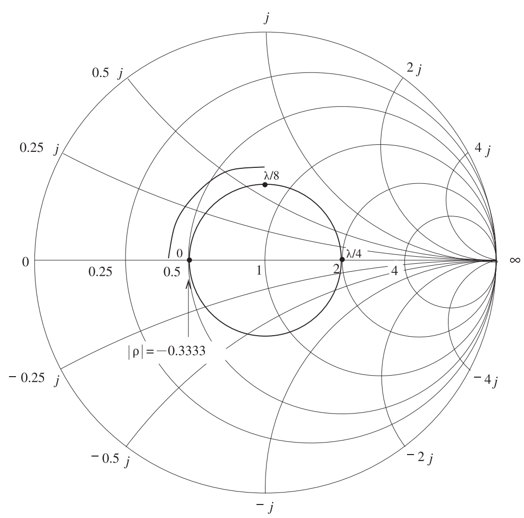

Figure 3-34: A Smith chart normalized to 50 Ω with the input reflection coefficient locus of a 50 Ω transmission line with a load of 25 Ω.

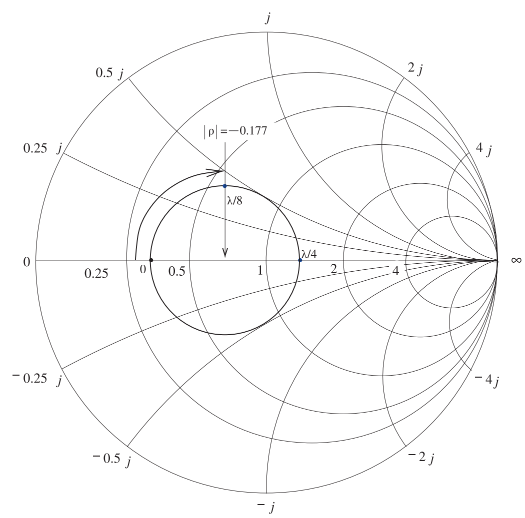

Figure 3-35: A Smith chart normalized to 75 Ω with the input reflection coefficient locus of a 50 Ω transmission line with a load of 25 Ω.

EXAMPLE 3.8 Reflection Coefficient, Reference Impedance Change

In the circuit to the right, a 50-Ω lossless line is terminated in a 25-Ω load. Plot the locus, with respect to the length of the line, of the reflection coefficient looking into the line, referencing it first to a 50-Ω reference impedance and then to a 75-Ω reference impedance.

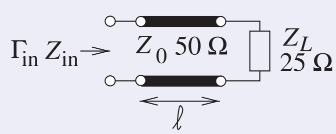

Solution:

Let the input reflection coefficient referenced to a 50-Ω system be $\Gamma_{\text{in},50}$, and when it is referenced to 75-Ω it is $\Gamma_{\text{in},75}$. In the 50-Ω system the reflection coefficient of the load is

$$\Gamma_{L,50} = \frac{Z_L - 50}{Z_L + 50} = \frac{25 - 50}{25 + 50} = -0.3333 \quad (3.42) \quad \text{and} \quad \Gamma_{\text{in},50} = \Gamma_{L,50}\mathrm{e}^{-\jmath 2\theta}, \quad (3.43)$$

where $\theta = (\beta\ell)$ is the electrical length of the line. The locus, with respect to electrical length, of $\Gamma_{\text{in},50}$ is plotted in Figure 3-34 as the length ℓ ranges from 0 to $\lambda/8$ to $\lambda/2$, and completes the circle at $\lambda/2$. Now

$$Z_{\text{in}} = 50\frac{1 + \Gamma_{\text{in},50}}{1 - \Gamma_{\text{in},50}}, \quad (3.44)$$

so that the 75-Ω reflection coefficient is

$$\Gamma_{\text{in},75} = \frac{Z_{\text{in}} - 75}{Z_{\text{in}} + 75}. \quad (3.45)$$

The locus of this reflection coefficient is plotted on a polar plot in Figure 3-35. This locus is the plot of $\Gamma_{\text{in},75}$ as the electrical length of the line, θ, is varied from 0 to π. The center of the circle in Figure 3-35 is taken from the chart and determined to be -0.177.

A circle is defined by its center and its radius, and Equations ((1.239)) and ((1.240)) of [11], enable the circles for the locus of $\Gamma_{\text{in},Z01}$ and $\Gamma_{\text{in},Z02}$ to be related. $\Gamma_{\text{in},Z01}$ has a center C_{Z01} and a radius R_{Z01}:

$$C_{Z01} = 0 \quad \text{and} \quad R_{Z01} = |\Gamma_{L,Z01}| \,. \tag{3.46}$$

In Equation ((1.239)) of [11] C_{Z01} replaces the center C_z and $|\Gamma_{L,Z01}|$ takes the place of the radius R_z. Similarly the center of the Γ_{Z02} circle, C_{Z02}, replaces C_w and the radius of the Γ_{Z02} circle, R_{Z02}, replaces R_w. So the locus of the reflection coefficient referenced to Z_{02} is described by a circle with center and radius

$$C_{Z02} = \frac{B - A/C}{1 - |C\Gamma_{L,Z01}|^2} + \frac{A}{C} \quad (3.47) \qquad R_{Z02} = \left|\frac{(BC - A)\Gamma_{L,Z01}}{1 - |C\Gamma_{L,Z01}|^2}\right| . \quad (3.48)$$

Since, from Equation (3.41), $A = 1$ and $B = C$ (B is given in Equation (3.41)), this further simplifies to

$$C_{Z02} = \frac{B - 1/B}{1 - |B\Gamma_{L,Z01}|^2} + \frac{1}{B} \quad (3.49) \qquad R_{Z02} = \left|\frac{(B^2 - 1)\Gamma_{L,Z01}}{1 - |B\Gamma_{L,Z01}|^2}\right| . \quad (3.50)$$

So the locus (with respect to frequency) of the input reflection coefficient of a terminated transmission line (of characteristic impedance Z_{01}) is a circle no matter what normalization impedance is used and the center of the circle will be on the real axis, the horizontal axis of the Smith chart.

EXAMPLE 3.9 Center of Reflection Coefficient Locus

In Example 3.8 the locus of the input reflection coefficient referenced to 75 Ω was plotted for a 50-Ω line terminated in a load with reflection coefficient (in the 50-Ω system) of $-1/3$. Calculate the center of the input reflection coefficient when it is referenced to 75 Ω.

Solution:

The center of the reflection coefficient normalized to Z_{01} is zero, that is, $C_{50} = 0$. From Equation (3.49), the center of the reflection coefficient normalized to $Z_{02} = 75\ \Omega$ is

$$C_{75} = \frac{B - 1/B}{1 - |B\Gamma_{L,50}|^2} + \frac{1}{B}, \tag{3.51}$$

where $$B = \frac{Z_{01} - Z_{02}}{Z_{01} + Z_{02}} = \frac{50 - 75}{50 + 75} = -0.2. \tag{3.52}$$

So $$C_{75} = \frac{-0.2 + 5}{1 - (0.2/3)^2} - 5 = -0.17857, \tag{3.53}$$

which compares favorably to a center of -0.177 determined manually from the polar plot in the previous example.

3.5.3 Reflection Coefficient Locus

The direction of the locus of the input reflection coefficient of a terminated transmission line is always clockwise with increasing frequency, even if the Smith chart uses a reference or normalization impedance different from the characteristic impedance of the line. In Figure 3-36, Z_{01} is the characteristic impedance of the line and Z_{02} is the normalization impedance. The center of the circle of the reflection coefficient normalized to Z_{02} is to the left of the origin if $Z_{02} > Z_{01}$, and to the right of the origin if normalized to $Z_{02} < Z_{01}$, but always on the real axis.

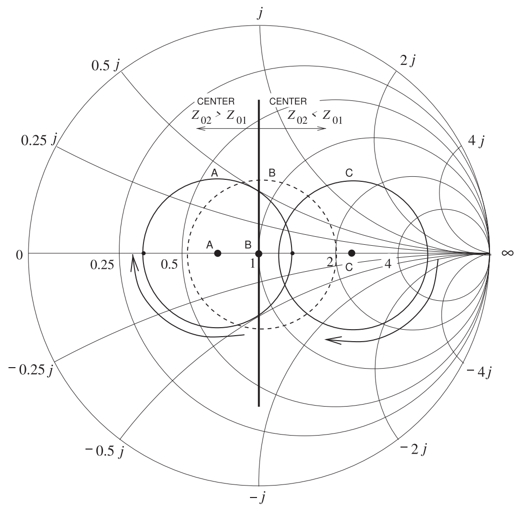

Figure 3-36: The locus of the input reflection coefficient normalized to Z_{02} of a terminated line of characteristic impedance Z_{01}. The locus is with respect to the electrical length of the line and the arrows show the direction of rotation of the reflection coefficient. (Note that for the same terminating impedance the radii will also change, but this is not shown here.)

3.5.4 Summary

Smith charts are indispensable tools for RF and microwave engineers. Even with the ready availability of CAD programs. Smith charts are generally preferred for portraying measured and calculated data because of the easy interpretation of S parameters. With experience, the properties of circuits can be inferred. Also, with experience they are an invaluable design tool enabling the designer to see the beginning and endpoints of a design and infer the type of circuitry required to go from start to finish.

3.6 Summary

Graphical representations of power flow enable RF and microwave engineers to quickly ascertain circuit performance and arrive at qualitative design decisions. Humans are very good at processing graphical information and seeing patterns, anomalies, and the path from one point to another. Two powerful techniques were introduced in this chapter that provide this insight. These are the signal flow graph and the Smith chart. Signal flow graphs enable engineers to solve algebraic problems without using algebraic equations. Signal flow graphs are also a convenient way to develop symbolic expressions. Developing these expressions using algebraic manipulations alone is error prone.

The Smith chart is a richly annotated polar plot for representing reflection and transmission coefficients, and more generally, scattering parameters. The Smith chart representation of scattering parameter data aligns very well with the intuitive understanding of an RF designer. The experienced RF designer is intrinsically familiar with the Smith chart and prefers that circuit performance during design be represented on one. Representing something as simple as an extension of a line length to a two-port is quite complex if described using network parameters other than scattering parameters. However, with scattering parameters this extension results in a change of the angle of a scattering parameter, or on a Smith chart an arc. Scattering parameters relate directly to power flow. So from a Smith chart an experienced designer can ascertain the effect of circuit design on power flow, which then relates to signal-to-noise ratio and power gain. The Smith chart will be an essential tool in many of the topics considered in later chapters.

3.7 References

[1] S. Mason, "Feedback theory-some properties of signal flow graphs," *Proc. of the IRE*, vol. 41, no. 9, pp. 1144–1156, Sep. 1953.

[2] A. Tustin, *Direct Current Machines for Control Systems*. The Macmillan Company, 1956.

[3] N. Balabanian, *Fundamentals of Circuit Theory*. Allyn and Bacon, 1961.

[4] J. Abrahams and G. Coverley, *Signal Flow Analysis*. Pergamon Press, 1965.

[5] J. Distefano, A. Stubberud, and I. Williams, *Theory and Problems of Feedback Control Systems*. McGraw-Hill, 1990.

[6] S. Mason, "Feedback theory-further properties of signal flow graphs," *Proc. of the IRE*, vol. 44, no. 7, pp. 920–926, Jul. 1956.

[7] P. Smith, *Electronic Applications of the Smith Chart: In Waveguide, Circuit, and Component Analysis*. SciTech Publishing, 2000.

[8] ——, "Transmission line calculator," *Electronics*, 1939.

[9] ——, "An improved transmission-line calculator," *Electronics*, 1944.

[10] ——, "R.F. transmission line nomographs," *Electronics*, vol. 22, pp. 112–117, Feb. 1949.

[11] M. Steer, *Microwave and RF Design, Transmission Lines*, 3rd ed. North Carolina State University, 2019.

3.8 Exercises

1. Reduce the following signal flow graph to two edges and three nodes. That is, write down the expression for b_2 in terms of a_1 and a_2, eliminating the variables x_1, x_2, and x_3.

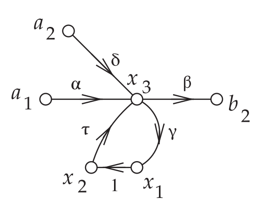

2. Reduce the following signal flow graph to one edge and two nodes. That is, write down the expression for b_2 in terms of a_1, eliminating the variables x_1 and x_2.

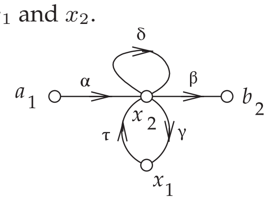

3. The scattering parameters of a two-port are $S_{11} = 0.25$, $S_{12} = 0$, $S_{21} = 1.2$, and $S_{22} = 0.5$. The system reference impedance is 50 Ω and the Thevenin equivalent impedance of the source at Port 1 is $Z_G = 50\ \Omega$. The power available from the source connected to Port 1 is 1 mW. The load impedance is $Z_L = 25\ \Omega$. Using SFGs, determine the power dissipated by the load at Port 2.

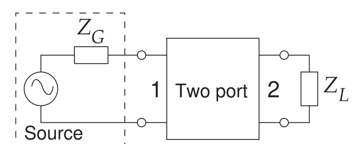

4. Draw the SFG of a two-port with a load at Port 2 having a voltage reflection coefficient of Γ_L, and at Port 1 a source reflection coefficient of Γ_S. Γ_S is the reflection coefficient looking from Port 1 of the two-port toward the generator. Keep the S parameters of the two-port in symbolic form (e.g., S_{11}, S_{12}, S_{21}, and S_{22}). Using SFG analysis, derive an expression for the reflection coefficient looking into the two-port at Port 2. You must show the stages in collapsing the SFG to the minimal form required.

5. A three-port has the scattering parameters:

$$\begin{bmatrix} 0 & \gamma & \delta \\ \alpha & 0 & \epsilon \\ \theta & \beta & 0 \end{bmatrix}.$$

Port 2 is terminated in a load with a reflection coefficient Γ_L. Reduce the three-port to a two-port using signal flow graph theory. Write down the four scattering parameters of the final two-port.

6. The 50-Ω S parameters of a three-port are

$$\begin{bmatrix} 0.2\angle 180^\circ & 0.8\angle -45^\circ & 0.1\angle 45^\circ \\ 0.8\angle -45^\circ & 0.2\angle 0^\circ & 0.1\angle 90^\circ \\ 0.1\angle 45^\circ & 0.1\angle 90^\circ & 0.1\angle 180^\circ \end{bmatrix}.$$

(a) Is the three-port reciprocal? Explain your answer.

(b) Write down the criteria for a network to be lossless.
(c) Is the three-port lossless? You must show your work.
(d) Draw the SFG of the three-port.
(e) A 50 Ω load is attached to Port 3. Use SFG operations to derive the SFG of the two-port with just Ports 1 and 2. Write down the two-port S parameter matrix.

7. The 50 Ω S parameters of a three-port are

$$\begin{bmatrix} 0.2\angle 180^\circ & 0.8\angle -45^\circ & 0.1\angle 45^\circ \\ 0.8\angle -45^\circ & 0.2\angle 0^\circ & 0.1\angle 90^\circ \\ 0.1\angle 45^\circ & 0.1\angle 90^\circ & 0.1\angle 180^\circ \end{bmatrix}.$$

(a) Is the three-port reciprocal? Explain.
(b) Write down the criteria for a network to be lossless.
(c) Is the three-port lossless? Explain.
(d) Draw the SFG of the three-port.
(e) A 150 Ω load is attached to Port 3. Derive the SFG of the two-port with just Ports 1 and 2. Write down the two-port S parameter matrix of the simplified network.

8. A system consists of 2 two-ports in cascade. The S-parameter matrix of the first two-port is $\mathbf{S}_A$ and the S parameter matrix of the second two-port is $\mathbf{S}_B$. The second two-port is terminated in a load with a reflection coefficient Γ_L. (Just to be clear, $\mathbf{S}_A$ is followed by $\mathbf{S}_B$, which is then terminated in Γ_L. Port 2 of $\mathbf{S}_A$ is connected to Port 1 of $[S_B]$.) The individual S parameters of the two-ports are as follows:

$$\mathbf{S}_A = \begin{bmatrix} a & c \\ c & b \end{bmatrix} \text{ and } \mathbf{S}_B = \begin{bmatrix} d & f \\ f & e \end{bmatrix}.$$

(a) Draw the SFG of the system consisting of the two cascaded two-ports and the load.
(b) Ignoring the load, is the cascaded two-port system reciprocal? If there is not enough information to decide, then say so. Give your reasons.
(c) Ignoring the load, is the cascaded two-port system lossless? If there is not enough information to decide, then say so. Give your reasons.
(d) Consider that the load has no reflection (i.e., $\Gamma_L = 0$). Use SFG analysis to find the input reflection coefficient looking into Port 1 of $[S_A]$. Your answer should be Γ_{in} in terms of $a, b, \ldots, f$.

9. A circulator is a three-port device that is not reciprocal and selectively shunts power from one port to another. The S parameters of an ideal circulator are

$$[S] = \begin{bmatrix} 0 & 1 & 0 \\ 0 & 0 & 1 \\ 1 & 0 & 0 \end{bmatrix}.$$

(a) Draw the three-port and discuss power flow.
(b) Draw the SFG of the circulator.
(c) If Port 2 is terminated in a load with reflection coefficient 0.2, reduce the SFG of the circulator to a two-port with Ports 1 and 3 only.
(d) Write down the 2×2 S parameter matrix of the (reduced) two-port.

10. The S parameters of a certain two-port are $S_{11} = 0.5 + \jmath 0.5$, $S_{21} = 0.95 + \jmath 0.25$, $S_{12} = 0.15 - \jmath 0.05$, $S_{22} = 0.5 - \jmath 0.5$. The system reference impedance is 50 Ω.
(a) Is the two-port reciprocal?
(b) Which of the following is a true statement about the two-port?
(A) It is unitary.
(B) Overall power is produced by the two-port.
(C) It is lossless.
(D) If Port 2 is matched, then the real part of the input impedance (at Port 1) is negative.
(E) A and C.
(F) A and B.
(G) A, B, and C
(H) None of the above.
(c) What is the value of the load required for maximum power transfer at Port 2? Express your answer as a reflection coefficient.
(d) Draw the SFG for the two-port with a load at Port 2 having a voltage reflection coefficient of Γ_L and at Port 1 a source reflection coefficient of Γ_S.

11. The 50-Ω S parameters of a three-port are

$$\begin{bmatrix} 0.2 & 0.8 & 0.1 \\ 0.8 & 0.2 & 0.1 \\ 0.1 & 0.1 & 0.1 \end{bmatrix}.$$

(a) Is the three-port reciprocal? Explain your answer.
(b) Write down the criteria for a network to be lossless.
(c) Is the three-port lossless? You must show your work.
(d) Draw the SFG of the three-port.
(e) A 50 Ω load is attached to Port 3. Use SFG operations to derive the SFG of the two-port with just Ports 1 and 2. Write down the two-port S parameter matrix.

12. The 50-Ω S parameters of a three-port are

$$\begin{bmatrix} 0.5 & 0.4 & 0.5 \\ 0.6 & 0.5 & 0.5 \\ 0.5 & 0.5 & 0.5 \end{bmatrix}.$$

    (a) Is the three-port reciprocal? Explain.
    (b) Write down the criteria for a network to be lossless.
    (c) Is the three-port lossless? Explain.
    (d) Draw the SFG of the three-port.
    (e) A 150 Ω load is attached to Port 3. Derive the SFG of the two-port with just Ports 1 and 2. Write down the two-port S parameter matrix.

13. In the distribution of signals on a cable TV system a 75-Ω coaxial cable is used, with a loss of 0.1 dB/m at 1 GHz. If a subscriber disconnects a television set from the cable so that the load impedance looks like an open circuit, estimate the input impedance of the cable at 1 GHz and 1 km from the subscriber. An answer within 1% is required. Estimate the error of your answer. Indicate the input impedance on a Smith chart, drawing the locus of the input impedance as the line is increased in length from nothing to 1 km. (Consider that the dielectric filling the line has $\epsilon_r = 1$.)

14. A resistive load has a reflection coefficient with a magnitude of 0.7. If a transmission line is placed in series with the load, on a polar plot sketch the locus of the input reflection coefficient looking into the input of the terminated line as the line increases in electrical length from zero to $\lambda/2$. By reading the Smith chart, determine the normalized input impedance of the line when it has an electrical length of $\pi/2$.

15. A complex load has a reflection coefficient of $0.5+\jmath 0.5$. If a transmission line is placed in series with the load, on a polar plot sketch the locus of the input reflection coefficient looking into the input of the terminated line as the line increases in electrical length from zero to $\pi/2$.

16. A resistive load has a reflection coefficient of -0.5. If a transmission line is placed in series with the load, on a polar plot sketch the locus of the input reflection coefficient looking into the input of the terminated line as the line increases in electrical length from 0 to $3\lambda/8$.

17. S_{21} of a two-port is 0.5. If a transmission line is placed in series with Port 1, on a polar plot sketch the locus of S_{21} of the augmented two-port as the electrical length of the line increases from zero to $\lambda/2$.

18. A load has an impedance $Z = 115 - \jmath 20\ \Omega$.
    (a) What is the reflection coefficient, Γ_L, of the load in a 50 Ω reference system?
    (b) Plot the reflection coefficient on a polar plot of reflection coefficient.
    (c) If a one-eighth wavelength long lossless 50-Ω transmission line is connected to the load, what is the reflection coefficient, Γ_{in}, looking into the transmission line? (Again, use the 50 Ω reference system.) Plot Γ_{in} on the polar reflection coefficient plot of part (b). Clearly identify Γ_{in} and Γ_L on the plot.
    (d) On the Smith chart, identify the locus of Γ_{in} as the length of the transmission line increases from 0 to $\lambda/8$ long. That is, on the Smith chart, plot Γ_{in} as the length of the transmission line varies.

19. A load has a reflection coefficient with a magnitude of 0.5. If a transmission line is placed in series with the load, on a polar plot sketch the locus of the input reflection coefficient looking into the input of the terminated line as the line increases in electrical length from zero to $\lambda/2$. What is the normalized input impedance of the line when it has an electrical length of $\lambda/2$?

20. A resistive load has a reflection coefficient with a magnitude of 0.7. If a transmission line is placed in series with the load, on a polar plot sketch the locus of the input reflection coefficient looking into the input of the terminated line as the line increases in electrical length from zero to $\lambda/4$. By reading the Smith chart, determine the normalized input impedance of the line when it has an electrical length of $\lambda/4$.

Problems 21 to 27 refer to the normalized Smith chart in Figure 3-38 with reference impedance $Z_{\text{REF}} = 50\,\Omega$ and reflection coefficient Γ, voltage reflection coefficient ${}^V\Gamma$, current reflection coefficient ${}^I\Gamma$, and normalized impedance $z = r + \jmath x$ and admittance $y = g + \jmath b$. Γ should be given in magnitude-angle format.

21. (a) What is ${}^V\Gamma$ at A?
    (b) What is ${}^I\Gamma$ at A?
    (c) What is r at B?
    (d) What is z at C?
    (e) What is y at D?
    (f) What is $|\Gamma|$ at F?
    (g) What is b at I?
    (h) What is Γ at P?
    (i) What is Γ at D?
    (j) What is Γ at T?

22. (a) What is z at A?
    (b) What is y at I?
    (c) What is z at E?
    (d) What is y at Z?
    (e) What is y at H?
    (f) What is $|\Gamma|$ at W?
    (g) What is b at F?
    (h) What is x at K?
    (i) What is Γ at K?
    (j) What is Γ at R?

23. (a) What is y at A?
(b) What is y at I?
(c) What is z at G?
(d) What is y at O?
(e) What is y at V?
(f) What is Γ at B?
(g) What is x at C?
(h) What is Γ at G?
(i) What is z at L, label this z_L?
(j) Use the Smith chart to find z_{in} of a 50 Ω $\lambda/8$-long line with load z_L?

24. (a) What is ${}^V\Gamma$ at M?
(b) What is ${}^I\Gamma$ at M?
(c) What is r at W?
(d) What is z at Y?
(e) What is y at V?
(f) What is $|\Gamma|$ at B?
(g) What is b at K?
(h) What is Γ at V?
(i) What is Γ at P?
(j) What is Γ at N?

25. (a) What is z at M?
(b) What is y at K?
(c) What is z at S?
(d) What is y at R?
(e) What is g at B?
(f) What is $|\Gamma|$ at F?
(g) What is b at B?
(h) What is x at I?
(i) What is Γ at I?
(j) What is Γ at Q?

26. (a) What is g at M?
(b) What is r at K?
(c) What is y at S?
(d) What is z at R?
(e) What is y at Z?
(f) What is Γ at W?
(g) What is x at Y?
(h) What is Γ at T?
(i) What is z at O, label this z_O?
(j) Using the Smith chart find z_{in} of a $3\lambda/8$-long 50 Ω line with load z_O?

27. (a) What is g at P?
(b) What is y at J?
(c) What is Γ at L?
(d) What is z at N?
(e) What is y at S?
(f) What is $|\Gamma|$ at U?
(g) What is ${}^V\Gamma$ at X?
(h) What is ${}^I\Gamma$ at X?
(i) What is g at B?
(j) What is x at I?

28. Design a short-circuited stub to realize a normalized susceptance of 2.15. Show the locus of the stub as its length increases from zero to its final length. What is the minimum length of the stub in terms of wavelengths?

29. Design a short-circuited stub to realize a normalized susceptance of -0.56. Show the locus of the stub as its length increases from zero to its final length. What is the minimum length of the stub in terms of wavelengths?

30. Design a short-circuited stub to realize a normalized susceptance of -2.2. Show the locus of the stub as its length increases from zero to its final length. What is the minimum length of the stub in terms of wavelengths?

31. A 75-Ω transmission line is terminated in a load with a reflection coefficient, Γ, normalized to 75 Ω, of $0.5\angle 45^\circ$. If Γ at the input of the line is $0.5\angle{-135^\circ}$, what is the minimum electrical length of the line in degrees.

32. An open-circuited 75-Ω transmission line has an input reflection coefficient with an angle of 40° what is the electrical length of the line in degrees? If there is more than one answer provide at least two correct answers.

33. Use a Smith chart to design a microstrip network to match a load $Y_L = 28 - \jmath 12$ mS to a source $Y_S = 6 + \jmath 12$ mS. Use transmission lines only and use short-circuited stubs. Use a reference impedance of 50 Ω.
(a) Draw the matching network problem labeling source and load admittances and labeling the admittance looking into the matching network from the source as Y_1.
(b) What is the condition for maximum power transfer at the source side of the matching network in terms of admittances?
(c) What is the condition for maximum power transfer at the source side of the matching network in terms of reflection coefficients?
(d) What is the reference admittance Y_{REF}?
(e) What is the value of the normalized source admittance?
(f) What is the value of the normalized load admittance?
(g) On a Smith chart (not a sketch) identify, i.e. draw, the electrical designs of two suitable matching networks. Identify the designs using the labels D1 and D2 on the loci.
(h) Develop the complete electrical design of a matching network using the Smith chart using 50 Ω lines only. You only need do one design.
(i) Draw the microstrip layout of the matching network and identify critical parameters such characteristic impedances and electrical length. Ensure that you identify which is the source side and which is the load side. You do not need to determine the widths of the lies or their physical lengths.

34. Repeat Exercise 33 with $Y_L = 20 + \jmath 20$ mS to a source $Y_S = 4 + \jmath 20$ mS.

35. Repeat Example 3.4 using the full impedance Smith chart of Figure 3-18.

36. Plot the normalized impedances $z_A = 0.5 + \jmath 0.5$, $z_A = 0.5 + \jmath 0.5$, and $z_B = 0.185 - \jmath 1.05$ on the full impedance Smith chart of Figure 3-18. [Parallels Example 3.4]

37. In Figure 3-37 the results of several different experiments are plotted on a Smith chart. Each experiment measured the input reflection coefficient from a low frequency (denoted by a circle) to a high frequency (denoted by a square) of a one-port. Determine the load that was measured. The loads that were measured are one of those shown below.

Load	Description
i	An inductor
ii	A capacitor
iii	A reactive load at the end of a transmission line
iv	A resistive load at the end of a transmission line
v	A parallel connection of an inductor, a resistor, and a capacitor going through resonance and with a transmission line offset
vi	A series connection of a resistor, an inductor and a capacitor going through resonance and with a transmission line offset
vii	A series resistor and inductor
viii	An unknown load and not one of the above

For each of the measurements below indicate the load or loads using the load identifier above (e.g., i, ii, etc.).

(a) What load(s) is indicated by curve A?

(a) What load(s) is indicated by curve A?

(b) What load(s) is indicated by curve B?

(c) What load(s) is indicated by curve C?

(d) What load(s) is indicated by curve D?

(e) What load(s) is indicated by curve E?

(f) What load(s) is indicated by curve F?

38. A 50-Ω lossy transmission line is shorted at one end. The line loss is 2 dB per wavelength. Note that since the line is lossy the characteristic impedance will be complex, but close to 50 Ω, since it is only slightly lossy. There is no way to calculate the actual characteristic impedance with the information provided. That is, problems must be solved with small inconsistencies. Microwave engineers do the best they can in design and always rely on measurements to calibrate results.

(a) What is the reflection coefficient at the load (in this case the short)?

(b) Consider the input reflection coefficient, Γ_{in}, at a distance ℓ from the load. Determine Γ_{in} for ℓ going from 0.1λ to λ in steps of 0.1λ.

(c) On a Smith chart plot the locus of Γ_{in} from $\ell = 0$ to λ.

(d) Calculate the input impedance, Z_{in}, when the line is $3\lambda/8$ long using the telegrapher's equation.

(e) Repeat part (d) using a Smith chart.

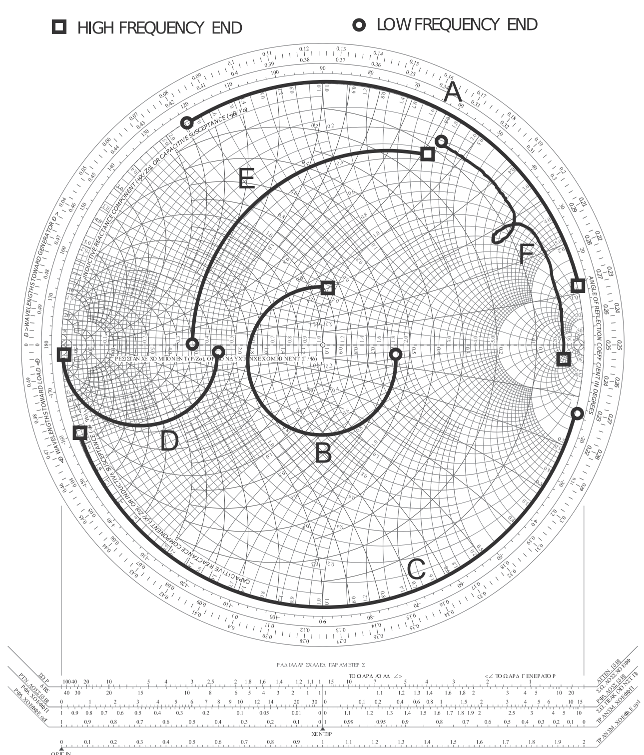

Figure 3-37: The locus of various loads plotted on a Smith chart.

39. Design an open-circuited stub with an input impedance of $+\jmath 75\ \Omega$. Use a transmission line with a characteristic impedance of $75\ \Omega$. [Parallels Example 3.5]
40. Design a short-circuited stub with an input impedance of $-\jmath 50\ \Omega$. Use a transmission line with a characteristic impedance of $100\ \Omega$. [Parallels Example 3.5]
41. A load has an impedance $Z_L = 25 - \jmath 100\ \Omega$.
    (a) What is the reflection coefficient, Γ_L, of the load in a $50\ \Omega$ reference system?
    (b) If a one-quarter wavelength long $50\ \Omega$ transmission line is connected to the load, what is the reflection coefficient, Γ_{in}, looking into the transmission line?
    (c) Describe the locus of Γ_{in}, as the length of the transmission line is varied from zero length to one-half wavelength long. Use a Smith chart to illustrate your answer
42. A network consists of a source with a Thevenin equivalent impedance of $50\ \Omega$ driving first a series reactance of $-50\ \Omega$ followed by a one-eighth wavelength long transmission line with a characteristic impedance of $40\ \Omega$ and an element with a reactive impedance of $\jmath 25\ \Omega$ in shunt with a load having an impedance $Z_L = 25 - \jmath 50\ \Omega$. This problem must be solved graphically and no credit will be given if this is not done.
    (a) Draw the network.
    (b) On a Smith chart, plot the locus of the reflection coefficient first for the load, then with the element in shunt, then looking into the transmission line, and finally the series element. Use letters to identify each point on the Smith chart. Write down the reflection coefficient at each point.
    (c) What is the impedance presented by the network to the source?
43. In the circuit below, a 75-Ω lossless line is terminated in a 40-Ω load. On the complex plane plot the locus, with respect to the length of the line, of the reflection coefficient, looking into the line referencing it first to a 50-Ω impedance. [Parallels Example 3.8]

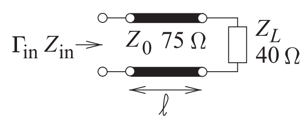

44. Consider the circuit below, a $60\ \Omega$ lossless line is terminated in a $40\ \Omega$ load. What is the center of the reflection coefficient locus on the complex plane when it is referenced to $55\ \Omega$? [Parallels Example 3.9]

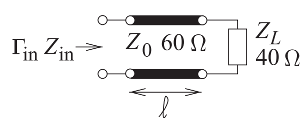

3.8.1 Exercises by Section

†challenging

§3.2 1, 2, 3†, 4†, 5†, 6†, 7†, 8†, 9†, 10†, 11, 12
§3.4 13, 14, 15, 16, 17, 18, 19, 20, 21, 22, 23, 24, 25, 26, 27, 28, 29, 30, 31, 32, 33, 34, 35, 36, 37†, 38†, 39†, 40†, 41†, 42†
§3.5 43†, 44†

3.8.2 Answers to Selected Exercises

1 $\dfrac{\beta}{1-\tau\gamma}(\alpha a_1 + \gamma a_2)$
3 0.940 mW
6 $\begin{bmatrix} -0.2 & 0.8\angle{-45^\circ} \\ -0.2 & 0.2 \end{bmatrix}$
8(d) $a + \dfrac{dc^2}{1-bd}$
13 $\Gamma_{\text{IN}} = 10^{-10}$
37(c) ii & iii
38(d) $8.37 - \jmath 49.3\ \Omega$
41 $0.825\angle{-50.9^\circ}$
42 $\approx 250 - \jmath 41\ \Omega$
44 0.0418

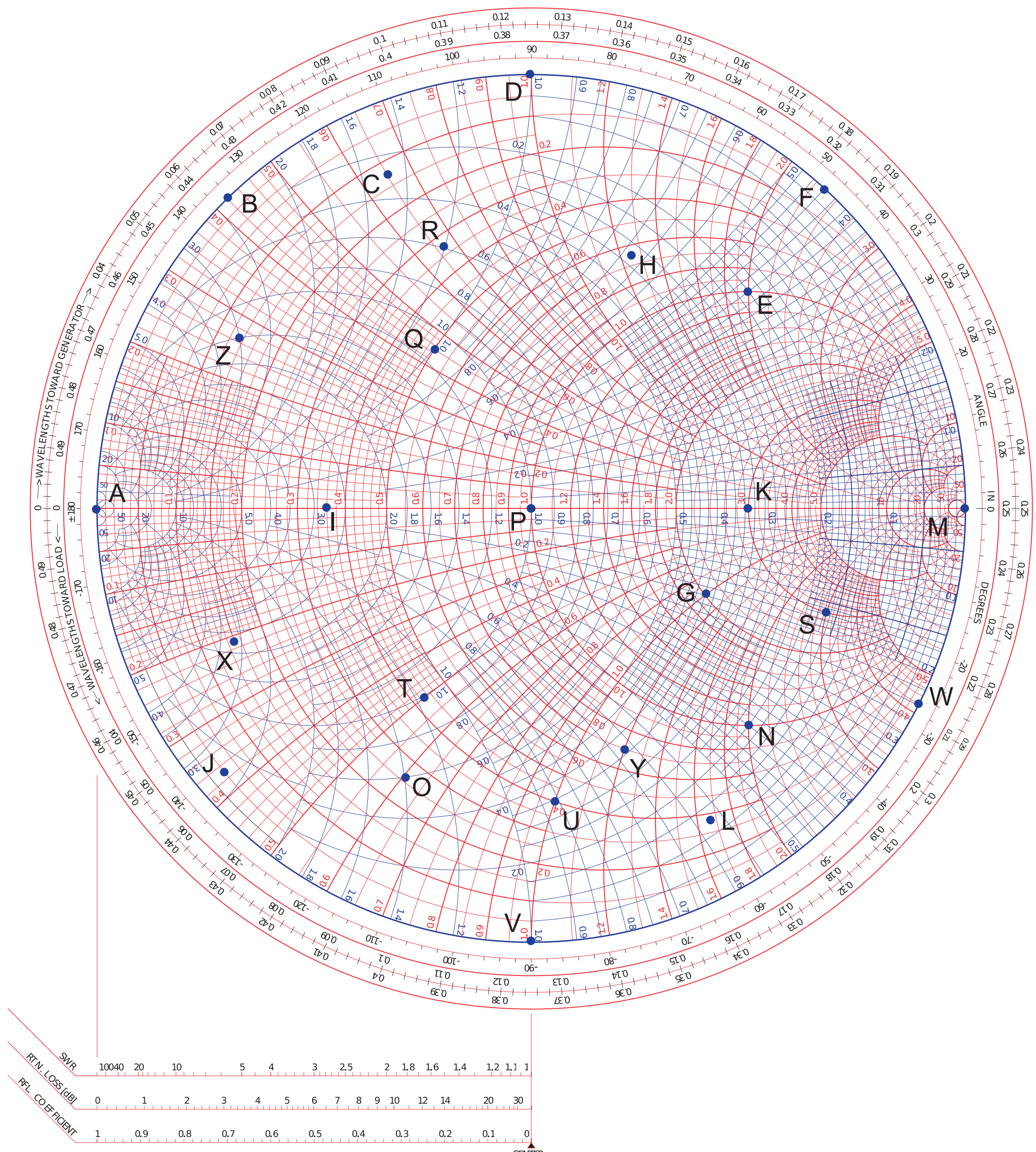
A
B
C
D
E
F
G
H
I
J
K
L
M
N
O
P
Q
R
S
T
U
V
W
X
Y
Z
SWR
RTN. LOSS [dB]
RFL. COEFFICIENT
CENTER

Figure 3-38

CHAPTER 4

Microwave Measurements

4.1 Introduction

At microwave frequencies it is almost never possible to measure voltage and current directly and so it is not possible to measure z and y parameters, and most other network parameters, directly. However S parameters are easy to measure as they are based on power flow and instead of relying on short and open circuit terminations, their definitions require matched loads which minimize reflections and also ensure that circuits are stable.

4.2 Measurement of Scattering Parameters

S parameters are measured using a network analyzer called an **automatic network analyzer** (**ANA**), or more commonly a **vector network analyzer** (**VNA**).

4.2.1 Vector Network Analyzer

The VNA is based on separating the forward- and backward-traveling voltage waves using a directional coupler. The separated traveling waves are then the total voltages on the coupled lines of the directional coupler. They are down-converted to perhaps 100 kHz and then sampled by an analog-to-digital converter [1]. Schematics of modern VNAs are shown in Figures 4-1 and 4-2 and comprise

1. A frequency synthesizer for stable generation of a sinewave.
2. A display plotting the S parameters in various forms, with a Smith chart being most commonly used.
3. An S parameter test set. This device generally has two measuring ports

so that when required S_{11}, S_{12}, S_{21}, and S_{22} can all be determined under program control. The main components are switches and directional couplers. Directional couplers separate the forward- and backward-traveling wave components. Network analyzers with more than two ports—four-port network analyzers are popular—have more switches and directional couplers. The mixers map the amplitude and phase of the RF signal to the IF, commonly around 100 kHz, which is sampled by the ADC.

4. A computer controller used in correcting errors and converting the results to the desired form.

For RF measurements up to a few tens of gigahertz, most of these functions are incorporated in a single instrument. At higher frequencies and with older equipment multiple units are used. An outline of such a system is shown in Figure 4-3(a) and a photograph in Figure 4-3(c). In the foreground of Figure 4-3(c) is a probe station that has a stage for an IC or RF circuit board and mounts for micropositioners to which **microprobes** are attached. The vertical tube-shaped object is a microscope-mounted camera.

The probes are mounted on micromanipulators such as those shown in Figure 4-4. These provide precision positioning with x-y-z movement and an axis rotation to accommodate probing on substrates that are not completely flat.

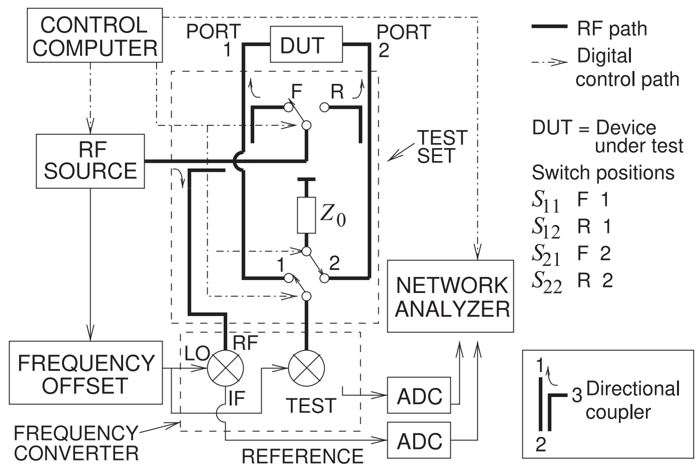

Figure 4-1: Switch-based vector network analyzer system with two receivers. The directional couplers selectively couple forward- or backward-traveling waves. With the directional coupler (see inset), a traveling wave inserted at Port 2 appears only at Port 1. A traveling wave inserted at Port 1 appears at Port 2 and a coupled version at Port 3. A traveling wave inserted at Port 3 appears only at Port 1. Switch positions determine which S parameter is measured.

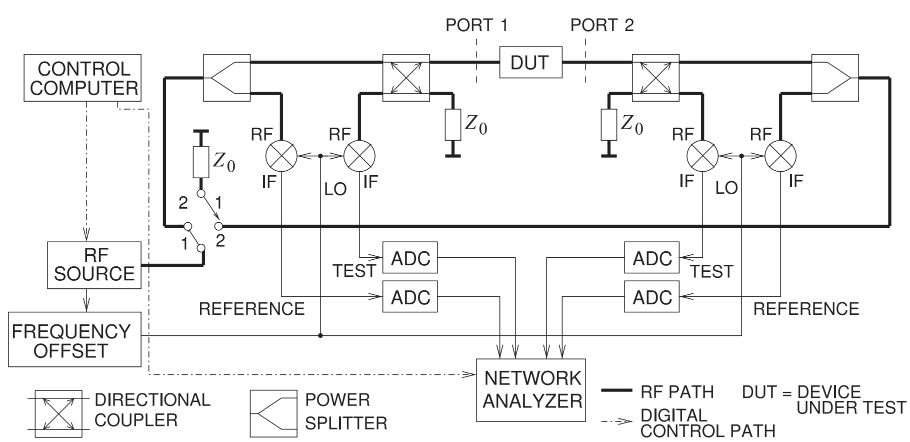

Figure 4-2: Vector network analyzer system with four receivers.

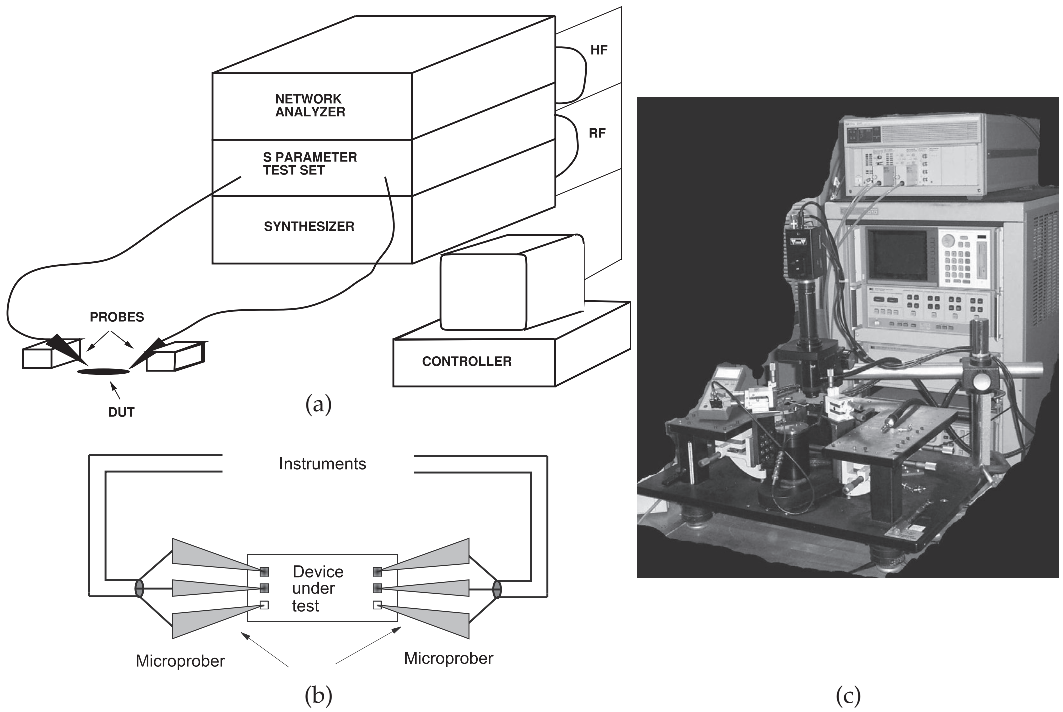

Figure 4-3: *S* parameter measurement system: (a) shown in a configuration to do on-chip testing; (b) details of coplanar probes with a GSG configuration and contacting pads; and (c) a vector network analyzer in the background with probe station including camera.

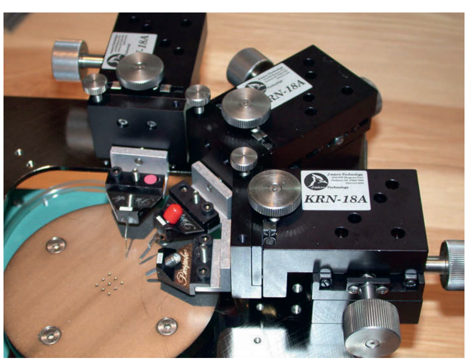

Figure 4-4: Micropositioners used with coplanar probes. Used with permission of J MicroTechnology, Inc.

Probing elements required for on-wafer measurements are shown in Figure 4-5. Figure 4-5(a) shows a single RF probe that is essentially an extended coaxial line. Figure 4-5(c) shows a microprobe making a connection to a transmission line on an IC and the lower image in Figure 4-5(b) shows greater detail of the contact area.

A typical microprobe is based on a micro coaxial cable with the center conductor (carrying the signal) extended a millimeter or so to form a needle-like contact. Two other needle-like contacts are made by attaching short extensions to the outer conductor of the coaxial line on either side of the signal connection (see the top image in Figure 4-5(b)). Such probes are called

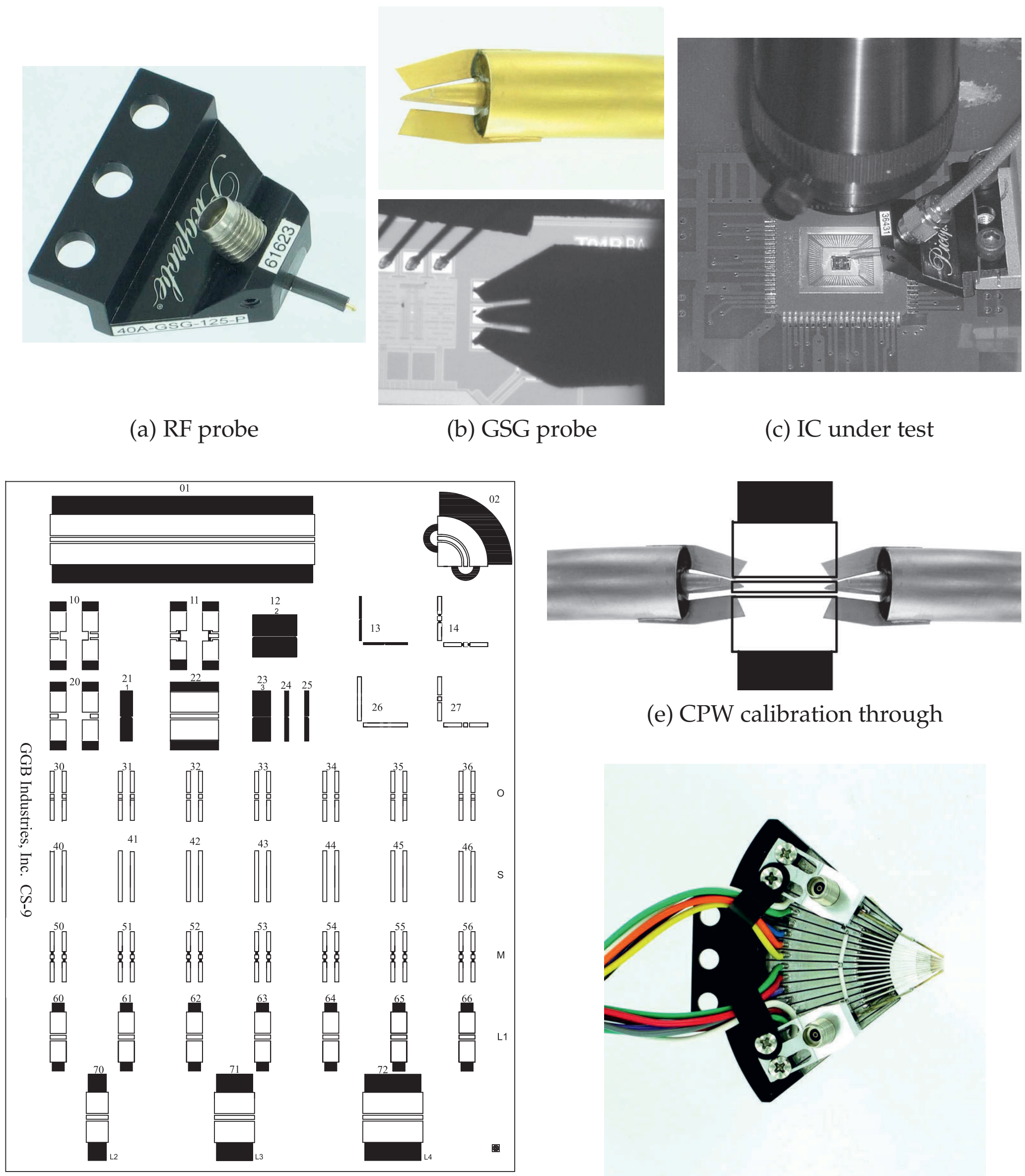

(a) RF probe (b) GSG probe (c) IC under test

(d) CPW calibration substrate (e) CPW calibration through (f) Probe card

Figure 4-5: RF probes: (a) single RF probe probe; (b) detail of a GSG probe and contacting an IC; (c) an IC under test; (d) layout of a calibration substrate used with GSG probes; (e) probes contacting a through CPW structure on the calibration substrate; and (f) a probe card with 2 RF probes (top and bottom) and 13 needle probes for DC and low-frequency connections. ((a), (b) top, (d), (e), (f) Copyright GGB Industries Inc., used with permission [2].)

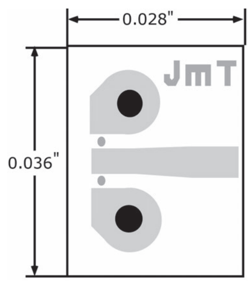

(a) Layout

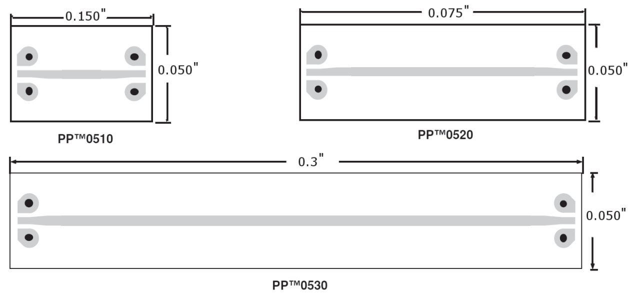

(b) Calibration microstrip lines

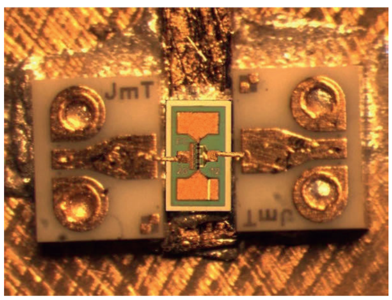

(c) Transistor under test

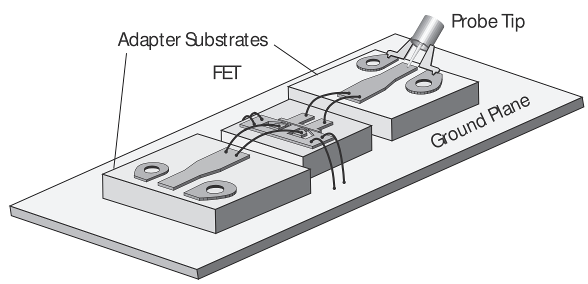

(d) Details of measurement configuration in (c)

Figure 4-6: Use of a CPW-to-microstrip adaptor enabling coplanar probes to be used in characterizing a non-CPW device. The adaptors provide a low insertion loss CPW-to-microstrip transition. Used with permission of J microTechnology, Inc.

ground-signal-ground (**GSG**) probes and transition from a coaxial cable to an on-wafer CPW line, providing a smooth transition of the EM fields from those of a coaxial line to those of the CPW line. The on-wafer pads can be as small as 50 μm on a side.

Measurement using CPW probes and manipulators enables repeatable measurements to be made from DC to above 100 GHz. Such measurements require repeatability of probe connections that are better than 1 μm. When the DUT has microstrip connections, it is necessary to use a CPW-to-microstrip adapter, as shown in Figure 4-6. The layout of a suitable adapter is shown in Figure 4-6(a). In Figure 4-6(c and d) two adaptors are shown in use in the characterization of a microwave transistor. GSG probes contact the adapters and the grounds are connected to the backside metalization by vias. Calibration uses the microstrip transmission line calibration substrates shown in Figure 4-6(b).

4.3 Calibration

The components of a microwave measurement system introduce substantial errors. Fortunately a network analyzer is a very stable instrument and the errors are faithfully reproduced. This means that a calibration procedure can be used to determine the errors and then the errors can be removed from raw measurements of the device being measured, which, by convention, is called

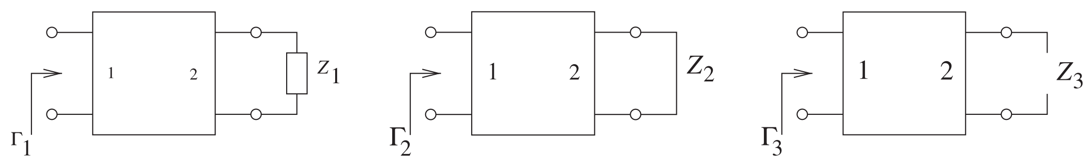

(a) Matched load (b) Short (c) Open

Figure 4-7: Two-port error network with three different calibration loads.

the **device under test** (**DUT**). All that is needed to determine the parameters of a two-port are three precisely known loads.

Calibration of the measurement system is critical, as the effect of cabling and connectors can be more significant than that of the device being measured. The process of removing the effect of cabling and connectors is called de-embedding. Ideally, perfect short, open, and matched loads would be available, but these can only be approximated, and numerous schemes have been developed for alternative ways of calibrating an RF measurement system. In some cases, for example, in measuring integrated circuits using what is called on-wafer probing, it is very difficult to realize a good match. A solution is to use calibration standards that consist of combinations of transmission line lengths and repeatable reflections. These calibration procedures are known mostly by combinations of the letters T, R, and L such as **through-reflect-line TRL** [3] (which relies on a transmission line of known characteristic impedance to replace the match); or **through-line** (**TL**), [4, 5] (which relies on symmetry to replace the third standard).

4.3.1 One-Port Calibration

In one-port measurements the desired reflection coefficient cannot be obtained directly. Instead, there is effectively an error network between the measurement plane at the load and the ideal internal network analyzer port. The network model [6] of the measurement system is shown in Figure 4-7 together with three ideal calibration standards. Calibration, here, is concerned with determining the S parameters of the error two-port.

Various calibration schemes have been developed, some of which are better in particular measurement environments, such as when measuring on-chip structures. Calibration schemes share certain commonalities. One of these is that the errors can be represented as a two-port (or several two-ports) that exists between an effective reference plane internal to the measurement equipment and the reference plane at the device to be measured. This device is commonly called the device under test (DUT). Known standards are placed at the device reference plane and measurements are made. The concept is illustrated by considering the determination of the S parameters of the two-port shown in Figure 4-7. With Z_1 being a matched load, the input reflection coefficient Γ_1 is S_{11}:

$$S_{11} = \Gamma_1. \tag{4.1}$$

The other commonly used calibration loads are $Z_2 = 0$ (a short circuit) and $Z_3 = \infty$ (an open circuit). In calibration precision shorts and opens are

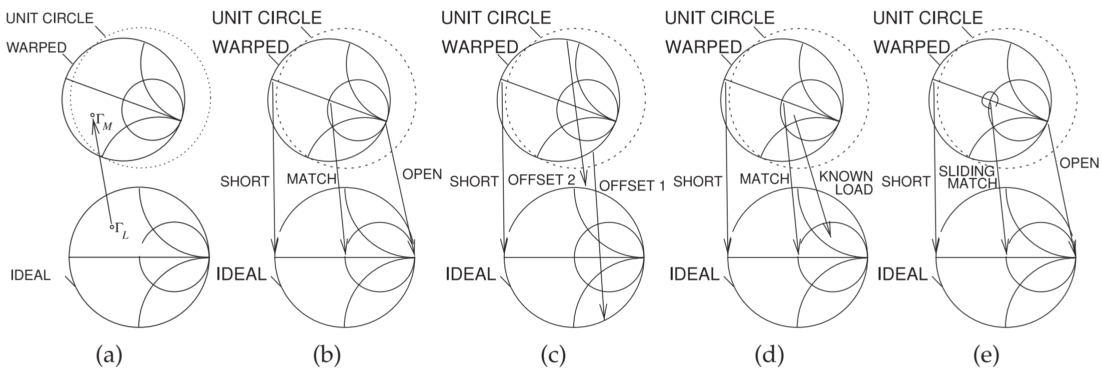

Figure 4-8: Calibrations as mapping operations with each calibration mapping having a warped Smith chart and an ideal Smith chart. The raw measurement of a reflection coefficient of a load is not the actual reflection coefficient, Γ_L, but instead is the raw measurement, Γ_M, which appears on a Smith chart that is warped (see (a)). In calibration, the raw measurements of standards also appear on the warped Smith chart although their actual values are known: (b) calibration as a mapping established using short, match, and open calibration standards; (c) mapping using short and two offset short calibration standards; (d) mapping using a short, a match, and a known load as calibration standards; and (e) mapping using a short, an open, and a sliding matched load as calibration standards.

are used and the errors involved are known and incorporated in the more detailed calibration procedure. From these, $S_{12} = S_{21}$ and S_{22} can be derived:

$$S_{22} = \frac{2S_{11} - \Gamma_2 - \Gamma_3}{\Gamma_2 - \Gamma_3} \tag{4.2}$$

and $$S_{21} = S_{12} = [(\Gamma_3 - S_{11})(1 - S_{22})]^{\frac{1}{2}}. \tag{4.3}$$

The error two-port modifies the actual reflection coefficient of a DUT to a warped (but calibrated) reflection coefficient according to Equation (3.12). In Equation (3.12), the load reflection coefficient, Γ_L, is a complex number that is scaled, rotated, and shifted before being presented at Γ_{in}. Moreover, circles of reflection coefficient are mapped to circles on the warped complex plane; that is, the ideal Smith chart is mapped to a warped Smith chart. Here the actual load reflection coefficient, Γ_L, is warped to present a measured reflection coefficient, Γ_M, to the internal network analyzer. Calibration can be viewed as a mapping operation from the complex plane of raw measurements to the complex plane of ideal measurements, as shown in Figure 4-8(a). That is, calibration develops the required mapping. Figure 4-8(b–e) shows how the corrected mapping is developed using different sets of calibration standards. The mapping operation shown in Figure 4-8(b) uses the short, open, and match loads. This one-port calibration procedure is called open-short-load or SOL calibration and is available as a calibration algorithm in all network analyzers. The three standards are well distributed over the Smith chart and so the mapping can be extracted with good precision. While ideal short, open, and match loads are not available, if the terminations are well characterized then appropriate corrections can be made. The mapping in the one-port case is embodied in the extracted S

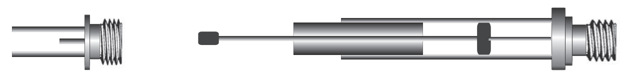

(a) Precision open. (b) Sliding load.

Figure 4-9: Precision calibration standards.

parameters of the two-port.

Figure 4-9(a) shows the longitudinal section of a precision coaxial open. The key feature is that the outer coaxial conductor is extended and the fringing capacitance at the end of the center conductor can be calculated analytically. Thus the precision open is not a perfect open, but rather an open that can be modeled as a small capacitor whose frequency variation is known. Figure 4-8(c) uses offset shorts (i.e., short-circuited transmission lines of various lengths). This circumvents the problem of difficult-to-produce open and matched loads. Care is required in the choice of offsets to ensure that the mapping can be determined accurately. The calibration scheme shown in Figure 4-8(d) introduces a known load. The mapping cannot be easily extracted here, but in some situations this is the only option. Figure 4-8(e) introduces a new concept in calibration with the use of a sliding matched load such as that shown in Figure 4-9(b). A perfect matched load cannot be produced and there is always, at best, a small resistance error and perhaps parasitic capacitance. When measured, the reflection will have a small offset from the origin. If the matched load is moved, as with a sliding matched load, a small circle centered on the origin will be traced out and the center of this circle is the ideal matched load.

4.3.2 De-Embedding

The one-port calibration described above can be repeated for two ports, resulting in the two-port error model of Figure 4-10(a), the error model for correcting two-port measurements. Using the chain scattering matrix (or $\mathbf{T}$ matrix[1]) introduced in Section 2.6, the $\mathbf{T}$ parameter matrix measured at the internal reference planes of the network analyzer is

$$\mathbf{T}_{\mathrm{MEAS}} = \mathbf{T}_A \mathbf{T}_{\mathrm{DUT}} \mathbf{T}_B, \tag{4.4}$$

where $\mathbf{T}_A$ is the $\mathbf{T}$ matrix of the first error two-port, $\mathbf{T}_{\mathrm{DUT}}$ is the $\mathbf{T}$ matrix of the device under test, and $\mathbf{T}_B$ is the $\mathbf{T}$ matrix of the right-hand error two-port. Manipulating Equation (4.4) leads to $\mathbf{T}_{\mathrm{DUT}}$:

$$\mathbf{T}_A^{-1} \mathbf{T}_{\mathrm{MEAS}} \mathbf{T}_B^{-1} = \mathbf{T}_A^{-1} \mathbf{T}_A \mathbf{T}_{\mathrm{DUT}} \mathbf{T}_B \mathbf{T}_B^{-1} \tag{4.5}$$

$$\mathbf{T}_{\mathrm{DUT}} = \mathbf{T}_A^{-1} \mathbf{T}_{\mathrm{MEAS}} \mathbf{T}_B^{-1}, \tag{4.6}$$

from which the S parameters of the DUT can be obtained.

4.3.3 Two-Port Calibration

The VNA architecture introduced in 1968 and still commonly used today is shown in Figure 4-1. A key component of the system is the test set that comprises mechanical microwave switches and directional couplers that selectively couple energy in either the forward- or backward-traveling waves. Many modern VNAs use multiple mixers and electronic switches to

[1] Note that there are several $\mathbf{T}$ matrices, so it necessary to be specific.

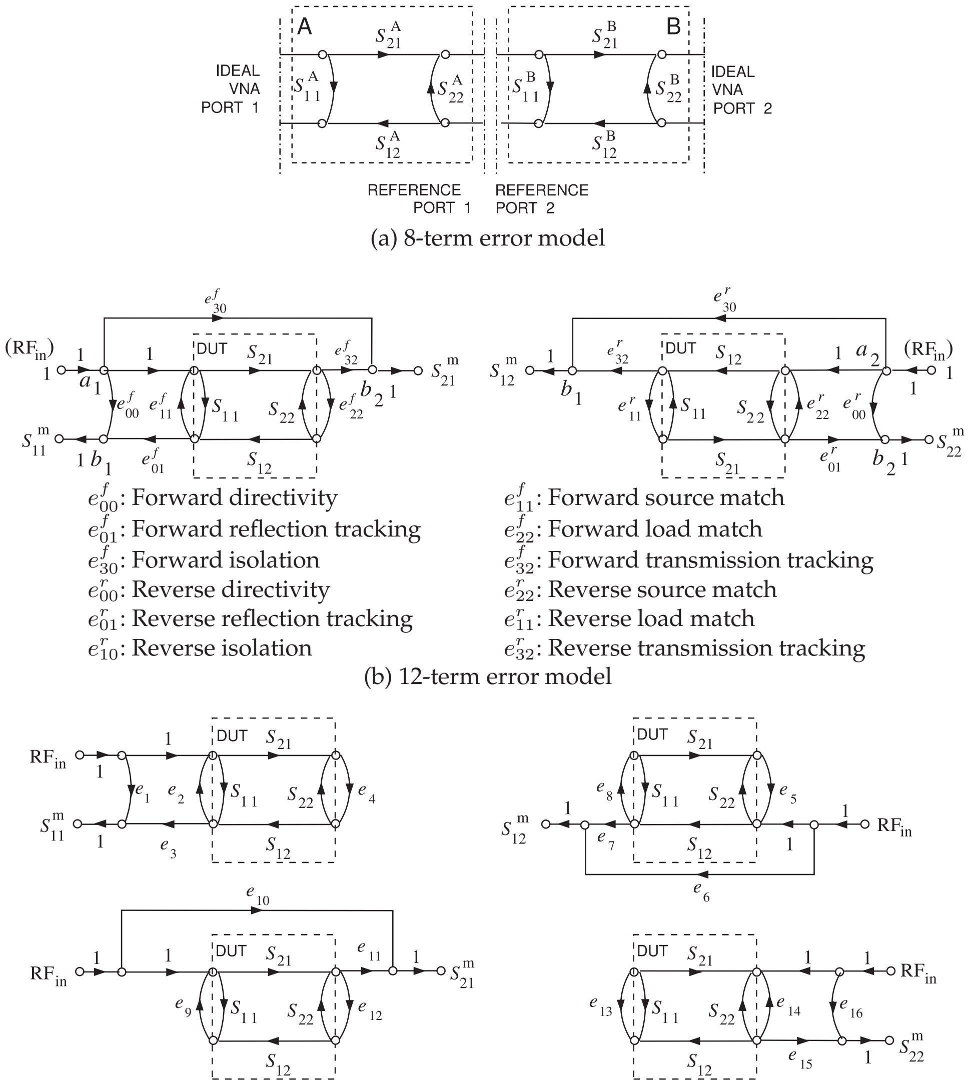

Figure 4-10: Two-port error models: (a) SFG representation of the 8-term two-port error model (1968) [1]); (b) SFG of the 12-term two-port error model (1978) [7]; and (c) SFG of the 16-term two-port error model (circa 1979) [8]. S_{ij}^{m} are the raw S parameter measurements, S_{ij} are the S parameters of the DUT, and e_{ij}, e_{ij}^r, and e_{ij}^f are error S parameters determined during calibration.

eliminate the need for mechanical switches. Operation is similar. Returning to the architecture of Figure 4-1, this architecture supports a single signal source and a single test port at which the RF signal to be measured is mixed down to a low frequency, typically 100 kHz, where it is captured by an ADC. The mixing component is called the frequency converter, and it mixes the RF signal with a version of the original RF signal offset in frequency to produce a low-frequency version of the RF signal. This has the same phase as the

RF signal and an amplitude that is linearly proportional to the RF signal. When Hackborn introduced this system in 1968 [1], he also introduced the 8-term error model shown in Figure 4-10(a). This is an extension of the one-port error model discussed in Section 4.3.1, with a two-port capturing the measurement errors to each port.

Closer examination of the VNA system of Figure 4-1 indicates that the signal path varies for each of the four scattering parameters for a DUT. Another imperfection that is not immediately obvious is that there is leakage in the system so that Ports 1 and 2 are coupled by a number of mechanisms that do not involve transmission of the signal through the DUT. Leakage is due to finite isolation in the mixers and direct coupling between probes used to make contact at Ports 1 and 2, among other possible causes. The first person to identify this was Shurmer [9] in 1973, leading eventually to the 12-term error model [7, 10] shown in Figure 4-10(b). Calibration yields the error parameters, and the S parameters of the DUT are found as follows:

$$S_{11} = \frac{1}{\delta}\left\{\left[\frac{S_{11}^{\mathrm{m}} - e_{00}^{f}}{e_{01}^{f}}\right]\left[1 + \frac{S_{22}^{\mathrm{m}} - e_{00}^{r}}{e_{01}^{r}} e_{22}^{r}\right] - e_{22}^{f}\left[\frac{S_{21}^{\mathrm{m}} - e_{30}^{f}}{e_{32}^{f}}\right]\left[\frac{S_{12}^{\mathrm{m}} - e_{10}^{r}}{e_{32}^{r}}\right]\right\} \tag{4.7}$$

$$S_{21} = \frac{1}{\delta}\left\{\left[\frac{S_{21}^{\mathrm{m}} - e_{30}^{f}}{e_{32}^{f}}\right]\left[1 + \frac{S_{22}^{\mathrm{m}} - e_{00}^{r}}{e_{01}^{r}}\left(e_{22}^{r} - e_{22}^{f}\right)\right]\right\} \tag{4.8}$$

$$S_{12} = \frac{1}{\delta}\left\{\left[\frac{S_{12}^{\mathrm{m}} - e_{10}^{r}}{e_{32}^{r}}\right]\left[1 + \frac{S_{11}^{\mathrm{m}} - e_{00}^{f}}{e_{01}^{f}}\left(e_{11}^{f} - e_{11}^{r}\right)\right]\right\} \tag{4.9}$$

$$S_{22} = \frac{1}{\delta}\left\{\left[\frac{S_{22}^{\mathrm{m}} - e_{00}^{r}}{e_{01}^{r}}\right]\left[1 + \frac{S_{11}^{\mathrm{m}} - e_{00}^{f}}{e_{01}^{f}} e_{11}^{f}\right] - e_{11}^{r}\left[\frac{S_{21}^{\mathrm{m}} - e_{30}^{f}}{e_{32}^{f}}\right]\left[\frac{S_{12}^{\mathrm{m}} - e_{10}^{r}}{e_{32}^{r}}\right]\right\} \tag{4.10}$$

$$\begin{aligned}\delta = &\left[1 + \frac{S_{11}^{\mathrm{m}} - e_{00}^{f}}{e_{01}^{f}} e_{11}^{f}\right]\left[1 + \frac{S_{22}^{\mathrm{m}} - e_{00}^{r}}{e_{01}^{r}} e_{22}^{r}\right] \\ &- e_{22}^{f} e_{11}^{r}\left[\frac{S_{21}^{\mathrm{m}} - e_{30}^{f}}{e_{32}^{f}}\right]\left[\frac{S_{12}^{\mathrm{m}} - e_{10}^{r}}{e_{32}^{r}}\right].\end{aligned} \tag{4.11}$$

The most complete model is the 16-term error model introduced in 1979 and shown in Figure 4-10(c), which incorporates a different model for each parameter and fully captures the various signal paths resulting from the different switch positions [8]. Nevertheless, the 12-term error model is the one most commonly used in microwave measurements and is sufficient to reliably extract the desired S parameters of the DUT from the raw VNA measurements. This process of extracting the de-embedded parameters is call de-embedding, or less commonly, unterminating.

The 12-term error model models the error introduced by leakage or crosstalk internal to the network analyzer. The 16-term error model captures the leakage or crosstalk of the 12-term error model, but in addition includes switch leakage that results in error signals reflecting from the DUT and leaking to the transmission port as well as common-mode leakage [11]. This method is called two-port 16-term singular value decomposition (SVD) calibration, as the equations are solved in a least squares sense using the singular value decomposition method [11]. In a coaxial environment, the

extra leakage terms are small, provided that the switches have high isolation. However, in wafer probing where direct coupling between the probes can be appreciable, the transmission-related leakage can be important and the 16-term error model captures errors that the 12-term error model does not.
These error models and the sequence of measurements to extract them are included in the VNA control software. The user must select which to use.

Coaxial Two-Port Calibration

If the DUT has coaxial connectors then precision open, short, and matched loads are available. While these are not ideal components, the open has fringing capacitance; for example, they are well characterized over frequency. The full set of standards required to develop the 12-term error model includes one-port measurements for each port with open, short, and match connections, a two-port measurement with a through connection, and a two-port measurement with opens at each port. The last measurement determines the internal isolation of the system. Most connectors come in male and female counterparts. As such it is not possible to create a perfect through by joining the connectors and a small delay is introduced. There are, however, sexless connectors, such as the Amphenol precision connector (APC-7) with a 7 mm outer diameter as it has a flush face that can be connected for a near-perfect through. The APC-7 connector is no longer commonly used, with most coaxial systems now using SMA connectors or the higher-tolerance APC 3.5 connectors that come in male and female connectors. The majority of the measurements desired these days are of ICs and other planar structures for which there is no clear connector. The connector, or fixture, problem has resulted in a variety of standards being used.

Planar Circuit Calibration

Calibration standards are required in microwave measurements. For measurements of microstrip and CPW systems, standard calibration alumina substrates are available, see Figure 4-5(d and e). These calibration substrates include various lengths of transmission lines that can be used as standards, as well as an open, a short, and a laser-trimmed matched load.

4.3.4 Transmission Line-Based Calibration Schemes

A drawback of all de-embedding techniques that use repeated fixture measurements during the de-embedding process is the generation of errors caused by the lack of fixture reproducibility during measurements of each of the required standards. These errors can be amplified during the course of de-embedding.
The TRL technique [3] is a calibration procedure used for microwave measurements when classical standards such as open, short, and matched terminations cannot be realized. There are now a family of related techniques, here denoted as TxL methods, with the commonality being the two-port measurement of a through connection and of the same structure with an inserted transmission line. The two-port connections required in the TRL procedure are shown in Figure 4-11. The concept behind the representation is that there is a measurement error that is captured by

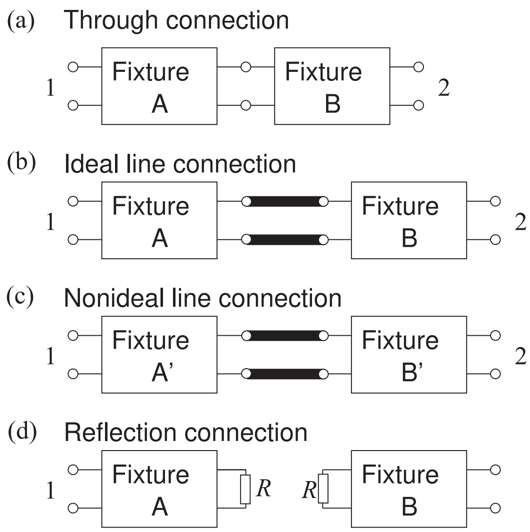

Figure 4-11: Measurement connections in two-port calibration using the TRL procedure: (a) through connection; (b) ideal line connection; (c) realistic configuration with nonidentical fixtures; and (d)with arbitrary reflection.

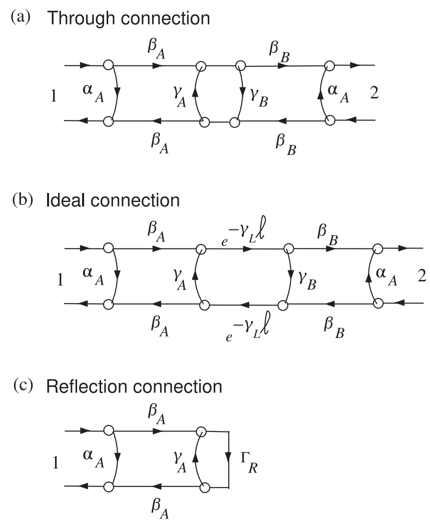

Figure 4-12: SFG representations of the two-port connections shown in Figure 4-11: (a) through connection; (b) ideal line connection; and (c) arbitrary reflection connection.

the fixture two-port. The TRL procedure allows the fixtures on either side, Fixtures A and B here, to have different two-port parameters. The SFG representations of the connections are shown in Figure 4-12. Assuming that the fixtures are faithfully reproduced when going from one connection to another, then the SFGs shown in 4-12(a–c) need to be considered. With each configuration, two-port measurements are made, and as the number of independent S parameter measurements exceed the number of unknowns, it would seem that it may be possible to solve the SFGs to obtain the unknown parameters of the fixtures. This is all that is required to de-embed measurements made with a DUT between the fixtures. Unfortunately this is not possible. However, Engen and Hoer [3] developed a procedure that enabled the complex propagation constant of the line to be extracted from the external S parameter measurements of the through and line connections. This procedure is considered in the next section.

4.3.5 Through-Line Calibration

The through and line measurement structures include fixtures as well as the direct connection (for the through) and the inserted line (for the line) (see Figure 4-11). Two-port measurements of these two structures yield the propagation constant $\gamma_L = \alpha + \jmath\beta$ of the line [3]. Similar but earlier work was presented by Bianco et al. [12]. For the through structure, the error networks between the ideal internal port of a network analyzer and the desired measurement reference plane are designated as Fixture A at Port 1 and Fixture B at Port 2. For the line measurement, fixturing is reestablished (following the through measurement) with the line inserted. In general, the fixturing cannot be faithfully reproduced and therefore becomes Fixtures A′ and B′, respectively (see Figure 4-11).

The following is based on the derivation of Engen and Hoer [3]. As well as presenting an important result indicating sources of error in microwave measurement, the development demonstrates a technique for solving measurement problems involving transmission lines.

The development begins using **cascading matrices**, $\mathbf{R}$, defined as

$$\begin{bmatrix} b_1 \\ a_1 \end{bmatrix} = \mathbf{R} \begin{bmatrix} a_2 \\ b_2 \end{bmatrix}, \tag{4.12}$$

which is related toscattering parameters $\mathbf{S}$ by

$$\mathbf{R} = \begin{bmatrix} R_{11} & R_{12} \\ R_{21} & R_{22} \end{bmatrix} = \begin{bmatrix} \dfrac{S_{12}\,S_{21} - S_{11}\,S_{22}}{S_{21}} & \dfrac{S_{11}}{S_{21}} \\ -\dfrac{S_{22}}{S_{21}} & \dfrac{1}{S_{21}} \end{bmatrix}. \tag{4.13}$$

Thus the parameters describing the A and B fixtures are $\mathbf{S}_A$, $\mathbf{S}_B$ and $\mathbf{R}_A$, $\mathbf{R}_B$, respectively. The cascading matrix of the through is simply a unity matrix and the line of length, ℓ_L, is described by

$$\mathbf{R}_L = \begin{bmatrix} e^{-\gamma_L \ell_L} & 0 \\ 0 & e^{\gamma_L \ell_L} \end{bmatrix}. \tag{4.14}$$

The characteristic impedance of the line is taken as the reference impedance, Z_0, of the measurement system and results in the off-diagonal zeros in the above definition for the line standard. Because of this simplifying assumption, γ_L can be computed using the equations that follow.

The cascading matrix of the through structure (i.e., the fixture-fixture cascade) is

$$\mathbf{R}_t = \mathbf{R}_A \mathbf{R}_B \quad \text{(the through)}. \tag{4.15}$$

For the line structure, a fixturing error Δ is introduced. Δ corresponds to a small additional electrical length of the A fixture (i.e., $\mathbf{R}'_A = \mathbf{R}_A \mathbf{R}_e$), then the cascading matrix of the fixture-line-fixture cascade is

$$\mathbf{R}_d = \mathbf{R}'_A \mathbf{R}_L \mathbf{R}_B = \mathbf{R}_A \mathbf{R}_e \mathbf{R}_L \mathbf{R}_B \ \text{(the line)} \quad \text{with } \mathbf{R}_e = \begin{bmatrix} \mathrm{e}^{-\Delta} & 0 \\ 0 & \mathrm{e}^{\Delta} \end{bmatrix}. \tag{4.16}$$

Now introduce the matrix

$$\mathbf{T} = \begin{bmatrix} t_{11} & t_{12} \\ t_{21} & t_{22} \end{bmatrix} = \mathbf{R}_d \mathbf{R}_t^{-1}. \tag{4.17}$$

Thus $\mathbf{T}$ combines the line and through measurements and approximately removes the through measurement from the line measurement. Most importantly, all of the elements of the $\mathbf{T}$ matrix are measured quantities. Continuing (note that if $\mathbf{A}$ and $\mathbf{B}$ are matrices, $(\mathbf{AB})^{-1} = \mathbf{B}^{-1}\mathbf{A}^{-1}$), and using Equations (4.15)–(4.17),

$$\begin{aligned} \mathbf{T}\mathbf{R}_A &= \mathbf{R}_d \mathbf{R}_t^{-1} \mathbf{R}_A = \mathbf{R}'_A \mathbf{R}_L \mathbf{R}_B \left(\mathbf{R}_A \mathbf{R}_B\right)^{-1} \mathbf{R}_A \\ &= \mathbf{R}_A \mathbf{R}_e \mathbf{R}_L \mathbf{R}_B \mathbf{R}_B^{-1} \mathbf{R}_A^{-1} \mathbf{R}_A \end{aligned} \tag{4.18}$$

and so $$\mathbf{T}\mathbf{R}_A = \mathbf{R}_A \mathbf{R}_e \mathbf{R}_L, \tag{4.19}$$

which is referred to as the TL (for through-line) equation.
Expanding Equation (4.19) leads to a system of equations:

$$t_{11}R_{A11} + t_{12}R_{A21} = R_{A11}\mathrm{e}^{-\Delta}\mathrm{e}^{-\gamma_L \ell_L} \tag{4.20}$$

$$t_{21}R_{A11} + t_{22}R_{A21} = R_{A21}\mathrm{e}^{-\Delta}\mathrm{e}^{-\gamma_L \ell_L} \tag{4.21}$$

$$t_{11}R_{A12} + t_{12}R_{A22} = R_{A12}\mathrm{e}^{\Delta}\mathrm{e}^{\gamma_L \ell_L} \tag{4.22}$$

$$t_{21}R_{A12} + t_{22}R_{A22} = R_{A22}\mathrm{e}^{\Delta}\mathrm{e}^{\gamma_L \ell_L}, \tag{4.23}$$

which upon solution yields the propagation constant of the line standard [3],

$$\gamma_L = \frac{1}{2\,\ell_L}\left[\ln\left(\frac{t_{11} + t_{22} \pm \zeta}{t_{11} + t_{22} \mp \zeta}\right) - 2\Delta\right] \tag{4.24}$$

$$\zeta = \left({t_{11}}^2 - 2\,t_{11}t_{22} + {t_{22}}^2 + 4\,t_{21}t_{12}\right)^{1/2}. \tag{4.25}$$

If the fixtures are faithfully reproduced, then networks A and A' are identical, as are networks B and B', and so $\Delta = 0$, and γ_L is

$$\gamma_L = \frac{1}{2\,\ell_L}\ln\left(\frac{t_{11} + t_{22} \pm \zeta}{t_{11} + t_{22} \mp \zeta}\right). \tag{4.26}$$

The sign to use with ζ is chosen corresponding to the root selection [3].
That is, two-port S parameter measurements of the through connection (shown in Figure 4-11(a)) and two-port S parameter measurements of the line connection (shown in Figure 4-11(b)) enable the propagation constant of the line to be determined. The characteristic impedance of the line standard can be determined as described in Section 4.5.
Extraction of the propagation constant of the transmission line standard is a common property of calibration techniques that use through and line measurements instead of match measurements. Such techniques are called TxL techniques, where x identifies an additional measurement used in calibration. Unfortunately the TxL calibration techniques often result in errors in de-embedding at frequencies where the length of the line standard is a multiple of one-half wavelength (called critical lengths [13, 14]). These are the lengths where the electrical length is a multiple of 180°. Buff et al. [15, 16] showed that small fixture repeatability errors result in errors incorporated in Δ. These errors affect the entire calibration and subsequent de-embedded measurements. These errors are minimized by using measurements where the line standard has an electrical length not within 20° of a critical length. Statistical means and the use of multiple lines have been proposed to minimize the error [17, 18], as well as an optimization scheme to determine the additional electrical length, Δ [15, 16]. The optimization scheme significantly reduces the uncertainty and is based on the assumption that a change of line length is the sole source of error in fixture reproducibility (the fixture here includes, of course, the probe and probe pad). This is seen in Figure 4-13 where the results of optimization are seen most clearly for the attenuation constant in Figure 4-13(a), the curve labeled fixture error de-embedded. The no fixture error curve was selected as the best results from a large number of calibrations (multiple repeats of probe-on-probe pad connections). The fixture error curve is the result of a typical calibration measurement.

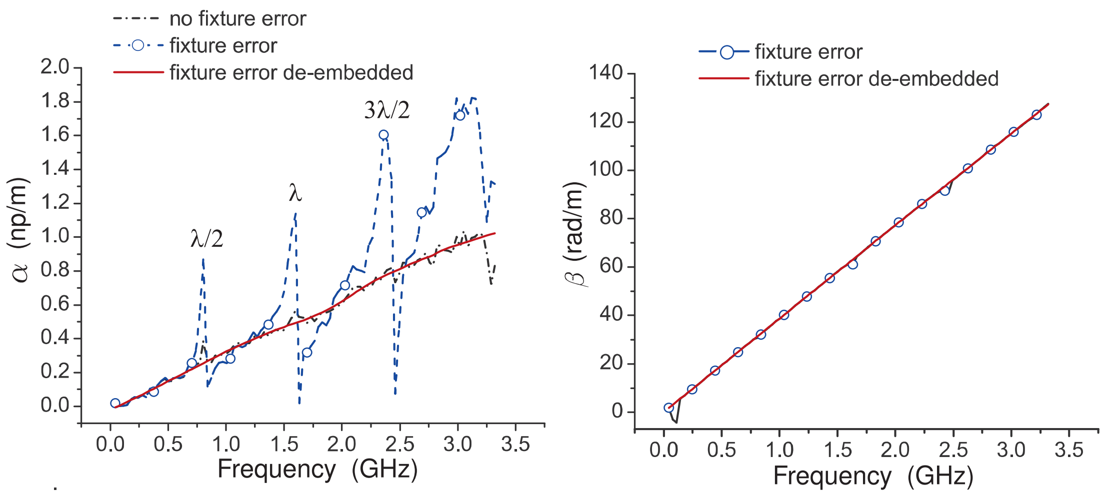

(a) Attenuation constant

(b) Phase constant

Figure 4-13: Extracted propagation constant from the through and line components of TRL with fixture error introduced during the line measurement.

In the following, several of the TxL calibration techniques are described. These are techniques incorporated in most vector network analyzers and are particularly useful in characterizing on-chip circuits. An example of an on-wafer two-port measurement is shown in Figure 4-14, showing on-chip calibration standards. The VNA software leads the user through the required set of calibration measurements and computes the error models to be used in de-embedding.

Through Short Delay

Matched loads can be difficult to realize, especially when probing ICs and planar circuits using probes. The through short delay (**TSD**) method uses reflection and transmission measurements [19]. The delay is realized using a line with a 50 Ω characteristic impedance. TSD experiences the $180°$ glitches common to TxL schemes. The through could be another delay, but then problems occur when the delay difference (the electrical length difference) of the through and delay is an integer multiple of $180°$.

Through Reflect Line

What has become known as the through reflect line (**TRL**) calibration technique was developed by Bianco et al. [12] and Engen and Hoer [3], who used a through connection, an arbitrary reflection standard, and a delay or line standard. The line standard can be of arbitrary length with its propagation constant unknown, but it is assumed to be nonreflecting. The result of this assumption is that the characteristic impedance of the line becomes the system reference impedance. Also, the reflection standard, can be any repeatable reflection load, with an open or short preferred. Again the transmission line introduces calibration uncertainties when the electrical

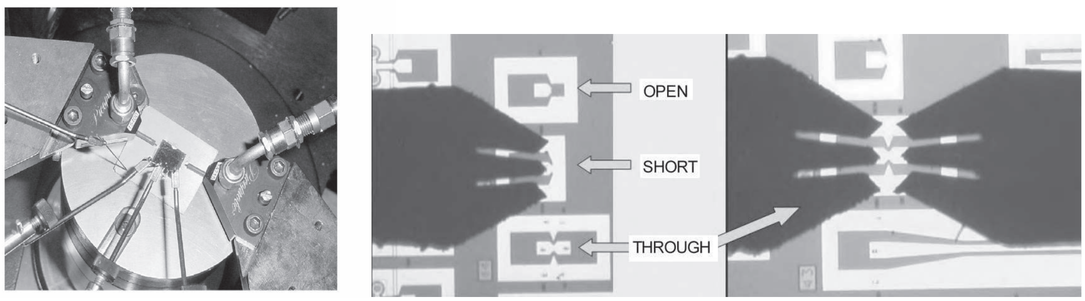

(a) Two-port DUT (b) Calibration standards

Figure 4-14: Two-port measurements: (a) two-port device under test with DC needle probes at the bottom and GSG probes on the left and right; and (b) open, short, and through calibration standards with GSG probes.

length is a multiple of one-half wavelength [3].

Through Reflect Match

Through reflect match (**TRM**) is a variation of TRL that replaces the through by a matched load and is useful only when a matched load can be realized. It retains the arbitrary reflection standard, which is particularly useful as it can be difficult to produce a short or open with planar circuits. For example, a via used in realizing a microstrip short circuit has finite resistance and inductance and so does not create a good through, but does create a useful repeatable arbitrary reflection. The technique does not have the critical length glitches, but repeatable fixturing is always important.

Other Distributed Calibration Techniques

TRL and TRM are the most commonly accepted standards used in calibrating measurements of planar circuit structures. There are several other related techniques that also use transmission lines and are useful in certain circumstances.

In 1982 Benet [20] developed the open-short-five-offset-line calibration technique. The key concept is that the multiple offset through lines trace out a circle on the Smith chart and the center of the circle provide the matched load. Through least squares fitting Benet derived the propagation constant of the through lines and the remaining error terms to develop the 12-term error model.

Pennock et al. [21] introduced the **double through line** (**DTL**) calibration system in 1987. This is useful for characterizing transitions between different mediums. There is sufficient information to develop the 6-term error model.

SOLT (short-open-load-through) calibration requires precisely characterized standards and is robust to 20 GHz.

SOLR (short-open-load-reciprocal-through) calibration is similar to SOLT using precisely defined reflect standards as a standard.

LRRM, (line-reflect-reflect-match) calibration uses a line instead of a through, one of the reflection standards is a short and the other is an open. This is

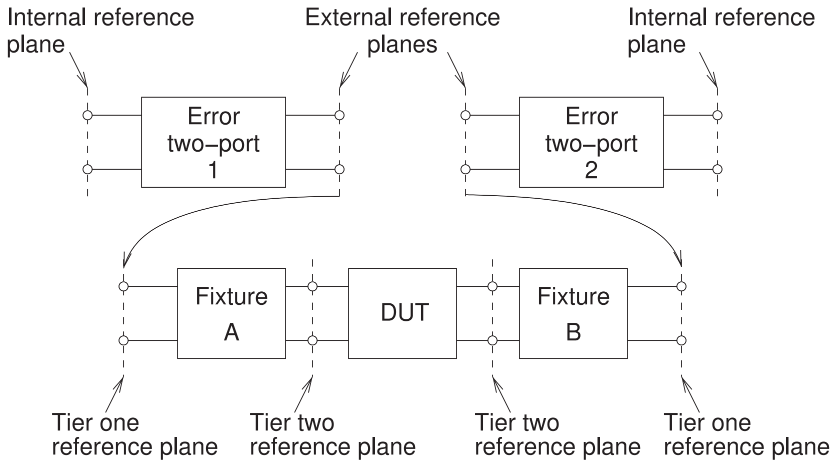

Figure 4-15: Two-tier calibration procedure.

usually the best calibration technique to use with probes, as these standards are straightforward to incorporate in calibration substrates. The calibration standards are the same as those used in SOLT, but LRRM does not require precision short and open standards. The essentials of what must be known are the characteristics of the through and the DC resistance of one of the load standards. The inductance of the load is automatically determined.
LRM, (load-reflect-match) calibration is similar to LRRM calibration but does not use a precision reflect standard. A modification is LRM+, for which the DC resistances of the loads are required.

4.3.6 Two-Tier Calibration

With measurements in noncoaxial systems, it is difficult to produce precision standards such as shorts, opens, and resistive loads. In these situations, two-tier calibration is sometimes used. In a two-tier calibration procedure, two sets of standards are used to establish first- and second-tier reference planes (see Figure 4-15). It is preferable to use a highly repeatable set of standards in Tier 1 (such as a non-TxL technique), and one that yields more precise characterization in a particular environment (such as a TxL technique for on-wafer measurement).
In the first-tier calibration, a precision set of standards is normally used. This can be achieved using coaxial standards or perhaps a standard calibration substrate used with probes. Referring to Figure 4-15, each of the 2 two-ports from the internal reference planes of the network analyzer to the external reference planes is established. Generally with the second tier, insitu calibration standards are used, and the additional (e.g. on-chip) fixturing is identical for the two ports. Precision calibration should be done using standards fabricated in the medium of the DUT.
Two-tier calibration generally results in the fixtures in the second tier being identical. This enables checks to be made for the integrity of the probe connection. Connections to IC pads can be problematic because of oxide build up, especially with aluminum pads. So ensuring symmetry of second-tier calibrations by comparing the two-port measurements of symmetrical structures such as transmission lines can greatly reduce the impact of the fixture-induced errors discussed in Section 4.3.5. Recall that small fixturing errors, such as bringing the probes down in slightly different positions,

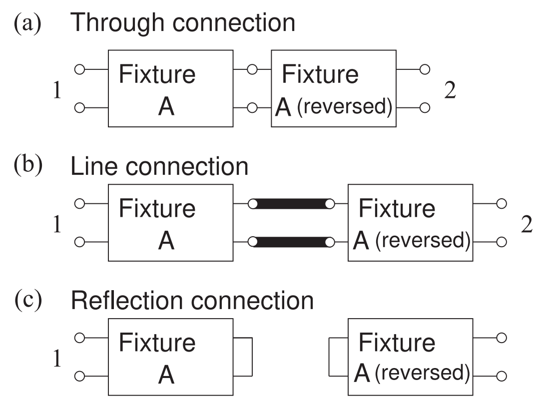

Figure 4-16: Measurement connections in two-port second-tier calibration using the TL calibration procedure: (a) through connection; (b) ideal line connection; (c) realistic configuration showing that the fixtures are not precisely reproduced; and (d) arbitrary reflection configuration.

results in measurement errors at the half-wavelength frequencies ($\lambda/2$, λ, $3\lambda/2$, etc.). For example, if the DUT is a device on a silicon wafer, the optimum measurement technique is to realize the calibration standards on the silicon wafer processed in the same way as for the DUT. The two-tier calibration procedure removes fixturing errors associated with fringing effects at the probes and with other nonidealities involved in creating the landing pads for the probes.

In an example two-tier calibration scheme, a first tier is used to establish the 12-term error model. Then a second calibration is used to develop a secondary six-term error model, as in Figure 4-10(a) with $S_{12} = S_{21}$. In such a situation the standards used in developing the 12-term error model would normally include an open, a short, and a matched load. These need not be precise standards. Thus the 12-term error model need not be precise, and this model does not suffer from the half-wavelength errors of the **TxL** techniques.

Through Line Symmetry

For planar measurements using probes, first-tier calibration using a standard calibration substrate is to the end of the probe tips, and errors with using other substrates (e.g., the probe pads are of different size or the substrate permittivity is different) will be common to both probes (fixtures) in a two-port measurement. With careful design, the fixtures employed in the second tier will be identical and have the same S parameters. In the second-tier calibration, measurements of a through and line will be symmetrical with $S_{11} = S_{22}$ and $S_{12} = S_{21}$. This symmetry is exploited in the **through line** (**TL**) technique which exploits symmetry and renders the half-wavelength errors of TxL insignificant [4, 5]. The TL calibration connections in second-tier calibration are shown in Figure 4-16. In the first calibration tier, a 12-term error model is developed using open, short, load, and delay. Consequently there are no half-wavelength glitches that occur when transmission line standards are used. In the second calibration tier, probes are used with two lengths of transmission line fabricated on the same substrate as the DUT. One of the lines becomes a through.

The procedure proceeds by calculating the propagation constant of the line using the technique developed for the TRL procedure (Equation (4.26)). There is fixture symmetry in the TL connections (see Figure 4-16) and this is reflected in the SFG representations of the connections as shown in Figure 4-17. As will be shown, this symmetry enables the arbitrary reflection used

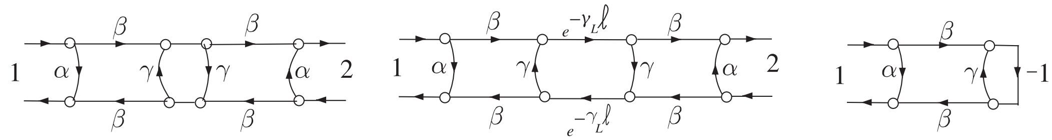

(a) Through connection (b) Line connection (c) Reflection connection

Figure 4-17: SFG representations of the two-port connections shown in Figure 4-16.

in the TRL procedure to be replaced by a virtual precise short or open circuit. Let the S parameters of Fixture A be $\alpha = S_{11}$, $\beta = S_{12} = S_{21}$, and $\gamma = S_{22}$. Using these parameters with the port reversal required to model the Fixture at Port 2, the SFG shown in Figure 4-17(a) relates the measured S parameters to the parameters of the fixtures. The input reflection coefficient of Fixture A with a short circuit placed at Port 2 of A is

$$\rho_{\rm sc} = \alpha - \frac{\beta^2}{1+\gamma}. \tag{4.27}$$

Let the measured S parameters of the through connection be designated by a leading superscript T. Using the self-loop (or Mason's) rule with the SFG in Figure 4-17(a) relates the measured S parameters to the fixture parameters:

$$^{T}S_{11} = \alpha + \frac{\beta^2\gamma}{1-\gamma^2} \quad \text{and} \quad ^{T}S_{21} = \frac{\beta^2}{1-\gamma^2}. \tag{4.28}$$

Subtracting these expressions yields

$$\begin{aligned} ^{T}S_{11} - {}^{T}S_{21} &= \alpha + \frac{\beta^2\gamma}{1-\gamma^2} - \frac{\beta^2}{1-\gamma^2} = \alpha + \frac{\beta^2\gamma - \beta^2}{(1-\gamma)(1+\gamma)} \\ &= \alpha - \frac{\beta^2(1-\gamma)}{(1-\gamma)(1+\gamma)} = \alpha - \frac{\beta^2}{1+\gamma} = \rho_{\rm sc}. \end{aligned} \tag{4.29}$$

That is, the input reflection coefficient of a fixture terminated in a virtual ideal short circuit can be obtained from the through measurement of the back-to-back fixtures in the through configuration:

$$\rho_{\rm sc} = {}^{T}S_{11} - {}^{T}S_{21}. \tag{4.30}$$

Similar results are obtained for a virtual ideal open circuit placed at Port 2 of Fixture A:

$$\rho_{\rm oc} = {}^{T}S_{11} + {}^{T}S_{21}. \tag{4.31}$$

Thus it is possible to effectively insert ideal open and short circuits within a noninsertable medium.

4.4 Extraction of Transmission Line Parameters

This section describes approaches for extracting the per unit length $RLGC$ parameters of a transmission line, and the effective permittivity and permeability of transmission line mediums, from measurements. The measurements could be made experimentally or through simulation.

Ideal Calibration

The procedure described here assumes ideal calibration to the ports of a uniform transmission line that will yield symmetrical transmission line S parameters with $S_{11} = S_{22}$ and $S_{12} = S_{21}$ for the reciprocal structure.
The propagation constant of a transmission line is

$$\gamma = \sqrt{(R + \jmath\omega L)(G + \jmath\omega C)} \tag{4.32}$$

and the characteristic impedance is

$$Z_0 = \sqrt{\frac{(R + \jmath\omega L)}{(G + \jmath\omega C)}}. \tag{4.33}$$

Then

$$R = \Re\{\gamma Z_0\}, \quad L = \Im\left\{\frac{\gamma Z_0}{\omega}\right\}, \quad G = \Re\{\gamma/Z_0\}, \quad C = \Im\left\{\frac{\gamma/Z_0}{\omega}\right\}. \tag{4.34}$$

These parameters can be extracted from the measured S parameters of a transmission line provided that sufficiently accurate calibration can be achieved. This extraction was described in [22–24], yielding the line's characteristic impedance

$$Z_0 = Z_{\text{REF}}\sqrt{\frac{(1 + S_{11})^2 - S_{21}^2}{(1 - S_{11})^2 - S_{21}^2}}, \tag{4.35}$$

where Z_{REF} is the reference impedance of the S parameters. The line's propagation constant is obtained from

$$\mathrm{e}^{-\gamma\ell} = \left(\frac{1 - S_{11}^2 + S_{21}^2}{2S_{21}} \pm K\right)^{-1}, \tag{4.36}$$

where $$K = \left[\frac{(S_{11}^2 - S_{21}^2 + 1)^2 - (2S_{11})^2}{(2S_{21})^2}\right]^{\frac{1}{2}}. \tag{4.37}$$

It is also possible to use specialized test structures to obtain the transmission line parameters. In [25] measurements of the input impedances of short- and open-circuited stubs are used to derive the transmission line parameters.

Nonideal Calibration

The measurement of the S parameters of a transmission line described above assumes that the error model of the fixtures can be accurately calibrated. Sometimes it can be difficult to achieve a sufficiently accurate calibration because of the difficulty of inserting a known resistive impedance standard. In the through-line calibration methods described in Section 4.3.5, measurement of a fixtured transmission line and measurement of back-to-back fixtures (a through connection) yields the propagation constant γ of the transmission line, even if an impedance standard is not available. One way of extracting the characteristic impedance, Z_0, of a line from measurements in this situation was described in Section 4.5. The key idea was varying the electrical length of a transmission line to trace out a circle on the Smith chart. The frequency-dependent characteristic impedance can be obtained by using a number of transmission lines of different length. So with γ and Z_0 known, the $RLGC$ parameters can be obtained using Equation (4.34).

4.4.1 Summary

The complexity and expense of equipment involved in measuring S parameters depends greatly on the frequency range with vector network analyzers able to measure S parameters above a hundred gigahertz costing many 100s of thousands of dollars. Also the time involved in calibration can be significant taking many hours to days at the very highest of microwave frequencies but only a few minutes at single-gigahertz frequencies. Microwave measurement requires the development of considerable expertise.

4.5 Determining Z_0 of a Line from the Smith Chart

It was shown in Section 3.5.2 that the reflection coefficient locus with respect to frequency of a terminated line is a circle on the Smith chart even if the characteristic impedance of the line is not the same as the reference impedance of the Smith chart. The one caveat here is that the reflection coefficient of the termination must be independent of frequency so a resistive termination is sufficient. If the characteristic impedance of the line is Z_{01} and the Smith chart is referenced to Z_{02}, which is usually the same as the system impedance of the measurement system, then Z_{01} can be determined from the center, C_{Z02}, and radius, R_{Z02}, of the reflection coefficient circle. Thus measurements can be used to determine the unknown impedance Z_{01}. Another situation where this is useful is in design where a transmission line circle can be drawn to complete a design problem and from this the characteristic impedance of the line found. In both situations C_{Z02}, R_{Z02}, and Z_{02} are known and Z_{01} must be determined.

A simple closed-form solution for the unkown characteristic impedance Z_{01} cannot be obtained from Equations (3.49) and (3.50). However, by substituting Equation (3.50) in Equation (3.49), and if Z_{01} and Z_{02} are close (so that B is small), then

$$C_{Z02} \approx B - \frac{1}{B} + \frac{1}{B} \approx B. \tag{4.38}$$

The approximation is better for smaller $|\Gamma_{L,Z01}|$. Also

$$R_{Z02} \approx |\Gamma_{L,Z01}|\,. \tag{4.39}$$

So provided that the characteristic impedance of the line, Z_{01}, is close to the system reference impedance, Z_{02},

$$\frac{Z_{01}}{Z_{02}} = \frac{1+B}{1-B} \approx \frac{1+C_{Z02}}{1-C_{Z02}} \tag{4.40}$$

and this is just the normalized impedance reading at the center of the circle. For example, if a line with a characteristic impedance (Z_{01}) of $55\ \Omega$ is terminated in a $45\ \Omega$ load, then in a ($Z_{02}\ =$) $50\ \Omega$ system, C_{Z02} = 0.0939 and R_{Z02} = 0.0996. Using Equation (4.40) the derived Z_{01} = 54.7 Ω and, using Equation (4.39), $\Gamma_{L,Z01}$ = 0.0996 compared to the ideal 0.1000.

Table 4-1 presents the actual characteristic impedance of the line as the ratio Z_{Z01}/Z_{Z02} for particular center and radius values measured on the polar plot referenced to Z_{02}. The actual value of impedance is compared to the approximate value for $Z_{Z01}/Z_{Z02} \approx 1 + C_{Z02}/1 - C_{Z02}$. It is seen that the approximation in Equation (4.40) provides a good estimate of the unknown characteristic impedance (Z_{01}) improving as the center of the locus is closer to the origin.

4.6 Summary

The vendors of microwave test equipment program their instruments so that they guide the user through the calibration procedure. Usually the calibration procedures take much longer than the actual DUT measurement. The higher the frequency the longer and more fastidious is calibration, with calibration at 200 GHz perhaps taking days. Still calibration is absolutely required and with it surprisingly accurate measurements can be made at microwave and millimeter-wave frequencies.

4.7 References

[1] R. Hackborn, "An automatic network analyzer system," *Microwave Journal*, pp. 45–52, May 1968.

[2] http://www.ggb.com.

[3] G. Engen and C. Hoer, "Thru-reflect-line: An improved technique for calibrating the dual six-port automatic network analyzer," *IEEE Trans. on Microwave Theory and Techniques*, vol. 27, no. 12, pp. 987–993, Dec. 1979.

[4] S. Goldberg, M. Steer, P. Franzon, and J. Kasten, "Experimental electrical characterization of interconnects and discontinuities in high-speed digital systems," *IEEE Trans. on Components, Hybrids, and Manufacturing Technology*, vol. 14, no. 4, pp. 761–765, Dec. 1991.

[5] M. Steer, S. Goldberg, G. Rinne, P. Franzon, I. Turlik, and J. Kasten, "Introducing the through-line deembedding procedure," in *1992 IEEE MTT-S Int. Microwave Symp. Dig.*,, Jun. 1992, pp. 1455–1458.

[6] J. Hunton, "Analysis of microwave measurement techniques by means of signal flow graphs," *IRE Trans. on Microwave Theory and Techniques*, vol. 8, no. 2, pp. 206–212, Mar. 1960.

[7] J. Fitzpatrick, "Error models for systems measurement," *Microwave Journal*, pp. 63–66, may 1978.

[8] A. A. M. Saleh, "Explicit formulas for error correction in microwave measuring sets with switching-dependent port mismatches," *IEEE Trans. on Instrumentation and Measurement*, vol. 28, no. 1, pp. 67–71, Mar. 1979.

[9] H. Shurmer, "Calibration procedure for computer-corrected s parameter characterisation of devices mounted in microstrip," *Electronics Letters*, vol. 9, no. 14, pp. 323–324, 12 1973.

[10] *De-embedding and Embedding S-paramater Networks Using a Vector Network Analyzer*, May 2004, agilent Application Note 1363–1.

[11] J. Butler, D. Rytting, M. Iskander, R. Pollard, and M. Vanden Bossche, "16-term error model and calibration procedure for on-wafer network analysis measurements," *IEEE Trans. on Microwave Theory and Techniques*, vol. 39, no. 12, pp. 2211–2217, Dec. 1991.

[12] B. Bianco, M. Parodi, S. Ridella, and F. F. Selvaggi, "Launcher and microstrip characterization," *IEEE Trans. on Instrumentation and Measurement*, vol. 25, no. 4, pp. 320–323, Dec. 1976.

[13] C. Hoer, "Choosing line lengths for calibrating network analyzers," *IEEE Trans. on Microwave Theory and Techniques*, vol. 31, no. 1, pp. 76–78, Jan. 1983.

[14] C. A. Hoer, "Some questions and answers concerning air lines as impedance standards," in *29th ARFTG Conf. Digest-Spring*, vol. 11, Jun. 1987, pp. 161–173.

[15] P. Buff, "Characterization of propagation on wires over lossy earth," Ph.D. dissertation, North Carolina State University, 2006.

[16] P. Buff, J. Nath, and M. Steer, "Origin of the half-wavelength errors in microwave measurements using through-line calibrations," *IEEE Trans. on Instrumentation and Measurement*, vol. 56, no. 5, pp. 1610–1615, Oct. 2007.

[17] R. Marks, "A multiline method of network analyzer calibration," *IEEE Trans. on Microwave Theory and Techniques*, vol. 39, no. 7, pp. 1205–1215, Jul. 1991.

[18] D. Williams, "De-embedding and unterminating microwave fixtures with nonlinear least squares," *IEEE Trans. on Microwave Theory and Techniques*, vol. 38, no. 6, pp. 787–791, Jun. 1990.

[19] N. R. Franzen and R. A. Speciale, "A new

Table 4-1: Table of the normalized characteristic impedance Z_{01}/Z_{02} of a terminated transmission line having characteristic impedance Z_{01} plotted on a Smith chart with a reference impedance of Z_{02} in terms of the center, C_{Z02}, of the circular locus (with respect to line length) of the line for various radii, R_{Z02}, of the circular locus. C_{Z02} and R_{Z02} are in terms of reflection coefficient measured on the Smith chart. Also shown is the approximation, $(1 + C_{Z02})/(1 - C_{Z02})$, of Z_{01}/Z_{02} (see Equation (4.40)) .

C_{Z02}	$Z_{01}/Z_{02} \approx \frac{(1+C_{Z02})}{(1-C_{Z02})}$	$R_{Z02} = 0.2$		$R_{Z02} = 0.3$		$R_{Z02} = 0.4$		$R_{Z02} = 0.5$	
			error	Z_{01}/Z_{02}	error	Z_{01}/Z_{02}	error	Z_{01}/Z_{02}	error
0.00	1.000	1.000	0%	1.000	0%	1.000	0%	1.000	0%
0.02	1.041	1.043	$< 1\%$	1.045	$< 1\%$	1.050	1%	1.050	1%
0.04	1.083	1.088	$< 1\%$	1.093	1%	1.100	2%	1.113	3%
0.06	1.128	1.130	$< 1\%$	1.140	1%	1.155	2%	1.175	4%
0.08	1.174	1.183	$< 1\%$	1.193	2%	1.210	3%	1.250	6%
0.10	1.222	1.230	$< 1\%$	1.245	2%	1.270	4%	1.310	7%
0.12	1.273	1.285	1%	1.305	2%	1.335	5%	1.385	8%
0.14	1.326	1.340	1%	1.365	3%	1.408	6%	1.465	10%
0.16	1.381	1.400	1%	1.428	3%	1.475	6%	1.550	11%
0.18	1.439	1.460	1%	1.495	4%	1.550	7%	1.645	13%
0.20	1.500	1.528	2%	1.565	4%	1.635	8%	1.745	14%
0.22	1.564	1.595	2%	1.645	5%	1.720	9%	1.860	16%
0.24	1.632	1.670	2%	1.725	5%	1.815	10%	1.980	18%
0.26	1.703	1.745	2%	1.810	6%	1.920	11%	2.120	20%
0.28	1.778	1.830	3%	1.905	7%	2.030	12%	2.270	22%
0.30	1.857	1.915	3%	2.005	7%	2.150	14%	2.450	24%
0.32	1.941	2.008	3%	2.110	8%	2.285	15%	2.655	27%
0.34	2.030	2.105	4%	2.225	9%	2.435	16%	2.885	30%
0.36	2.125	2.215	4%	2.350	10%	2.600	18%	3.125	32%
0.38	2.226	2.325	4%	2.490	11%	2.785	20%	3.515	37%
0.40	2.333	2.455	5%	2.640	12%	3.000	22%	3.925	40%
0.42	2.585	2.585	5%	2.805	13%	3.240	24%	–	–
0.44	2.730	2.730	6%	2.985	14%	3.535	27%	–	–
0.46	2.704	2.885	6%	3.180	15%	3.865	30%	–	–

C_{Z02}	$Z_{01}/Z_{02} \approx \frac{(1+C_{Z02})}{(1-C_{Z02})}$	$R_{Z02} = 0.6$		$R_{Z02} = 0.7$	
		Z_{01}/Z_{02}	error	Z_{01}/Z_{02}	error
0.00	1.000	1.000	0%	1.000	0%
0.02	1.041	1.065	2%	1.080	4%
0.04	1.083	1.135	5%	1.170	7%
0.06	1.128	1.208	7%	1.265	11%
0.08	1.174	1.285	9%	1.375	15%
0.10	1.222	1.370	11%	1.500	19%
0.12	1.273	1.465	13%	1.640	22%
0.14	1.326	1.565	15%	1.800	26%
0.16	1.381	1.685	18%	1.990	31%
0.18	1.439	1.820	21%	2.230	35%
0.20	1.500	1.965	24%	2.515	40%
0.22	1.564	2.130	27%	2.915	46%
0.24	1.632	2.330	30%	3.440	53%
0.26	1.703	2.555	33%	4.380	61%
0.28	1.778	2.830	37%	–	–
0.30	1.857	3.205	42%	–	–